

**Elucidation of strigolactone-dependent
seed germination pathway in the parasitic plant
*Striga hermonthica***

寄生植物ストライガにおける
ストリゴラクトン依存的発芽促進経路の解明

YAP Jia Xin

Division of Biological Science
Graduate School of Science
Nagoya University

A thesis submitted in partial fulfillment of the requirements
for the degree of Doctor of Philosophy

September 2023

Table of Contents

List of Figures	iv
List of Tables	vi
List of Abbreviations	vii
Main Abstract	1
Main Introduction	
Parasitic plant <i>Striga hermonthica</i> threatens food security in Africa	2
Host-derived strigolactones (SLs) as germination stimulants of <i>Striga</i>	2
SL perception and signaling mechanism in land plants	5
HYPOSENSITIVE TO LIGHT (HTL)-mediated germination in <i>Arabidopsis</i>	7
Convergent evolution of HTL as SL receptors in parasitic plants	9
Dynamics of SL perception in <i>S. hermonthica</i>	11
Involvement of other plant hormones in <i>S. hermonthica</i> germination	13
The aims of this research	14
Chapter 1	
Gibberellins promote seed conditioning by up-regulating strigolactone receptors in the parasitic plant <i>Striga hermonthica</i>	
Abstract	15
1.1 Introduction	16
1.2 Results	
<i>Striga</i> seeds depleted of GA during conditioning showed reduced germination	19
Exogenous GA rescued PAC inhibition during conditioning	22
PAC decreased the sensitivity of <i>Striga</i> seeds towards SLs	24
GA deficit seeds displayed low expression of ShHTL genes	26
Lack of GA reduced and delayed SL perception during germination	29
GA promotes conditioning at sub-optimal temperature	33
1.3 Discussion	35
1.4 Materials and Methods	39

1.5 Supplementary Materials

Supplementary table	42
Supplementary figures	44

Chapter 2

Functional analysis of parasitic plant *Striga hermonthica* germination inhibitor RTC2

Abstract	56
2.1 Introduction	57
2.2 Results	
Identification of RTC2 as inhibitor of SPL7-induced <i>Striga</i> germination	58
Structure-activity relationship (SAR) studies of RTC2	62
RTC2 decoupled binding of ShHTLs to downstream MAX2 and SMAX1.....	66
RTC2 further destabilized SPL7-bound ShHTL7	68
2.3 Discussion	70
2.4 Materials and Methods	73
2.5 Supplementary Materials	
Supplementary table	79
Supplementary figures	80
Concluding Remarks	87
Acknowledgement	88
Reference	89

List of Figures

Main Introduction

Figure 1 Chemical structures of canonical SLs.	4
Figure 2 Proposed models for SLs signal activation.	6
Figure 3 Chemical structures of KAR and GR24.	8
Figure 4 HTL and D14 signaling pathways in parasitic and non-parasitic plants.	10
Figure 5 Chemical structures of YLG and dynamics of SL perception during germination process of <i>S. hermonthica</i>	12

Chapter 1

Figure 1 Timeline and effect of PAC treatment during seed germination or conditioning of <i>S. hermonthica</i> and <i>O. minor</i>	21
Figure 2 Promotion of seed conditioning by GA.	23
Figure 3 Effect of GA on sensitivity of <i>Striga</i> seeds towards SLs.	25
Figure 4 Effect of GA on SL signaling and GA metabolic components.	28
Figure 5 Time-lapse images showing GA affected on the dynamics of SL perception during <i>Striga</i> germination.	30
Figure 6 Quantitative analysis on the changes in YLGW fluorescence pattern in representative <i>Striga</i> embryos conditioned in DMSO, PAC or GA ₃	31
Figure 7 Effect of GA on seed conditioning at sub-optimal temperature.	34
Figure 8 Proposed models for interaction between GA and <i>HTL</i> signaling pathways in non-parasitic and parasitic plants.	38
Supplementary Figure 1 Effect of GA biosynthetic inhibitors on the root elongation of germinating <i>Striga</i> seedlings.	44
Supplementary Figure 2 Timeline and effect of BX-112 treatment during <i>Striga</i> seed germination or conditioning.	45
Supplementary Figure 3 Exogenous GA added simultaneously with GR24 was less effective in alleviating PAC inhibition on <i>Striga</i> seed conditioning.	46
Supplementary Figure 4 Phylogenetic analysis of GA biosynthesis, catabolic and signaling genes in <i>S. hermonthica</i>	47

Supplementary Figure 5 Time-lapse movie images of green fluorescence produced from YLGW hydrolysis by ShHTL receptors.	49
Supplementary Figure 6 Germination rate of <i>Striga</i> embryos in YLGW time-lapse movies and kymographs of germinating embryos.	50
Supplementary Figure 7 Kymographs of non-germinating embryos.	52
Supplementary Figure 8 Wake-up wave velocity and pause duration of germinating seeds.	54
Supplementary Figure 9 Radicle emergence of <i>Striga</i> seeds conditioned for 7 d in DMSO, PAC or GA ₃	55

Chapter 2

Figure 1 9 RTCs suppressed <i>Striga</i> germination induced by SPL7 and bind to ShHTLs.	60
Figure 2 Chemical synthesis and structure-activity relationship studies of RTC2 derivatives. ...	64
Figure 3 RTC2 weakened SPL7-dependent protein-protein interactions of ShHTLs with downstream ShMAX2 and AtSMAX1 in Y2H and Y3H assays.	67
Figure 4 RTC2 destabilized SPL7-bound ShHTL7 <i>in vitro</i> and <i>in planta</i>	69
Figure 5 A proposed model for allosteric inhibition of RTC2.	72
Supplementary Figure 1 The flow of chemical suppressor screening.	80
Supplementary Figure 2 YLG binding assay of 41 germination inhibitors at 10 μM final concentration.	81
Supplementary Figure 3 Comparison of RTC2 from chemical library and synthesized compound.	82
Supplementary Figure 4 ACC treatment partially rescued RTC2 inhibition.	83
Supplementary Figure 5 Protein-protein interactions of ShHTLs, ShMAX2 and AtSMAX1 in Y2H and Y3H assays.	84
Supplementary Figure 6 Time course degradation of ShHTL7 induced by SPL7.	86

List of Tables

Chapter 1

Supplementary Table 1: List of primers used for RT-qPCR.	42
--	----

Chapter 2

Supplementary Table 1: List of primers used for Y2H and Y3H assays.	79
---	----

List of Abbreviations

2-OGD	2-oxoglutarate-dependent dioxygenases
4DO	4-deoxyorobanchol
5DS	5-deoxystrigol
ABA	Abscisic acid
ABC-ring	Tricyclic lactone moiety of strigolactones
ACC	1-Aminocyclopropane-1-carboxylate
ACS	1-Aminocyclopropane-1-carboxylate Synthase
AM fungi	Arbuscular mycorrhizal fungi
AVG	Aminoethoxyvinylglycine
BX-112	Prohexadione-calcium
CHX	Cycloheximide
CLIM	Covalently linked intermediate molecule
CTH	C-terminal α -helix
D3	DWARF3
D14	DWARF14
D53	DWARF53
DAD2	DECREASED APICAL DOMINANCE2
DMSO	Dimethylsulfoxide
D-ring	Methylbutenolide moiety of strigolactones
DSF	Differential scanning fluorimetry
GA	Gibberellins
GA2ox	Gibberellin 2-oxidase
GA3ox	Gibberellin 3-oxidase
GA20ox	Gibberellin 20-oxidase
GAI	GIBBERELIC ACID INSENSITIVE
GGDP	Geranyl geranyl diphosphate
GID	GIBBERELLIN-INSENSITIVE DWARF
GR24	Synthetic strigolactone
HTL/KAI2	HYPOSENSITIVE TO LIGHT/KARRIKIN INSENSITIVE2

IC ₅₀	Half maximal inhibitory concentration
KARs	Karrikins
KAO	<i>ent</i> -kaurenoic acid oxidase
KL	KAI2 ligand
KO	<i>ent</i> -kaurene oxidase
LGS1	LOW GERMINATION STIMULANT 1
LRR	Leucine-rich repeat
MAX2	MORE AXILARRY GROWTH2
MS	Murashige and Skoog
ORO	Orobanchol
PAC	Paclobutrazol
PP2C	Protein Phosphatase 2C
RGA	REPRESSOR-OF- <i>gal-3</i>
RGL	REPRESSOR-OF- <i>gal-3</i> -LIKE
RTC	Receptor-Targeting Compound
SAR	Structure-activity relationship
SCF	Skp1-Cullin-F-box-protein
SD	Standard deviation
SLs	Strigolactones
SLR	SLENDER RICE
SLY	SLEEPY1
SMAX1	SUPPRESSOR OF MORE AXILLARY GROWTH2 1
SMXL	SUPPRESSOR OF MORE AXILLARY GROWTH2 1-LIKE
SNE	SNEEZY1
SPL7	Sphynolactone-7
STR	Strigol
Y2H	Yeast two-hybrid
YLG	Yoshimulactone Green
YLGW	Yoshimulactone Green Double

Main Abstract

Expanding infestations of a root parasitic plant *Striga hermonthica* on staple crops pose serious threats to agricultural production especially for smallholder farmers in Africa. Eradication of this noxious weed remains challenging due to its unusual parasitic adaptations where the seeds stay dormant but viable in soil for decades until the presence of host plants. Dormant seeds of *S. hermonthica* require a period of conditioning under warm temperature and moisture before they become responsive to germination stimulants exuded from the host roots called strigolactones (SLs). Understandings on seed germination are important for developing solutions to deplete *S. hermonthica* seedbank in the soil, yet the current knowledge is limited. In this research, I applied chemical genetic approaches to study the strigolactone-dependent seed germination pathway in *S. hermonthica*. In Chapter 1, I will describe a positive role of plant hormone gibberellins on seed conditioning that indirectly regulates the seed germination of *S. hermonthica*. In Chapter 2, I will describe the discovery of a SL receptor-targeting germination inhibitor and discuss its mode-of-action.

Main Introduction

Parasitic plant *Striga hermonthica* threatens food security in Africa

Striga hermonthica, or commonly known as purple witchweed, is a root parasitic plant that belongs to the *Orobanchaceae* family. It is classified as an obligate parasite that depends on its hosts to complete its life cycle and a hemiparasite that obtains nutrients from hosts but photosynthetic at certain degree. Expanding *Striga* infestations are causing devastating yield losses in Africa and threatening food security across the continent (Ejeta 2007). Among *Striga* genus, damage caused by *S. hermonthica* poses the deadliest threat to agriculture because it infests a wide range of staple crops including sorghum, finger millet, rice and maize. Therefore, studies on *S. hermonthica* are crucial for parasitic plant control and to improve food supply.

Host-derived strigolactones (SLs) as germination stimulants of *Striga*

Challenges in *Striga* eradication arise from its unusual parasitic adaptation where the seeds can stay dormant but viable in soil for decades, and only germinate when they sense germination stimulants called strigolactones (SLs) that are exuded from the roots of host plants when hosts grow in proximity. SLs are a new class of plant hormones which were first isolated from root exudates of cotton as germination stimulants for *Striga lutea* Lour. (Cook et al., 1966). In land plants, SLs are mainly produced in roots through carotenoid pathway and function in regulating shoot branching, root development, leaf senescence and drought stress responses (Gomez-Roldan et al., 2008; Umehara et al., 2008; Ruyter-Spira et al., 2011; Ueda and Kusaba, 2015; Ha C. V. et al., 2014). Under nutrient deficient conditions, in particular phosphate deficiency, SLs are rapidly produced and exuded into the rhizosphere to stimulate hyphal branching of symbiotic arbuscular mycorrhizal (AM) fungi, allowing them to grow towards plant roots for nutrient exchange (Akiyama et al., 2005; Besserer et al., 2006). However, parasitic plants like *Striga* exploit these rhizosphere signals as germination cues for themselves that indicate the presence of suitable host plants.

Chemical structure of canonical SLs consists of a tricyclic lactone (ABC-ring) connected to a methylbutenolide (D-ring) through an enol ether linkage. While chemical modifications on the ABC-ring contribute to diversity in SL structures, D-ring with *R* configuration at C2' position

is conserved in all natural SLs identified thus far and is important for SL activity (Fig. 1; reviewed in Takahashi and Asami, 2018). SLs are exuded into the rhizosphere in different compositions among different plants and mixture of SLs in plant root exudates is important to establish interaction with AM fungi and determines the susceptibility of parasitic plant infestation. In fact, various SLs present in the rice root exudates were shown to stimulate parasitic plant seed germination and AM fungal hyphal branching at very different extents (Cardoso et al., 2014).

Striga seeds are extremely sensitive to SLs in which they can detect and germinate at picomolar concentration of SLs present in the soil. Structure-activity relationship studies showed that strigol-type SLs with β -oriented C-ring are more preferred germination stimulants for *S. hermonthica* than the orobanchol-type SLs with α -oriented C-ring (Fig. 1; Nomura et al., 2013). 5-deoxystrigol (5DS) present in root exudates of sorghum (*Sorghum bicolor*), natural host of *S. hermonthica*, represents one of the most potent germination stimulants. Sorghum genotypes that produce higher concentration of 5DS were shown to stimulate higher germination of *S. hermonthica* than those that produce higher concentration of orobanchol (ORO) in field experiments (Mohammed et al., 2016). More recently, it was shown that loss-of-function of *LOW GERMINATION STIMULANT 1 (LGS1)* that encodes a sulfotransferase in sorghum resulted in drastic reduction of *Striga* germination stimulating activity due to dominant production of ORO over 5DS in root exudates (Gobena et al., 2017). Altogether, these results suggested that *Striga* possibly recognize its host and avoid non-host plants based on the composition of SLs present in host root exudates.

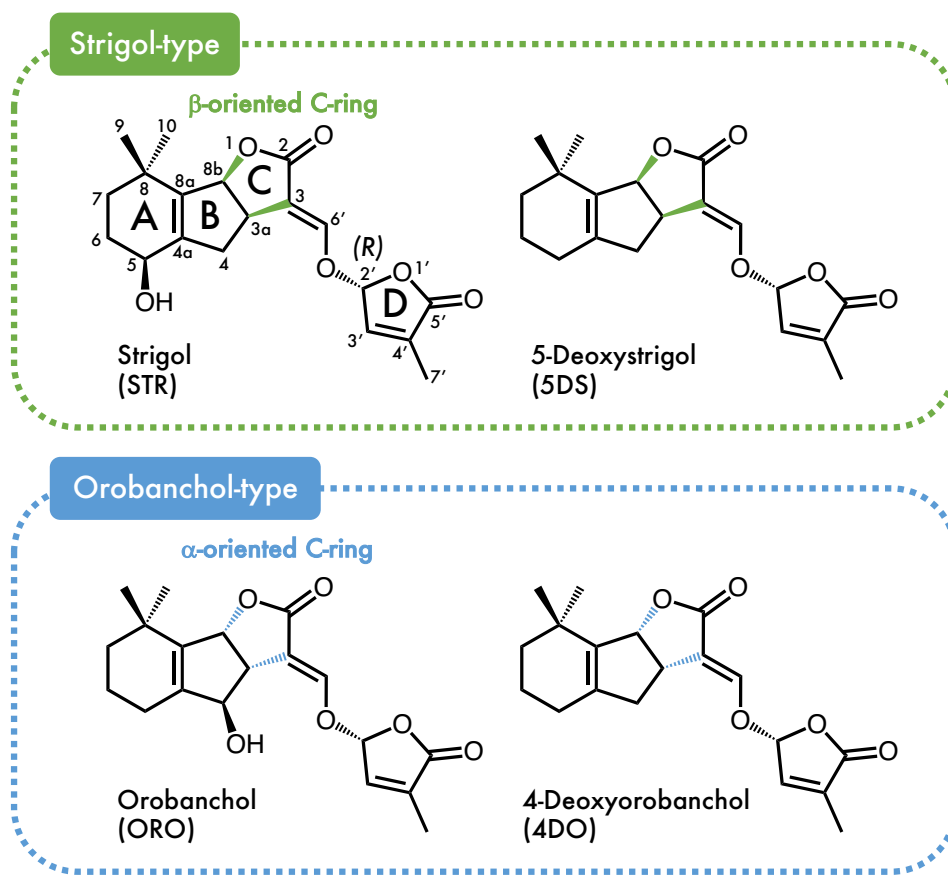


Figure 1 Chemical structures of canonical SLs. Variable modifications on the tricyclic lactone (ABC-ring) contribute to diverse SL structures but methylbutenolide (D-ring) structure with *R* configuration is invariant and important for SL activity. Strigol-type SLs (green) have β -oriented C-ring whereas orobanchol-type SLs (blue) have α -oriented C-ring. All natural SLs identified thus far have conserved *R* configuration at C2' position.

SL perception and signaling mechanism in land plants

In non-parasitic plants, SLs are perceived by DWARF14/DECREASED APICAL DOMINANCE2 (D14/DAD2) that act as SL receptor in rice, *Arabidopsis thaliana* (D14) or petunia (DAD2) respectively (Arite et al., 2009; Scaffidi et al., 2014; Hamiaux et al., 2012). D14 receptors are members of the α/β hydrolase superfamily with conserved catalytic triad comprising of serine, histidine and aspartic acid residues. Thus, they retain enzymatic activity to bind and hydrolyze SLs, but the activation mechanism of SL signaling remains debatable.

The first model proposed a hydrolysis-dependent signal activation, where upon binding to the receptors, SL enol ether bond is hydrolyzed, cleaving off ABC-ring while D-ring moiety binds covalently to histidine in the catalytic site and forms covalently linked intermediate molecule (CLIM) (Nakamura et al., 2013; de Saint Germain et al., 2016; Yao et al., 2016). Crystallographic study on AtD14 showed that CLIM formation changes conformation of the receptor that enables its binding to an F-box protein, DWARF3 (D3) to activate downstream signaling event. In contrast to the first model, the second model proposed a binding-dependent signal activation, where binding of intact SLs leads to active signaling state of AtD14 (Seto et al., 2019). This is supported by *AtD14^{D218A}* that confers active site mutation and defective in SL hydrolysis was able to complement *Atd14* mutant phenotype. In this case, SL hydrolysis is considered as a step for deactivation of bioactive SLs after signal activation.

While the signal activation mechanism remains puzzled, it is confirmed that D14 receptors signal through F-box protein, D3 in rice or its ortholog in *Arabidopsis*, MORE AXILLARY GROWTH2 (MAX2), that are part of the Skp1-Cullin-F-box-protein (SCF) E3 ubiquitin ligase complex, to direct polyubiquitination and proteasomal degradation of downstream negative regulators of SL signaling, DWARF53 (D53) in rice and SUPPRESSOR OF MORE AXILLARY GROWTH2-LIKE6 (SMXL6), SMXL7 and SMXL8 in *Arabidopsis*, to suppress shoot branching (Jiang et al., 2013; Zhou et al., 2013; Wang et al., 2015). Shortly after D53/SMXLs are degraded, D14 receptors also undergo MAX2-dependent proteasomal degradation as a feedback regulation to deactivate SL perception (Chevalier et al., 2014; Hu et al., 2017).

Recent crystallographic study of D3 revealed two conformational states of the F-box protein: the last C-terminal α -helix (CTH) that is highly dynamic can either engage with (closed) or dislodge from (open) its leucine-rich repeat (LRR) domain. The dislodged CTH in the D3/MAX2 open form binds to and inhibits the hydrolytic activity of SL-bound D14 to recruit D53/SMXLs for ubiquitination. Then, D14 hydrolysis is restored and CTH folds back to closed form to direct degradation of D53/SMXLs and eventually D14 (Shabek et al., 2018; Tal et al., 2022). It was reasoned that adaptation of such conformational switch adds another layer of regulation to prevent premature hydrolysis of SLs and helps to orchestrate ligand perception, signal activation and SL metabolism in a highly coordinated manner. However, SL-D14 signaling pathway does not affect seed germination since *Atd14* loss-of-function mutant shows no obvious defect in seed germination (Waters et al., 2012).

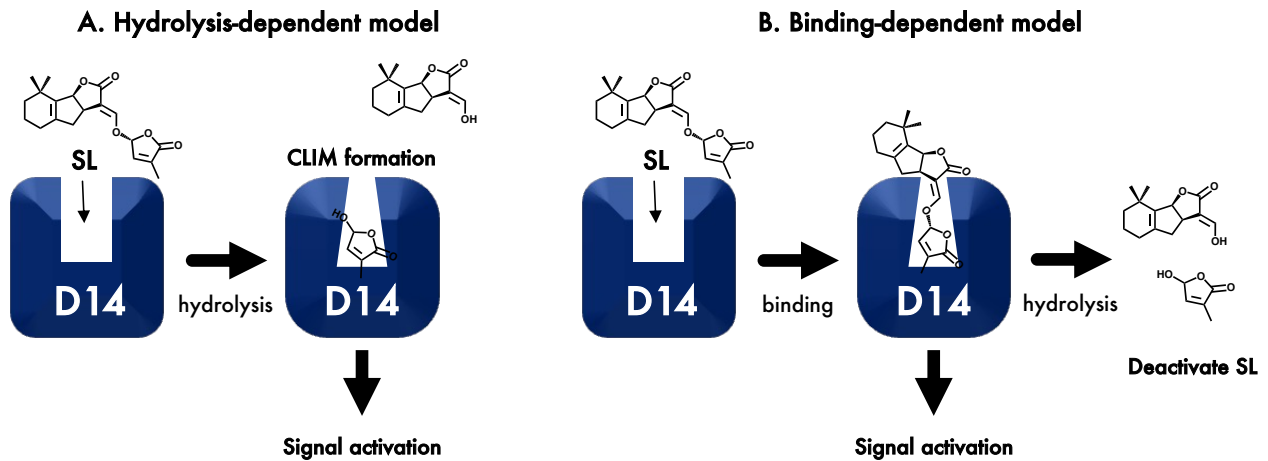


Figure 2 Proposed models for SLs signal activation. (A) D14 binds and hydrolyses SL into ABC-ring and D-ring. While ABC-ring is released, D-ring forms CLIM with active site residue and changes the conformation of the receptor to allow it to bind downstream proteins to activate signal transduction. (B) Binding of intact SL change conformation of receptor to induce interaction with downstream proteins to activate signaling pathway. After signal transduction, SL is hydrolyzed to deactivate signal.

HYPOSENSITIVE TO LIGHT (HTL)-mediated germination in *Arabidopsis*

Phylogenetic analyses suggested that *D14* evolved from their ancestral paralogues *HYPOSENSITIVE TO LIGHT/KARRIKIN INSENSITIVE2 (HTL/KAI2)* through gradual neofunctionalization. While *HTL* is conserved in land plants, *D14* is only found in seed plants (Delaux et al., 2012; Bythell-Douglas et al., 2017). Similarly, HTL receptors are also α/β hydrolase-fold proteins with conserved catalytic triad and have similar overall structure with *D14*, but nonetheless, they have a smaller ligand binding pocket (Kagiyama et al., 2013).

In *Arabidopsis*, growing evidences are supporting that the endogenous ligand of AtHTL, tentatively termed KAI2 ligand (KL), should exist in plants but remain unidentified, as *Athtl* loss-of-function mutant has increased primary seed dormancy, elongated hypocotyl and is defective in various seedling and root developments as well as drought and stress responses (Sun et al., 2016; Waters et al., 2012; Sun and Ni, 2010; Swarbreck et al., 2019; Villaécija-Aguilar et al., 2019; Li et al., 2017; Wang et al., 2018). On the other hand, exogenous ligands called karrikins (KARs) can overcome primary dormancy of *Arabidopsis* seeds in a AtHTL-dependent manner. KARs are smoke-derived compounds of burning vegetative that serve as seed germination cues after forest fire (Waters et al., 2012). Unlike the CLIM-bound AtD14, crystal structure of KAR₁-bound AtHTL showed an intact ligand binding at the entrance of active site but was distal from the catalytic triad (Guo et al., 2013). Yet, contradicting results from other biochemical analysis showed that KARs are unable to activate AtHTL *in vitro* but need to be converted into active form before they bind to AtHTL *in planta* (Waters et al., 2015b). Aside from that, it is intriguing that chemical structures of KARs contain butanolide moiety that resembles D-ring of SLs (Fig. 3). Although AtHTL is unable to bind natural SLs with 2'*R* configuration, it can recognize non-natural stereoisomers of synthetic SLs with 2'*S* configuration (Waters et al., 2012; Scaffidi et al., 2014). Especially when *Arabidopsis* is treated with GR24, one of the widely applied synthetic SLs that is usually used as a racemic mixture in plant research, (+)-GR24 with natural 2'*R* configuration signals through D14 whereas (-)-GR24 with non-natural 2'*S* configuration acts through both HTL and D14, which confers complicated results (Scaffidi et al., 2014). Consistent with this observation, AtHTL is able to bind and hydrolyze (-)-GR24 *in vitro* like D14 receptors (Toh et al., 2014). Whether KARs or GR24, they are either exogenous signals or synthetic molecule, ligand perception by AtHTL therefore remains elusive until the identification of endogenous KL.

Like D14, AtHTL also signals through MAX2 but targets to different negative regulators, SUPPRESSOR OF MAX2 1 (SMAX1) and SMXL2, which are the homologs of SMXLs 6-8 that regulate SL signaling (Stanga et al., 2013). Thus, MAX2 mediates SL-signal from AtD14 as well as KL-signal from AtHTL but results in two distinct functions through binding to different downstream suppressors and domains of SMAX1 and SMXL7 that are responsible for specific binding to AtHTL or AtD14 were recently identified (Nelson et al., 2011; Khosla et al., 2020). Nevertheless, differences between two signaling mechanisms were also highlighted. Firstly, aside from KARs-induced and MAX2-dependent degradation, SMAX1 is also subjected to proteolysis that is independent of MAX2. Secondly, unlike AtD14, KARs-induced proteasomal degradation of AtHTL is MAX2-independent and was recently shown to be associated with binding to SMAX1/SMXL2 (Waters et al., 2015a; Khosla et al., 2020).

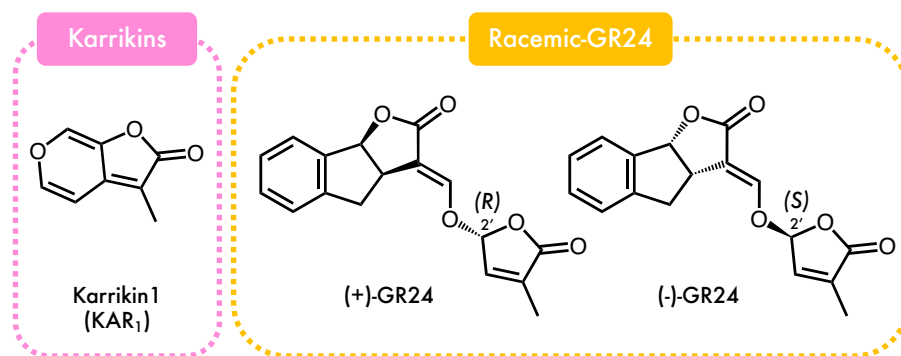


Figure 3 Chemical structures of KAR and GR24. (A) KAR₁ has a similar structure with D-ring of SL. (B) (+)-GR24 has natural *R* configuration whereas (-)-GR24 has non-natural *S* configuration at C2' position.

Convergent evolution of HTL as SL receptors in parasitic plants

Riding on the findings from D14 and HTL, parasitic plants were thought to have opted similar system to perceive host-derived SLs for germination. This is further supported by *MAX2* which is highly conserved in parasitic plants and *ShMAX2* is able to rescue most of the *Atmax2* mutant phenotypes (Liu et al., 2014). Evolutionary study of parasitic plants in the *Orobanchaceae* family revealed that they encode at most a single copy of *D14*, but great amplification of *HTL* is observed (Conn et al., 2015). In *S. hermonthica*, at least eleven copies of *HTL* were identified and they all encode α/β hydrolases with conserved catalytic triad but have different binding pocket volume and ligand preferences. Eleven *ShHTLs* can be further categorized into three subclades: conserved clade containing *ShHTL1* that is closest to ancestral *HTL*, intermediate clade containing *ShHTL2* and *ShHTL3* that has intermediate properties of *HTL* and *D14* as well as divergent clade containing *ShHTL4-ShHTL11* that evolve larger active site cavities that resembles D14. Interestingly, the fastest-evolving divergent clade contains the highest copy number of *HTLs*.

To date, there is still no suitable transformation method reported for *S. hermonthica*, mainly because it is an outcrossing species with high degree of heterozygosity and it requires host to grow, which makes it difficult to create stable transgenic line to study mutant phenotype of gene-of-interest such as *ShHTLs* in *S. hermonthica* itself. Instead, the function of *ShHTLs* was elucidated by individually transforming the gens into *Athtl* mutant. In addition to regulating seed primary dormancy mentioned above, AtHTL pathway can also alleviate thermoinhibition, which is seed dormancy induced under high temperature of 30 °C (Toh et al., 2012). Therefore, the function of *ShHTLs* in germination has been evaluated through functional complementation of *Athtl* germination phenotype under these specific conditions (Conn et al., 2015; Toh et al., 2015). Briefly, most members of the divergent clade, especially *ShHTLs 4-9*, were able to rescue germination of *Athtl* mutant in a SL-dependent manner, suggesting that they are most likely the important receptors to trigger germination in response to host-derived SLs in *S. hermonthica*. Among them, *ShHTL7* showed highest sensitivity to SLs at picomolar concentrations, implying that it is the key receptor in *S. hermonthica*. On the other hand, *ShHTL2* and *ShHTL3* of the intermediate clade were less sensitive to SLs but responded well to KARs, although KARs are unable to induce germination of *S. hermonthica*. Lastly, *ShHTL1* of the conserved clade was unable to rescue germination regardless of ligands tested. Strikingly, *ShHTL10* and *ShHTL11* of the divergent clade

also neither rescue *Athl* mutant through SLs nor KARs, although these two receptors are able to bind and hydrolyze SLs *in vitro* (Tsuchiya et al., 2015). Nevertheless, the HTL receptors have evolved from sensing KL in non-parasitic plants to sensing SLs throughout evolution of parasitic plants.

Based on the current findings, it is suggested that *ShHTLs* are likely to mediate germination through the same core components of *MAX2* and *SMAX1*. This is further supported by extensive biochemical studies such as pull-down experiments and yeast-two-hybrid assays that show ligand dependent protein-protein interactions of *ShHTLs* with *MAX2* and *SMAX1* (Yao et al., 2017; Xu et al., 2018; Wang et al., 2021).

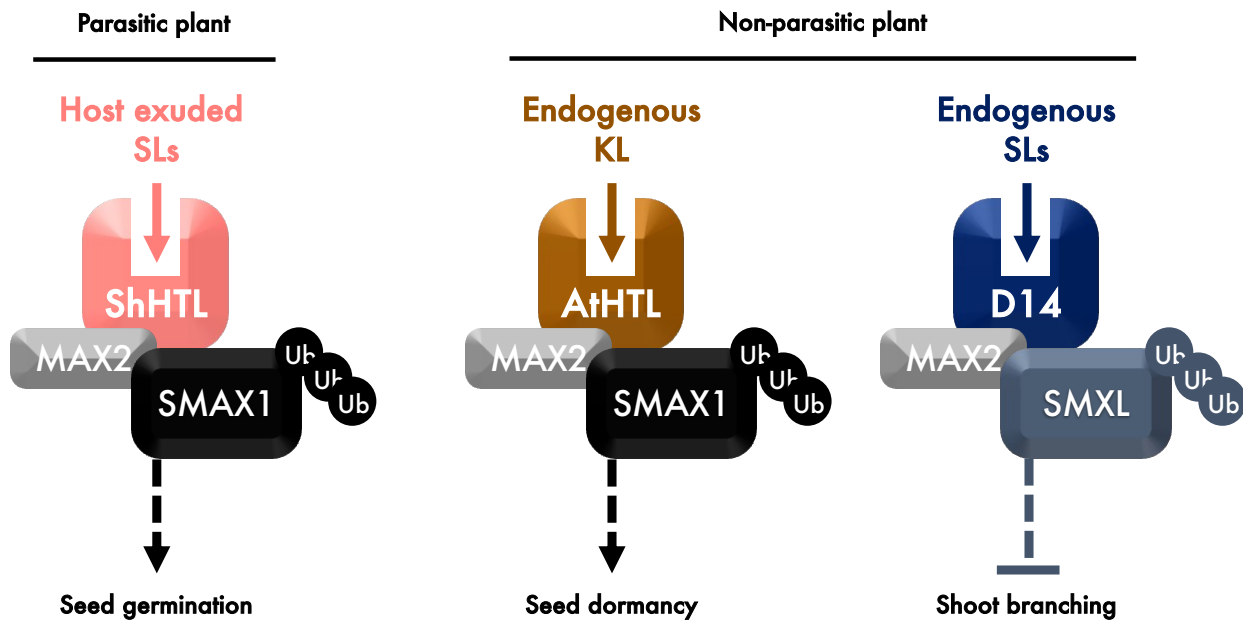


Figure 4 HTL and D14 signaling pathways in parasitic and non-parasitic plants. In parasitic plants like *S. hermonthica*, *ShHTLs* perceive host-derived SLs to stimulate seed germination via *MAX2* and *SMAX1* pathway. In non-parasitic plants like *Arabidopsis*, *AtHTL* perceives unknown endogenous KL to regulate seed dormancy via *MAX2* and *SMAX1* whereas *AtD14* perceives SLs to regulate shoot branching via *MAX2* and *SMXL6, 7* and *8*. The receptors bind to F-box protein *MAX2* in a ligand-dependent manner to target negative regulator *SMAX1* or *SMXL6, 7*, and *8* for ubiquitination and proteasomal degradation to elicit diverse functions.

Dynamics of SL perception in *S. hermonthica*

To probe the function of ShHTLs, a fluorogenic SL mimic called Yoshimulactone Green (YLG) was designed based on the hydrolytic property of SLs by the receptors (Tsuchiya et al., 2015). YLG carries a chemical structure of a D-ring moiety attached to a fluorescein. When hydrolyzed by SL receptors like D14 and ShHTLs, it produces green fluorescence as the D-ring is cleaved off and the free fluorescein can be excited. *In vivo*, YLG retains SL activities in both *Arabidopsis* and *S. hermonthica* whereas *in vitro*, it has been applied to set up a competitive binding assay with ShHTL2- ShHTL11, excluding ShD14 and ShHTL1 that do not hydrolyze YLG, to test the binding of ligand-of-interest by monitoring the changes in fluorescence level produced from YLG hydrolysis. Using this system, binding affinity of each ShHTLs to different SLs was compared by calculating their half maximal inhibitory concentration (IC₅₀) on YLG hydrolysis, and the receptors were shown to portray different preferences for different SLs, but ShHTLs 4-9 that are important for germination mainly bind most SLs at higher affinities. Among the natural SLs tested, 5DS binds to all of the receptors but ORO only binds to certain ShHTLs at lower affinity, which is consistent with the finding that 5DS is a stronger germination stimulant than ORO as previously mentioned. Differential selectivity of ShHTLs towards different SLs also suggests why *S. hermonthica* is able to distinguish host and non-host plants and able perceive different SLs released from its host plants.

On the other hand, a variant of YLG, Yoshimulactone Green Double (YLGW), with two D-rings attached to a fluorescein, has a reduced fluorescence background but still stimulate *S. hermonthica* germination. YLGW is used to track the *in planta* dynamics of SL signal perception by ShHTLs in *S. hermonthica* seeds. Live-imaging with YLGW showed that seed germination of *S. hermonthica* is a 3-step process: a first fluorescence wave propagates from root tip to cotyledon (wake-up wave), and disappeared (pre-germination pause), then the second fluorescence wave appears from root tip and root elongation begins (elongation tide). Treatment with protein translation inhibitor, cycloheximide (CHX), delayed the arrival of wake-up wave and inhibited seed germination, suggesting protein translation is required to produce the factors that ‘wake up’ the embryo (Tsuchiya et al., 2015).

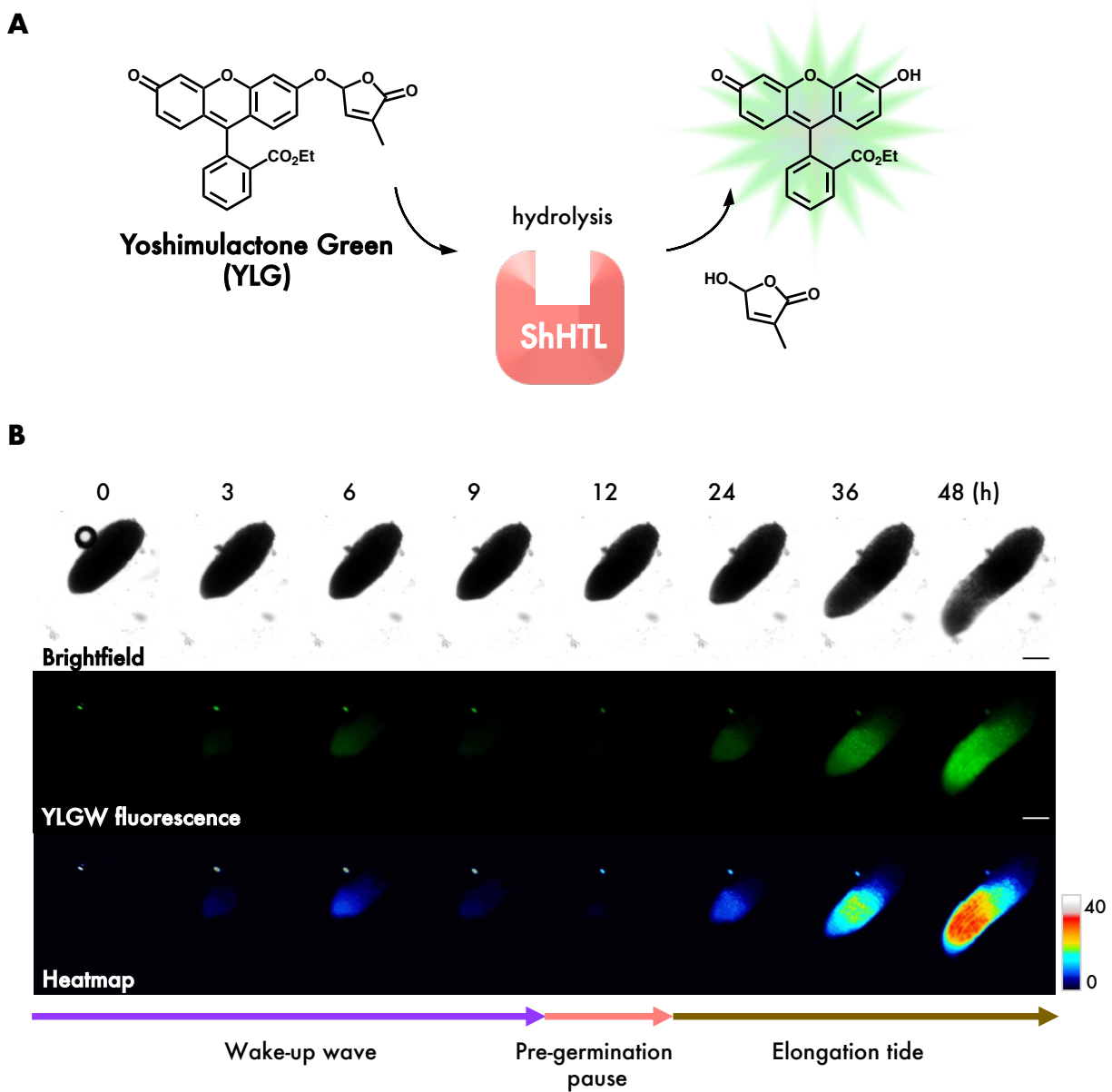


Figure 5 Chemical structures of YLG and dynamics of SL perception during germination process of *S. hermonthica*. (A) After hydrolysis by SL receptors, the free fluorescein moiety of YLG is released to produce fluorescence. (B) Three-step germination process of *S. hermonthica* where YLGW is first perceived and propagated from the root tip (wake-up wave) and disappears (pre-germination pause), then the second fluorescence wave propagates from root tip and root elongation begins (elongation tide).

Involvement of other plant hormones in *S. hermonthica* germination

Ethylene was shown to trigger germination in *Striga* independently of SLs in the early studies (Egley et al., 1970). Later, it was shown to work downstream of SLs in stimulating *S. hermonthica* seed germination, as GR24 increased the production of 1-aminocyclopropane-carboxylate (ACC), a key intermediate in ethylene biosynthesis, by up-regulating mRNA expression of *ACC synthase1* (*ShACSI*). It encodes a key enzyme that catalyzes the synthesis of direct ethylene precursor ACC, and inhibition of the enzyme by aminoethoxyvinylglycine (AVG) suppressed seed germination induced by GR24 (Sugimoto et al., 2003). Moreover, AVG was shown to reduce the intensity of fluorescence wave induced by YLGW without affecting the fluorescence pattern, suggesting that ShHTLs are activated by ethylene via feed forward regulation (Tsuchiya et al., 2015 & 2018).

In non-parasitic plants, it is well established that seed germination is negatively regulated by plant hormone abscisic acid (ABA) and positively regulated by GA. In contrast, the role of ABA and GA in parasitic plants is not well characterized. In the case of *S. hermonthica*, it was shown that neither bioactive GA₃ nor ABA biosynthesis inhibitor fluridone could independently stimulate germination efficiently (Toh et al., 2012). Yet interestingly, co-application of both GA₃ and fluridone stimulate germination to a level comparable to that of GR24. However, this mechanism is poorly understood, and a later study showed that seeds of *S. hermonthica* is insensitive to ABA due to a dominant mutation in a *protein phosphatase 2C* (*ShPP2C1*) that constitutively suppresses ABA signaling pathway. As a result, ABA does not affect GR24-dependent germination in *S. hermonthica* (Fujioka et al., 2019). Yet, this contradicts with the observation using fluridone but the reason is still unknown.

More recently, it was shown that *Arabidopsis* seeds expressing *ShHTLs 4-9* germinated in response to SLs even when they were treated with GA biosynthesis inhibitor paclobutrazol (PAC) to deplete them of GA (Bunsick et al., 2020). This pathway requires *MAX2*, since introducing *max2* loss-of-function mutation into *ShHTL4* or *ShHTL7* line resulted in loss of ability to germinate in the absence of GA. Additionally, *smax1* loss-of function mutant is also highly resistant to PAC inhibition of seed germination. Altogether, the findings proposed that ShHTLs can bypass GA requirement to germinate in response to SLs through conserved core components of *HTL* signaling pathway, but why *Striga* does not germinate in response to GA remains elusive.

The aims of this research

Understandings on seed germination of *S. hermonthica* are crucial especially for the development of efficient methods for parasitic plant control. For instance, one current promising solution in the field is called the “suicidal germination” that utilizes highly potent and selective SL agonists of ShHTLs to induce seed germination of *S. hermonthica* in the absence of host plants (Uraguchi et al. 2018). Without hosts, germinated seedlings die after two weeks and eventually depletes the number of parasitic seeds in the soil. In this case, identification and characterization of the ShHTLs receptors helps to accelerate the development of such suicidal germination molecules. Nonetheless, the details of seed germination in *S. hermonthica* are still largely unknown.

Overall, my research aims to contribute towards better understanding of *S. hermonthica* seed germination from two aspects. In Chapter 1, I first elucidated the role of GA in *S. hermonthica* germination. In Chapter 2, I studied the ShHTLs signaling pathway by chemical biology approach.

Chapter 1

Gibberellins promote seed conditioning by up-regulating strigolactone receptors in the parasitic plant *Striga hermonthica*

Abstract

Seeds of a parasitic witchweed *Striga hermonthica* (hereinafter referred to as *Striga* in this chapter) stay dormant and viable in soil until sensing host-derived signals called strigolactones (SLs) to germinate. This germination process is elicited by expanded SL receptors encoded by the *HYPOSENSITIVE TO LIGHT (HTL)* genes in *Striga*. Before the seeds become responsive to SLs, they require a period of incubation in warm and moist conditions, namely a process called “seed conditioning”. However, the detail mechanism behind this process is largely unknown. In this chapter, I elucidated that plant hormone gibberellins (GA) is required and positively regulates seed conditioning in *Striga*. GA acts through up-regulation of *ShHTLs* genes during conditioning to render competence of the seeds for sensing SLs. When GA biosynthesis was inhibited by paclobutrazol in conditioning, germination stimulated by SLs was greatly impaired. Additionally, *in planta* dynamics of SL perception visualized by a fluorogenic SL mimic, yoshimulactone green W, was disrupted in GA deficit seeds. Hence, this study uncovered an indirect contribution of GA to germination of parasitic plants, which is strongly in contrast to its role as the dominant germination regulator in autotrophic plants. Here, I proposed a detour model for how the role of GA became indirect throughout the evolutionary context of parasitic plants. Also, I highlighted the potential contribution of this study to the agricultural field to combat *Striga* infestations that are threatening the food security in Africa.

1.1 Introduction

Seed germination is a tightly regulated process in which plants sense the environmental signals such as temperature, light and nutrient availability to decide the adequate time for germination. Seeds remain in dormant state to overcome unfavorable environment and initiate germination process when conditions turn optimum. In most of the plant species, seed dormancy is positively regulated by plant hormone abscisic acids (ABA) whereas seed germination is promoted by another plant hormone gibberellins (GA). These two hormones act antagonistically to modulate the endogenous levels of one another in response to environmental cues (Bewly 1997). Essentially, the ability of dormant seeds to endure stresses along with their precision in germination control has allowed the plants to survive and propagate under constantly fluctuating environments.

The criteria for optimum conditions can, however, differ greatly between plant species. One astonishing example is the seed germination of parasitic plant *Striga hermonthica* (*Striga*). *Striga* is an obligate root parasite that depend heavily on the host to complete its life cycle and for growth. *Striga* seeds exhibit strong dormancy when the primary food source – host is absent. But if host grows in proximity, the seeds recognize strigolactones (SLs) that are released from the roots of host plant and germinate (Cook et al., 1966). Germinated seedlings then attach themselves to the host roots through a specialized organ called haustorium that hijacks the vasculature of host plant to absorb carbon, nutrients and water from host for their own growth. Considering the presence of host plant is indispensable for survival, it is therefore not surprising for parasitic plants like *Striga* to evolve into sensing host-derived signals as its predominant germination cues over other signals like light and nutrients as usually observed in autotrophic plants (Bewly, 1997).

Interestingly, dry and dormant *Striga* seeds are unable to immediately germinate in response to SLs after seed imbibition (Brown and Edwards, 1946). Instead, a period of 2-14 days incubation in moist and warm condition of around 30-40 °C is a prerequisite for germination in *Striga* (Lechat et al., 2015). This pre-incubation process is termed “seed conditioning”, and it takes relatively longer time compared to seed germination that occurs within 24 h after SLs application. But after conditioning, *Striga* seeds become extremely sensitive to exogenous SLs for eliciting germination. Thus, it is apparent that seed conditioning serves as an important period for the seeds

to acquire competence for sensing environmental SLs, possibly by establishing machineries required for seed germination. In addition to that, prolonged conditioning period is usually required under sub-optimal temperatures of 25 °C or below in order to reach maximum germination rate, hence physiological role of seed conditioning might also include sensing optimal environments for growth (Aflakpui et al., 1998). However, the mechanism behind this process is poorly understood.

On the contrary, more insights on seed germination of *Striga* are provided by the recent research of SLs in non-parasitic plants, and were described in details in the main introduction. Briefly, SL receptors in *Striga* evolve from *HYPOSENSITIVE TO LIGHT/KARRIKIN INSENSITIVE2* (*HTL/KAI2*) that perceives unknown endogenous KAI2-ligand (KL) to regulate seed dormancy through MORE AXILLARY GROWTH 2 (MAX2)-dependent degradation of negative regulator SUPPRESSOR OF MAX2 1 (SMA1) in non-parasitic plants (Stanga et al. 2013, Khosla et al. 2020). Remarkably, *Striga* genome encodes diverged copies of at least eleven *HTL/KAI2* genes, but throughout the evolution of parasitic plants, most ShHTLs have undergone functional shift from perceiving endogenous KL to sensing host-derived SLs in the environment (Conn et al., 2015; Tsuchiya et al., 2015; Toh et al., 2015). Among them, ShHTLs 4-9 are evidently the main SL receptors that account for stimulating *Striga* germination, likely also through MAX2-SMA1 pathway (Toh et al., 2015; Bunsick et al., 2020). The transcripts of these genes are gradually up-regulated during seed conditioning, which is in agreement with the acquisition of SL sensitivity during this phase (Tsuchiya et al., 2015). Also, fluorogenic SL probes called Yoshimulactone Green (YLG) and its variant YLGW revealed unique binding profile of ShHTLs to different SLs, as well as intriguing three-step germination process in *Striga* that is dynamically regulated by ShHTLs with reinforcement from other factors such as plant hormone ethylene (Tsuchiya et al., 2015).

The dominant role of host-derived SLs as germination cues in *Striga* is strongly in contrast to the dominant role of endogenous GA in promoting germination of non-parasitic plants (Bewly 1997). Optimum conditions for seed germination of non-parasitic plants like *Arabidopsis* include ambient temperature and light, and GA biosynthesis is required for this process as GA biosynthesis mutant *gal-3* is defective of seed germination (Koorneef and van der Veen, 1980). GA is first synthesized from geranyl geranyl diphosphate (GGDP) into *ent*-kaurene, then subsequently

converted by cytochrome P450 monooxygenases, *ent*-kaurene oxidase (KO) and *ent*-kaurenoic acid oxidase (KAO), before eventually catalyzed into the bioactive form by 2-oxoglutarate-dependent dioxygenases (2-OGD), GA 20-oxidases (GA20ox) and GA 3-oxidases (GA3ox) (Yamaguchi, 2008). GA homeostasis is tightly regulated in the plants, and bioactive GA is mainly catabolized by GA 2-oxidases (GA2ox) that also belongs to the 2-OGD superfamily. During *Arabidopsis* germination, biosynthesis genes like *AtKO1*, *AtGA20ox3* and *AtGA3ox1* were up-regulated within 8 h after seed imbibition and down-regulated afterwards whereas catabolic genes like *AtGA2ox2* were suppressed (Ogawa et al., 2003; Yamaguchi, 2008). Consistently, GA biosynthesis inhibitor paclobutrazol (PAC) that targets AtKOs also severely inhibits *Arabidopsis* germination (Jacobsen and Olszewski 1993). On the other hand, GA core signaling components also activate the pathway via the ubiquitin-proteasome system like SLs. In this case, GA receptor encoded by *GIBBERELLIN-INSENSITIVE DWARF1* (*GID1*) perceives GA to direct degradation of DELLA repressors, GIBBERELLIC ACID INSENSITIVE (*GAI*), REPRESSOR-OF-*gal-3* (*RGA*), *RGA-LIKE1* (*RGL1*), *RGL2*, and *RGL3* in *Arabidopsis* and *SLENDER RICE1* (*SLR1*) in rice, through F-box protein *SLEEPY1* (*SLY1*) or *SNEEZY1* (*SNE*) in *Arabidopsis* and *GID2* in rice (Ueguchi-Tanaka et al., 2005; Griffiths et al., 2006; Peng et al., 1997; Silverstone et al., 1998; Lee et al., 2002; Wen and Chang, 2002; Cheng et al., 2004; Ikeda et al., 2001; Sasaki et al., 2003; Gomi et al., 2004; McGinnis et al., 2003; Dill et al., 2004; Fu et al., 2004; Dohmann et al., 2010; Ariizumi et al., 2011)

It is currently unknown how the dominant germination cue switches from endogenous GA in autotrophic plants to exogenous SLs in parasitic plants. In fact, exogenous application of GA only stimulates weak *Striga* germination at high concentration (Toh et al., 2012). Nonetheless, GA-mediated autonomous germination should be suppressed in order to leave *Striga* seeds solely dependent on host-derived signals for germination. Intriguingly, *Arabidopsis* germination impaired by PAC can be rescued in seeds expressing *ShHTLs* in a SL-dependent manner (Bunsick et al. 2020). It thus appears that SL-*ShHTLs* pathway can bypass GA requirement for germination. Based on the current findings, there are a few possibilities of how *Striga* germination became SL-dependent: either GA is no longer required for *Striga* germination, or its role has become indirect. To evaluate these hypotheses, I investigated the role of GA in SL-dependent germination pathway in *Striga* by taking chemical genetic approaches as *Striga* mutant is currently not available.

1.2 Results

***Striga* seeds depleted of GA during conditioning showed reduced germination**

First, I confirmed if GA is required for germination of conditioned *Striga* seeds by testing the effect of GA biosynthesis inhibitor PAC on germination stimulated by a widely used synthetic SLs called GR24. I observed that even if high concentration of 100 μM PAC was used, *Striga* germination rate was only slightly reduced (Fig. 1A). Instead, the germinated seedlings showed shorter root phenotype in response to PAC treatment (Fig. S1A). These observations agreed with the previous report, that GA plays minimal role in *Striga* germination, but GA biosynthesis is important for root elongation (Bunsick et al., 2020). Consistently, another report also detected increased amount of bioactive GA₁ at 24 h after GR24 treatment, which corresponded to the timing after seed coat protrusion (Toh et al., 2012).

The observed results also raised other possibilities, for instance GA does not act downstream of SLs pathway or GA functions in other process to indirectly regulate germination. Indeed, GA₁ was shown to be readily accumulated in *Striga* after seed conditioning, suggesting that it might function during conditioning period (Toh et al., 2012). To test this hypothesis, I depleted *Striga* seeds of GA by adding PAC during conditioning and washed out PAC before inducing germination with GR24. Surprisingly, germination of PAC conditioned seeds was already severely impaired at 10 μM PAC (Fig. 1B). Notably, even though PAC was not included during germination, *Striga* seeds were still unable to germinate well. This suggested that GA plays a major role in seed conditioning instead of seed germination.

I also performed complementary experiments using another GA biosynthesis inhibitor called prohexadione-calcium (BX-112) that acts on the 2-OGD and has different target from PAC (Nakayama et al., 1990). Like PAC, *Striga* seeds conditioned with BX-112 also showed reduced germination whereas germination rate was not affected when it was simultaneously applied with GR24 but only the roots were shorter (Fig. S1B, S2). However, the inhibitory effect of BX-112 was a lot weaker as it required much higher concentration, perhaps because the target sites of this inhibitor are the enzymes that catalyze the last few steps of GA metabolism.

Besides *Striga*, the genus *Orobanche* from the same family contains obligate parasitic plant species that also requires host-derived SLs for germination. Therefore, I investigated if the role of GA in seed conditioning is conserved in other parasitic plants by performing the same experiments using PAC to test for its effect on seeds of *Orobanche minor*. Similar results were obtained, except high PAC concentration could also reduce germination of *O. minor* when co-applied with GR24, but seeds conditioned with PAC had greater germination impairment at lower concentration (Fig. 1C, D). Collectively, it is strongly evident that GA functions more importantly in seed conditioning rather than seed germination of parasitic plants.

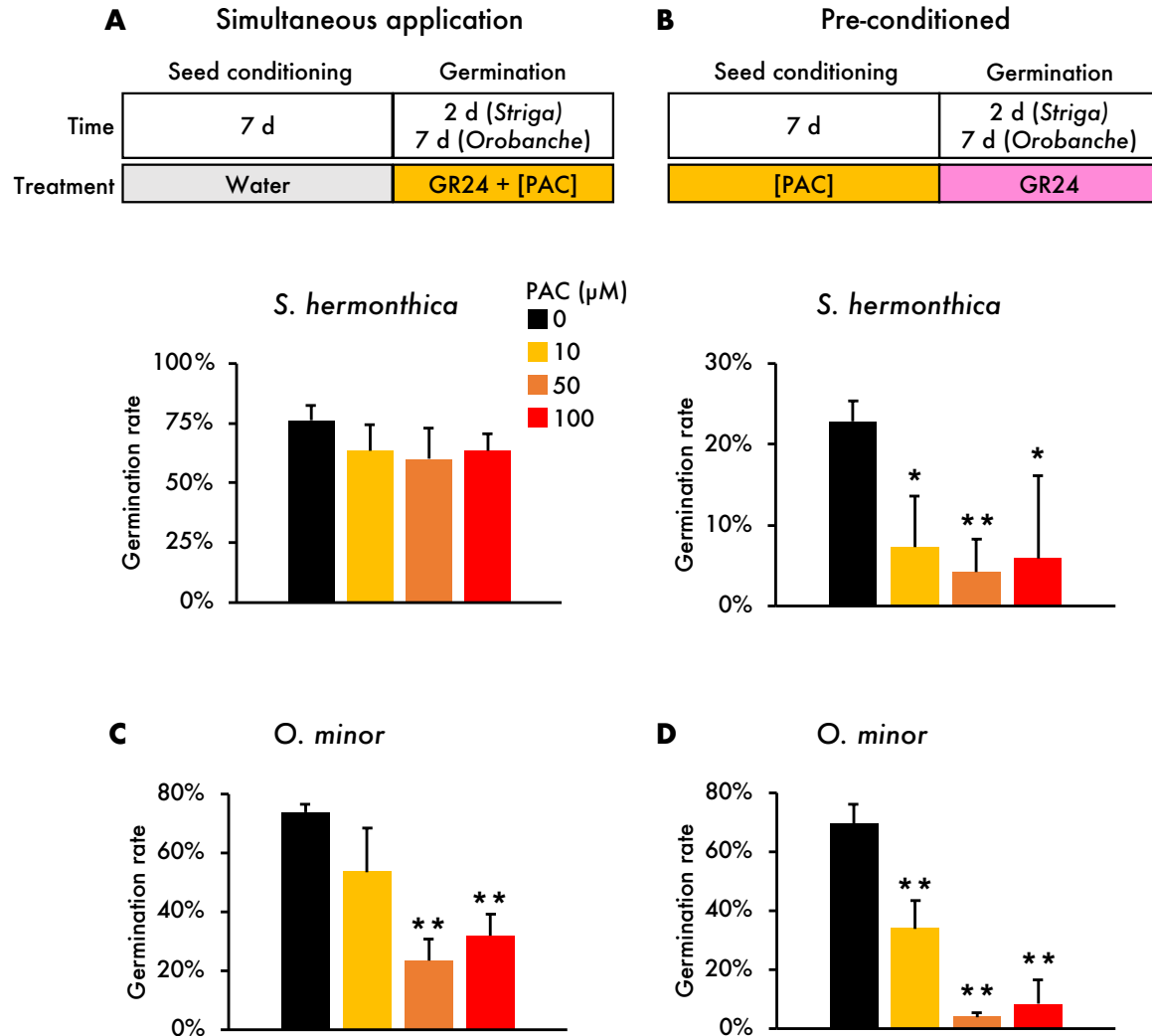


Figure 1 Timeline and effect of PAC treatment during seed germination or conditioning of *S. hermonthica* and *O. minor*. (A) *Striga* seeds were conditioned in water for 7 d and induced germination with GR24 and increasing concentrations of PAC. (B) *Striga* seeds were conditioned in PAC for 7 d, washed with water to remove PAC, and induced germination with GR24. Germination of *Striga* was counted after 2 d. (C) *O. minor* seeds were conditioned in water for 7d and treated with GR24 and PAC simultaneously, or (D) conditioned in PAC for 7 d and washed out before inducing germination with GR24. Germination of *O. minor* was counted after 7 d. 10 μM , 50 μM or 100 μM PAC was used and germination was induced with 0.1 μM GR24 and counted as radicle emergence. 0.1 % DMSO was used as control. Error bars represent SD (n = 3). Asterisks indicate significant differences compared to DMSO control (Student's *t*-test, * p < 0.05, ** p < 0.01). Brackets highlighted changing in PAC concentrations.

Exogenous GA rescued PAC inhibition during conditioning

I focused my studies on *Striga* hereafter and tested if the inhibitory effect of PAC on seed conditioning is reversible by exogenous GA application. Likewise, I treated *Striga* seeds with GA₃, one of the bioactive GA, together with or without 10 μM PAC during conditioning. The ligands were then washed out before stimulating germination with GR24. As anticipated, increasing concentrations of GA₃ gradually alleviated PAC suppression and 100 nM GA₃ was sufficient to restore germination rate back to DMSO control level (Fig. 2A). Hence, inhibition by PAC was most likely due to reduced endogenous GA level. On the other hand, I took an alternate approach to add GA₃ and GR24 simultaneously after seeds were conditioned with PAC. However, GA rescue was less efficient in this case as hundred-fold higher dose of 10 μM GA₃ was required to reach similar germination rate with DMSO only control (Fig. S3). Therefore, exogenous GA application that works more effectively during conditioning stage agrees with the promotive role of GA in seed conditioning. Besides, I also repeatedly observed that when *Striga* seeds were conditioned with high concentrations of 1 μM GA₃ and above, a few seeds germinated without SLs during conditioning, suggesting that high amount of exogenous GA could also weakly induce germination of unconditioned seeds as reported for conditioned seeds (Toh et al., 2012; Bunsick et al., 2020).

In addition to rescue experiments, transcript levels of GA metabolic genes during conditioning were also investigated, since regulation of these genes, especially *GA 20-oxidases*, *GA 3-oxidases* and *GA 2-oxidases*, were demonstrated to be important for maintaining bioactive GA level in *Arabidopsis* germination where GA plays a vital role (Yamaguchi, 2008). Firstly, BLAST search was performed against recently published genome sequence of *S. hermonthica* to identify the homologs of these genes (Fig. S4A; Qiu et al., 2022). Next, I focused on *Striga* homologs that are classified in the same clade as *AtGA20ox3*, *AtGA3ox1* and *AtGA2ox2* that participate in *Arabidopsis* germination process, and quantified their mRNA expression level during seed conditioning. In strong agreement with the findings thus far, up-regulation of two GA biosynthetic genes, *ShGA20ox1* and *ShGA3ox1*, were detected during conditioning of *Striga* seeds whereas a GA catabolic gene, *ShGA2ox1* was down-regulated (Fig. 2B). Moreover, the genes encoding GA core signaling components were also conserved in *Striga* (Fig. S4B-D). Altogether, the results strongly suggested that GA accumulates during seed conditioning and positively regulates this process in *Striga*.

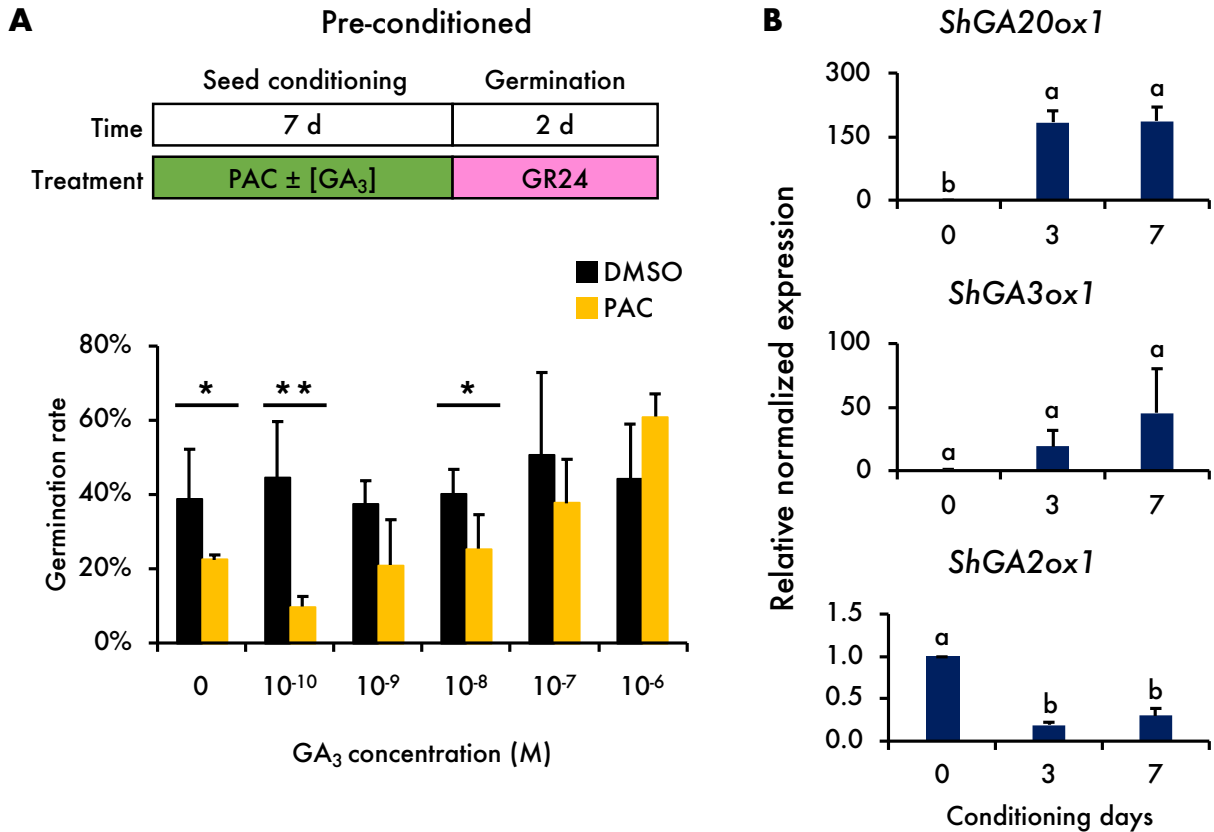


Figure 2 Promotion of seed conditioning by GA. (A) Timeline and effect of exogenous GA application in alleviating PAC inhibition on seed conditioning. *Striga* seeds were conditioned for 7 d in increasing concentration of GA₃ ranging from 100 pM to 1 μM together with or without 10 μM PAC. After conditioning, PAC and GA₃ were washed out by water. Germination was then stimulated with 0.1 μM of GR24 and germination rate was calculated after 2 d. 0.1 % DMSO was used as control. Error bars represent SD (n = 3). Asterisks indicate significant differences compared to DMSO control (Student's *t*-test, **p* < 0.1, ***p* < 0.05). Brackets highlighted changing in GA₃ concentrations. (B) Changes in expression level of GA metabolic genes during conditioning. Expression of GA biosynthetic genes (*ShGA20ox1* and *ShGA3ox1*) and GA catabolic gene (*ShGA2ox1*) of *Striga* seeds before (0 d) and after 3 d and 7 d conditioning in water was shown as relative value to 0 d. *ShUBQ1* was used as the internal control. Data represents the mean from three independent samples and error bars represent SD. Letters indicate the significance differences by one-way ANOVA with post-hoc Tukey HSD test (*p* < 0.05).

PAC decreased the sensitivity of *Striga* seeds towards SLs

Since the biological significance of seed conditioning is to prompt the *Striga* seeds to become extremely responsive to germination signals in which they become capable of sensing picomolar range of SLs released from the host root to germinate, I then examined if GA has influence on the sensitivity of *Striga* seeds toward SLs. To test this, the seeds were conditioned with PAC or GA₃ or both and triggered germination by increasing range of GR24. In contrast to DMSO control that progressively germinated in a dose dependent manner, PAC treated seeds started to germinate at ten-fold higher concentration of GR24, which indicated that sensitivity towards SLs was reduced (Fig. 3). Also, these seeds constantly exhibited low germination rates and were not rescued by high concentration of GR24, suggesting that components in the SL signaling pathway might become the limiting factors when GA is depleted. Nevertheless, sensitivity towards SLs could also be restored by exogenous GA application (Fig. 3).

Notably, after the seeds were conditioned with GA₃, they became slightly more responsive to germination stimulants as shown by slightly higher germination rates compared to DMSO at picomolar concentrations of GR24 (Fig. 3). Albeit germination rates were not significantly different, extra GA₃ seemed to be able to further enhance the competence of *Striga* towards host signals. However, this observation contradicted with a previous report that noticed a decrease in *Striga* germination after the seeds were conditioned with GA₃ (Mallu et al., 2022), and the difference could possibly be due to different treatment methods or concentration of ligands used.

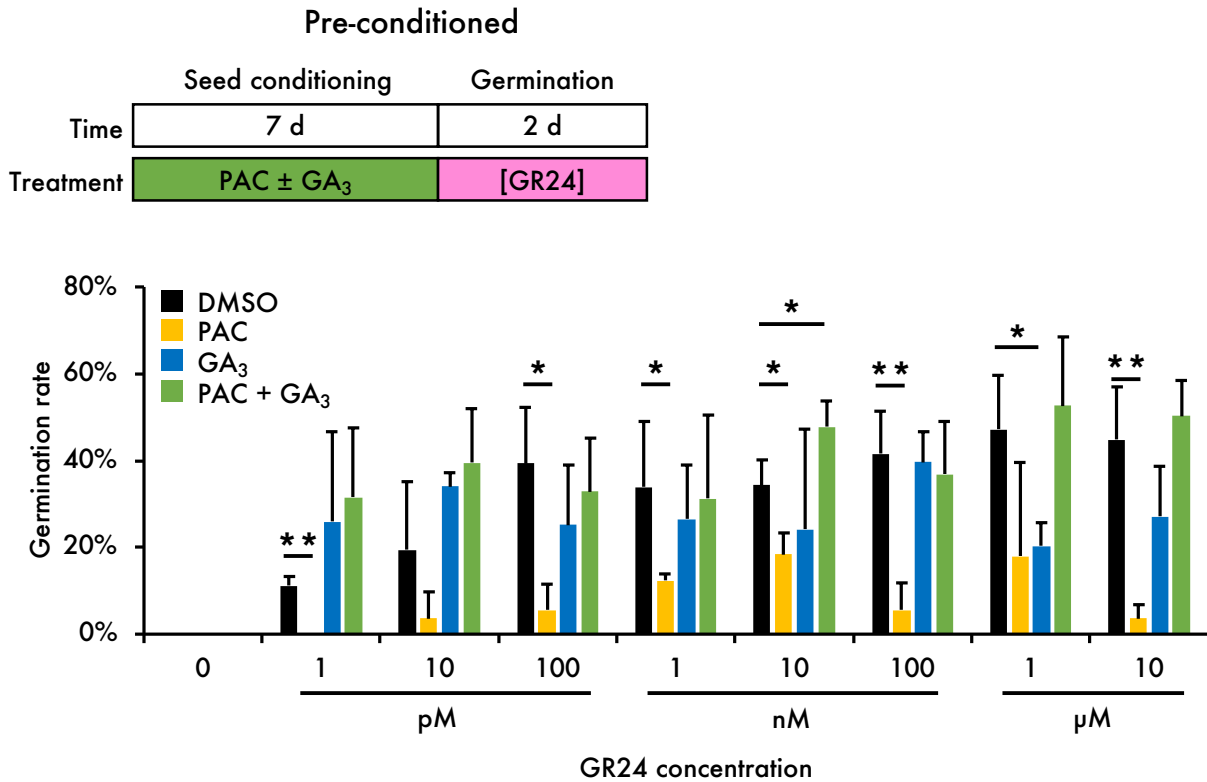


Figure 3 Effect of GA on sensitivity of *Striga* seeds towards SLs. *Striga* seeds were conditioned for 7 d in 10 μM PAC, 100 nM GA₃ or 10 μM PAC + 100 nM GA₃. PAC and GA₃ were removed after conditioning and germination were stimulated with GR24 ranging from 1 pM to 10 μM . Germination rate was counted after 2 d. 0.1 % DMSO was used as control. Error bars represent SD (n = 3). Asterisks indicate significant differences compared to DMSO control (Student's *t*-test, * $p < 0.05$, ** $p < 0.01$). Brackets highlighted changing in GR24 concentrations.

GA deficit seeds displayed low expression of *ShHTL* genes

In an attempt to clarify the limiting factors in SL signaling pathway for germination of GA deficit seeds, I first focused on the core signaling components of SLs. One possible candidate is the SL receptors, since they are crucial to *Striga* germination and the expressions of most *ShHTLs* are up-regulated during conditioning (Tsuchiya et al., 2015). Moreover, a recent study using a ShHTL antagonist revealed that it impinged on *Striga* germination most greatly when added during seed conditioning, suggesting that ShHTLs might also have unknown function in the conditioning stage (Arellano-Saab et al., 2022). Thus, I decided to check the expression levels of these genes after the seeds were conditioned with PAC or GA₃ or both.

In line with my speculation, transcript levels of most *ShHTLs*, especially *ShHTLs 4-9* that are important for germination, were greatly reduced in PAC conditioned seeds (Fig. 4A). This implied that GA mediates the up-regulation of *ShHTLs* during conditioning to indirectly contribute to *Striga* germination, and when GA is depleted by PAC, low level of ShHTLs are likely responsible for germination defects. Interestingly, it was previously shown that PAC treatment also decreased the expression of *AtHTL* during seed imbibition of *Arabidopsis*, suggesting a conserved role of GA in modulating expression of *HTL* genes in both parasitic and non-parasitic plants (Bunsick et al., 2020). However, additional GA₃ did not further up-regulate the expression of *ShHTLs* despite it increased the sensitivity of seeds towards SLs. Also, even though GA₃ could alleviate the effect of PAC as shown by relatively higher transcript amount of most *ShHTLs* in seeds conditioned with PAC + GA₃ compared to PAC alone, the expressions did not reach back to DMSO control level yet germination rate was fully restored under the same treatment (Fig. 3, 4A). Therefore, GA likely also regulates other genes to assist *Striga* germination process.

On the other hand, opposite expression patterns of *ShHTL2* and *ShHTL3* were noticed. These genes were previously shown to be mainly expressed in unconditioned seeds and gradually down-regulated after conditioning (Tsuchiya et al., 2015). Hence, the higher expression level of these two genes observed in PAC conditioned seeds was more likely due to hampered down-regulation rather than a differential up-regulation of the genes (Fig. 4A). Although ShHTL2 and ShHTL3 are not considered to be the key SL receptors for germination based on the results from

cross-complementation assay in *Arabidopsis*, they could instead have function during seed conditioning that remain uncovered.

I also checked the expression level of GA metabolic genes in the same set of seeds. Interestingly, expression of the GA biosynthetic genes was higher in PAC conditioned seeds but was lower when GA was present, indicating that these genes might be subjected to negative feedback regulation by GA to maintain the optimal level of bioactive hormone (Fig. 4B).

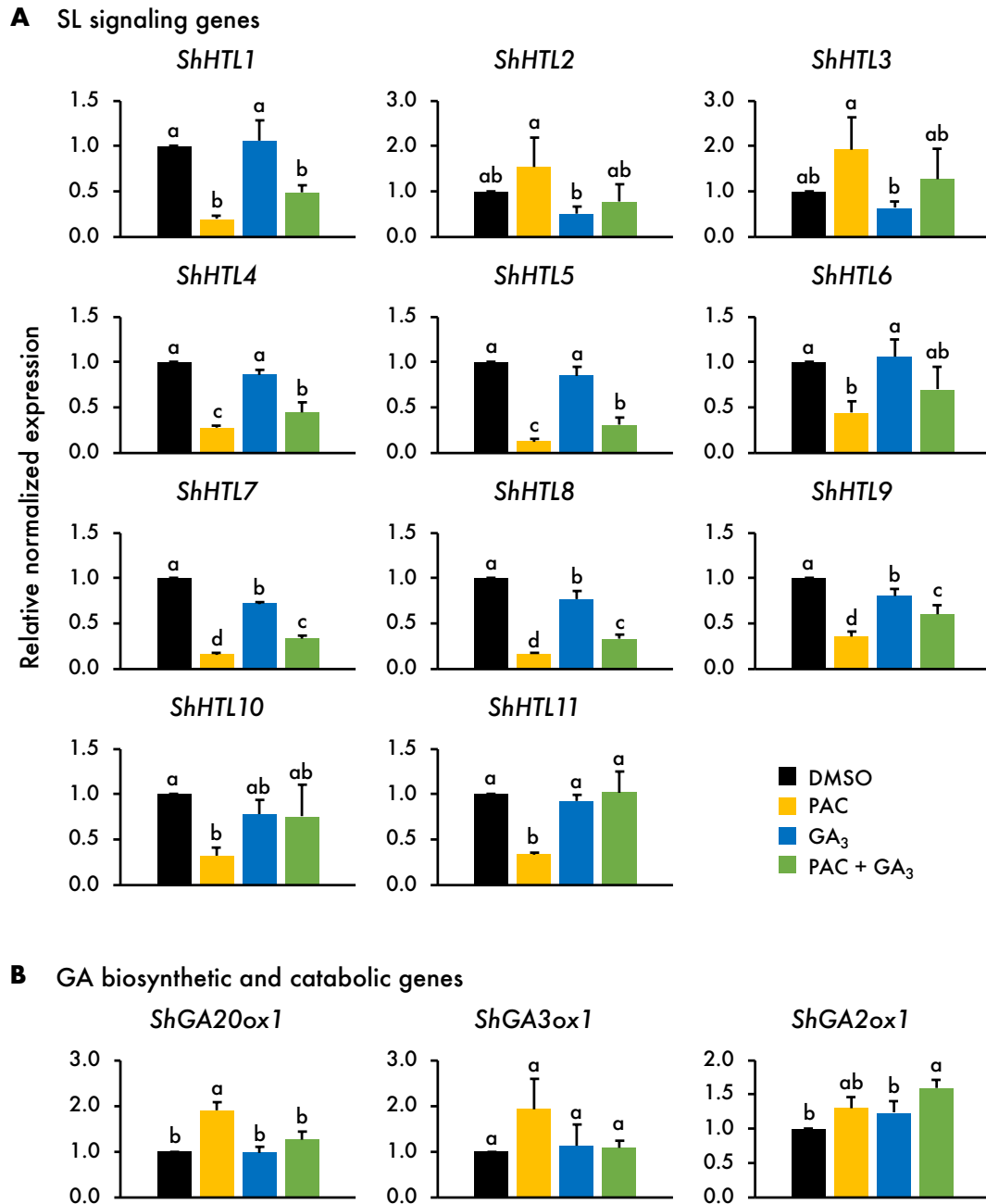


Figure 4 Effect of GA on SL signaling and GA metabolic components. Expression of (A) SL receptor genes (*ShHTL1* to *ShHTL11*) or (B) GA biosynthetic (*ShGA20ox1* and *ShGA3ox1*) and catabolic (*ShGA2ox1*) genes of *Striga* seeds after 7 d conditioning in 10 μ M PAC, 100 nM GA₃ or 10 μ M PAC + 100 nM GA₃ was shown as relative value to 0.1% DMSO control. *Sh18SrRNA* was used as the internal control for (A) and *ShUBQ1* was used for (B). Data represents the mean from three independent samples and error bars represent SD. Letters indicate the significance differences by one-way ANOVA with post-hoc Tukey HSD test ($p < 0.05$).

Lack of GA reduced and delayed SL perception during germination

To investigate if GA deficiency would also affect the dynamics of SL perception in *Striga* germination that exhibits a unique three-step process as probed by fluorogenic SL mimic, YLGW introduced above (Tsuchiya et al., 2015), embryos of seeds conditioned with PAC or GA₃ were treated with YLGW to stimulate germination and YLGW-derived fluorescent pattern was recorded (Fig. 5, S5, S6B-D, S7). Firstly, germination rate of PAC treated embryos was still lower when the seed coats were removed (Fig. S6A). Secondly, fluorescence intensities of PAC treated embryos in both wave-up wave and elongation tide were reduced, which is consistent with the low expression level of *ShHTLs* (Fig. 4A, 5B, 6B, D, E). Intriguingly, the appearance of wake-up wave was also delayed and elongated but pre-germination pause duration was not varied, which eventually leads to later initiation of elongation tide as well as root elongation time (Fig. 6F-I, S8). Furthermore, the root elongation rate seemed impeded and percentage elongation at 48 h was lower (Fig. 6J). Altogether, these observations inferred that GA possibly also regulate other factors that are required for proper propagation of the SL signal perception as well as cell elongation. This hypothesis is subsequently supported by the fluorescence pattern visualized in GA₃ conditioned embryos which in overall perceived wake-up wave earlier and the embryos tend to start elongating slightly amidst wake-up wave propagation (Fig. 6C, F, I).

Next, I wondered if the above-mentioned observation would reflect on faster seed coat protrusions in germinating seeds and tracked the radicle emergence of seeds conditioned with PAC or GA₃ every 12 h under two conditions: germination stimulated by GR24 at 30 °C or by YLGW at 25 °C, which respectively represents the general condition for germination assay and time-lapse imaging. Firstly, I observed that radicle emergence proceeded faster when seeds were germinated under optimum temperature of 30 °C (Fig. S9A, B). PAC conditioned seeds consistently germinated slower under 30 °C or were unable to germinate at 25 °C. However, differed from original anticipation, GA shared a similar emergence velocity with DMSO, perhaps because the observed initial elongation that preceded in embryos conditioned with GA₃ was insufficient to efficiently break through the seed coats until it was accelerated during the elongation tide.

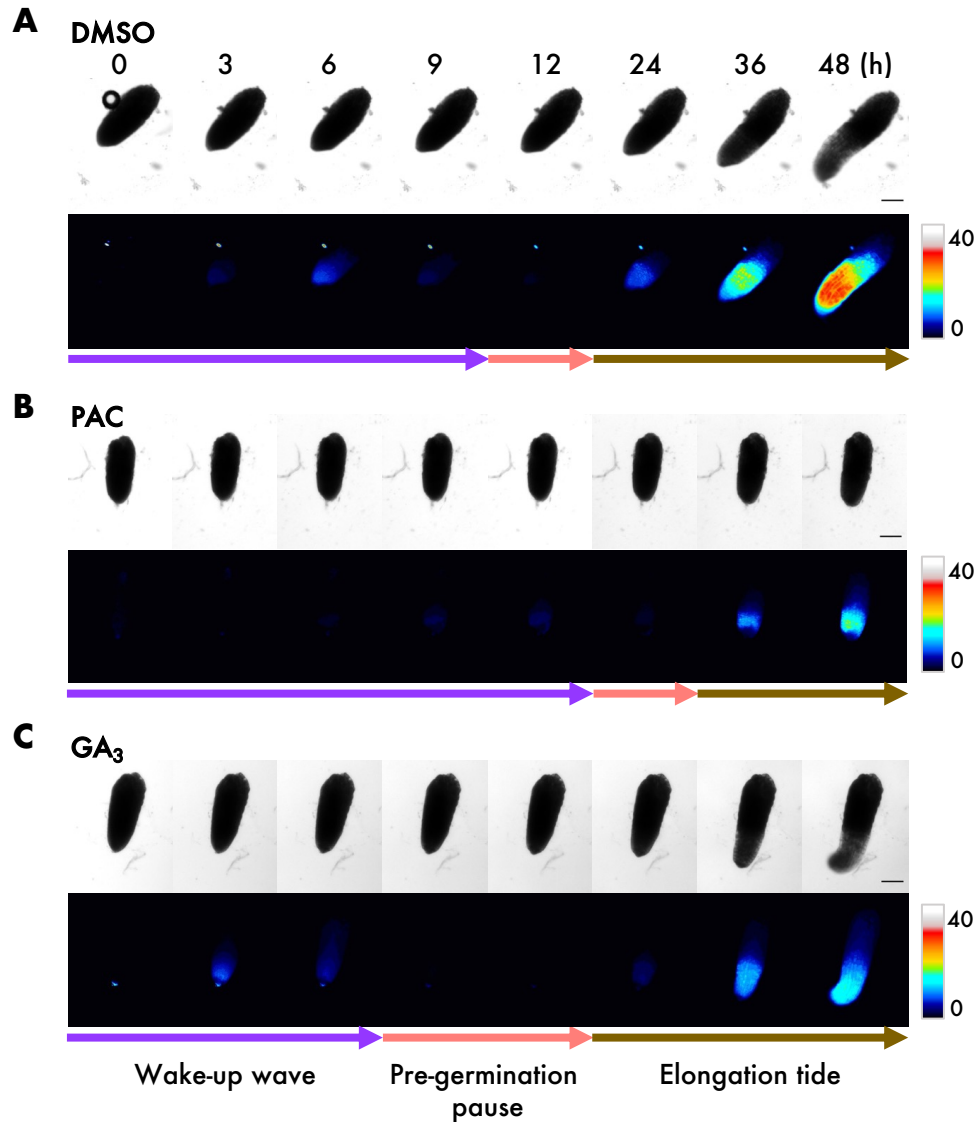


Figure 5 Time-lapse images showing GA affected on the dynamics of SL perception during *Striga* germination. Images of representative germinating *Striga* embryos that were conditioned for 10 d in (A) 0.1 % DMSO control, (B) 10 μ M PAC, or (C) 100 nM GA₃. PAC and GA₃ were removed by washing with water before dissecting the seed coats. Selected germination time point after 10 μ M YLW application were presented and the fluorescence of wake-up wave (purple arrow), pre-germination pause (pink arrow) and elongation tide (brown) in respective treatments were shown as a heatmap. Look-up table indicating grey value was shown on right.

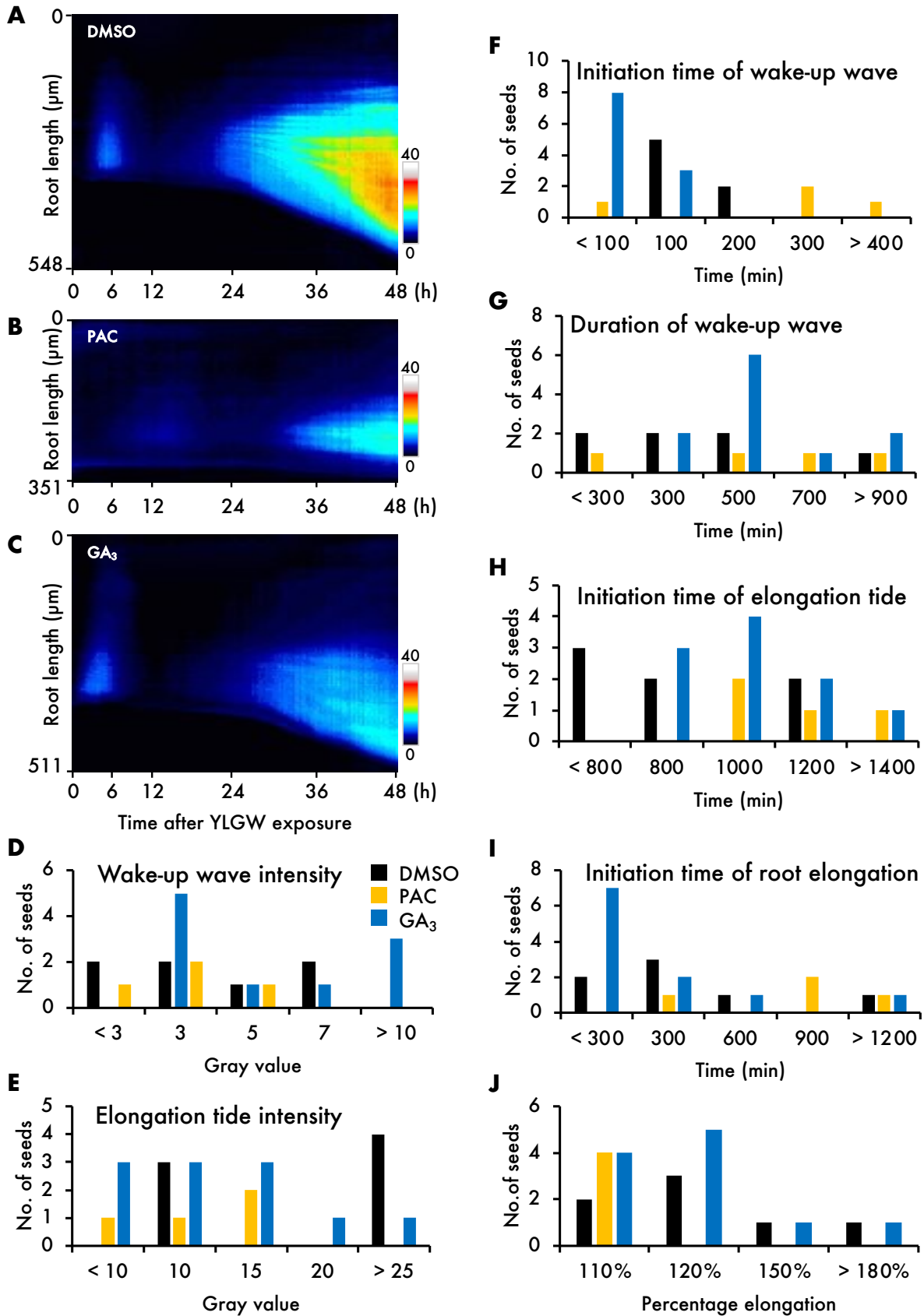


Figure 6 Quantitative analysis on the changes in YLGW fluorescence pattern in representative *Striga* embryos conditioned in either (A) DMSO or (B) 10 μ M PAC or (C) 100 nM GA₃. Kymographs were generated from the fluorescence produced by YLGW hydrolysis and presented as heatmaps, where x-axis represents time after 10 μ M YLGW application and y-axis represents root elongation. Look-up table indicating grey value was shown on right. (D) Maximum fluorescence intensities of the wake-up wave and (E) elongation tide were scored as gray value. (F) Initiation time and (G) total duration of wake-up wave as well as (H) initiation time of elongation tide were also calculated. (I) Root elongation initiation time represented the time when *Striga* embryo started to elongate. (J) Lengths of each embryo at 48 h were compared to 0 h and presented as percentage elongation.

GA promotes conditioning at sub-optimal temperature

Finally, to further strengthen the findings, I evaluated if exogenous GA application could promote seed conditioning. When *Striga* seeds were conditioned at optimal temperature of 30 °C, seeds treated with 10 µM GA₃ required only 3 days to reach a similar germination rate as the DMSO control seeds on day 7. This suggested exogenous GA could potentially shorten the conditioning period (Fig. 7).

Alternatively, the seeds were challenged under sub-optimal conditioning temperatures of 25 °C and 15 °C, which usually leads to extended conditioning period for SL-induced germination rate to saturate. Under these conditions, GA₃ exposure generally helped the seeds to germinate better in a concentration dependent manner, implying that exogenous GA could also enhance conditioning under sub-optimal conditions.

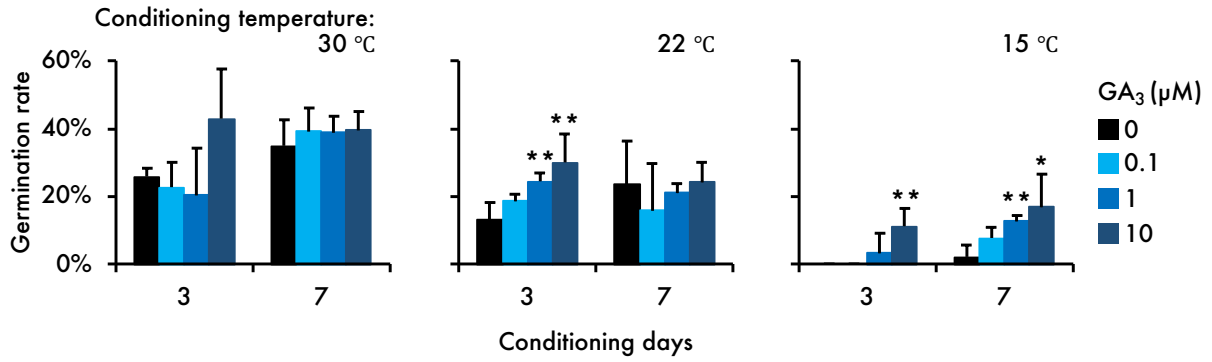


Figure 7 Effect of GA on seed conditioning at sub-optimal temperature. *Striga* seeds were conditioned at 30 °C, 22 °C or 15 °C in dark with increasing concentrations of GA₃. After 3 d or 7 d of conditioning, seeds were washed and treated with 0.1 μM GR24 to induce germination at 30 °C. Germination was counted after 2 d. Error bars represent SD (n = 3). Asterisks indicate significant differences compared to DMSO control (Student's *t*-test, **p* < 0.1, ***p* < 0.05).

1.3 Discussion

GA is well established as the dominant promoter of seed germination in many plant species, but not in the case of obligate parasitic plants like *Striga* that are dependent on host-derived SLs for germination. In contrast to recent extensive studies on the SL pathway, the role of GA in *Striga* is not well characterized perhaps because GA was thought to play a minor role in *Striga* germination and that placed it away from the research interest that mainly focuses on development of suicidal germination tools for *Striga* control. In this chapter, I performed a *Striga*-based study to elucidate that GA function is still required, but the role has become indirect in seed germination of *Striga*. Instead, results from this study consistently reinforced the positive role of GA in regulating seed conditioning of parasitic plants like *Striga*. Indeed, a few early studies on *Orobanchae* species already suggested that GA biosynthesis is required for seed conditioning (Takeuchi et al., 1995; Zehhar et al., 2002; Song et al. 2005), but the detail mechanism, for instance how it impacted on SL-induced germination was not further investigated.

During seed imbibition of *Arabidopsis*, GA functions as the dominant regulator to integrate environmental signals such as light and temperature to directly promote germination, and is required to up-regulate expression of *AtHTL* (Bunsick et al., 2020). However, *AtHTL* pathway plays a minor role under normal germination conditions and GA pathway continues to stimulate germination autonomously. Whereas in *Striga*, GA is still required to sense environmental conditions such as warm temperature and moisture, and has a conserved role to stimulate the expression of *ShHTLs* during conditioning. Yet, a sharp distinction is that the endogenous GA accumulated during conditioning is unable to directly stimulate *Striga* germination, which redirects germination to solely depend on *ShHTLs* that now become the dominant pathway to elicit host-dependent germination. In slight contrast to the bypass model previously proposed by Bunsick et al., findings from this study proposed a detour model to explain how the dominant role of GA in seed germination has switched to environmental SLs in parasitic plant *Striga* (Fig. 8). The major difference lies on the proposal that the indirect regulation of GA on HTL-mediated pathway, that is usually masked by direct GA dominant pathway in germination of non-parasitic plants, has become prominent in seed conditioning of parasitic plants.

Nevertheless, the loss-of-function of GA in directly regulating germination in *Striga* should not arise from insensitivity of GA, as the core signaling components are conserved and exogenous GA₃ could rescue PAC suppression. One possibility could be mutation of a repressor functioning downstream of direct GA pathway that leads to constitutive suppression of that pathway in *Striga*. Another possibility could arise from the DELLA repressors that mediate different subsets of GA responses, for instance *RGL2*, but not *GAI* and *RGA*, play major role in regulating seed germination (Lee et al., 2002). In this regard, *RGL2* should regulate the direct pathway whereas other DELLA proteins might act on the indirect pathway. Interestingly, the homologs in *Striga* carry mutated DELFA or DEHFA motif instead of the conserved DELLA motif that is important for GA-induced degradation in most plants species (Dill et al., 2011), which might lead to a different function mediated by these repressors. Alternatively, the indirect pathway might be regulated in a DELLA-independent manner, which recent studies in *Arabidopsis* showed that some GA-regulated genes were not regulated by DELLA proteins (Ito et al., 2018).

Besides the expression of *ShHTLs*, there must be other important genes that are also regulated by GA as suggested from the results of GA₃ rescue experiments where germination can be fully restored whereas *ShHTLs* expressions were not, as well as the effect of PAC treatment on SL perception dynamics that could not be explain from low *ShHTLs* expressions alone. One example could be the ethylene biosynthesis genes, since they were previously shown to be either accumulated during conditioning or up-regulated by SL pathway during germination, and ethylene was thought to be required to amplify the propagating signals during SL perception (Sugimoto et al., 2003; Tsuchiya et al., 2015). Meanwhile, it is also intriguing that exogenous application of GA₃ that supposedly mis-express *ShHTLs* in the *Striga* seeds still retain the three-step germination pattern, indicating that localization of SL receptors is tightly regulated for *Striga* germination and unlikely to be affected by endogenous GA because PAC treated seeds also showed the same direction of signal perception and propagation from the root tip.

On the other hand, although the results obtained consistently supported the finding of GA in promoting conditioning, this study that is based primarily on chemical approaches do have some major drawbacks, such as off-target of small-molecules. For instance, it is possible that PAC might target to P450 monooxygenases in other hormone pathway when high concentration was used in

Arabidopsis (Desta and Amare, 2021). In this context, conventional genetics approach would provide the most direct evidence, but it is still not applicable for *Striga* to date. In view of this, a facultative parasitic plant might be the best candidate to explore, since it specially adapted two germination modes that can either germinate and grow by itself or switch to depend on host under nutrient deficient condition.

Nevertheless, I considered this study to aid in solving *Striga* problem in the field from different perspectives. On one end, GA biosynthesis inhibitors such as PAC or BX-112 can be applied to *Striga* seeds in the soil during the conditioning period to prevent the seeds from germinating when host plants are around and eventually reduce *Striga* emergence. Since PAC and BX-112 are widely applied plant growth regulators in the field to usually improve crop yields (Desta and Amare, 2021), they can be used more readily than developing a new tool. However, many more aspects on this part should be evaluated, such as whether PAC inhibition is a long-term effect, or when will be the most effective timing for application during the conditioning timing in natural environment. On the other end, exogenous GA can be applied in conjunction with suicidal germination probe to further elevate the sensitivity of the seeds towards germination cues that should help to further deplete *Striga* seedbank. Yet bioactive GA is usually unstable and excess GA in field might incur growth effects on crop plants as well. Therefore, a solution to this could be to develop a potent *Striga*-specific GA analog. In anyways, I envisage that the findings from this study will stimulate new opportunities for development of more effective solutions to successfully eradicate *Striga* in the field.

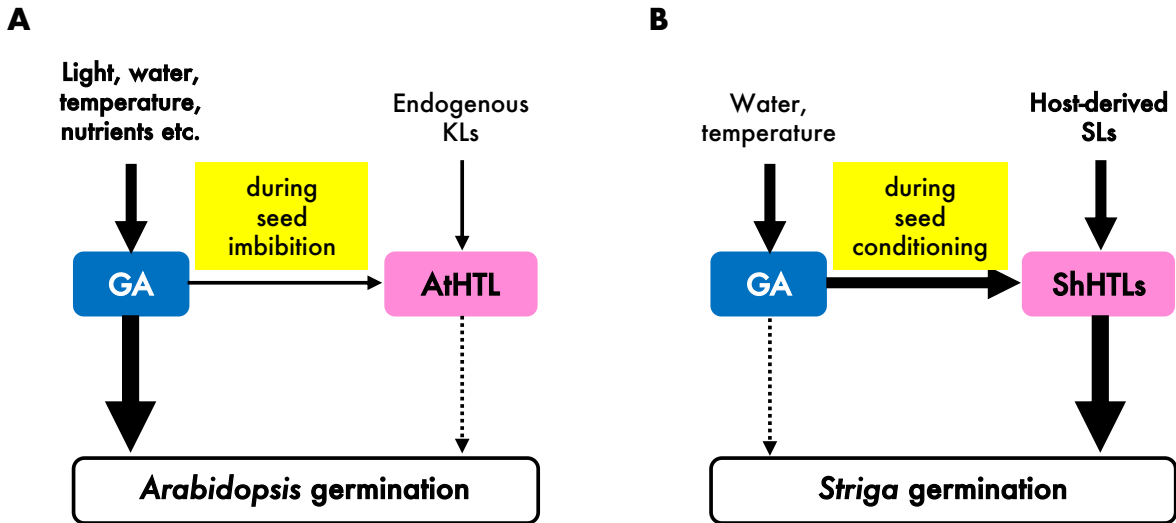


Figure 8 Proposed models for interaction between GA and *HTL* signaling pathways in non-parasitic and parasitic plants. (A) In non-parasitic plants like *Arabidopsis*, GA signaling pathway dominantly integrate environmental signals such as sufficient light and favorable temperature to promote seed germination. During the seed imbibition process, GA interacts with the HTL pathway by up-regulating the expression level of *AtHTL* where the receptor perceives unknown endogenous KAI2 ligand (KL) that play a minor role in stimulating *Arabidopsis* germination under normal condition. (B) In obligate parasitic plants like *S. hermonthica*, the role of GA to integrate surrounding signals such as moisture and temperature. The conserved positive regulation of *ShHTL* expressions promote the seed conditioning, but GA signaling lost its function to directly induce *Striga* germination. Instead, this indirect role of GA leads the predominant germination cues redirected to SLs released from the hosts that act through ShHTLs signaling pathway, by which *Striga* seeds only germinate when host plants, the major nutrient source for growth, are present.

1.4 Materials and Methods

Plant materials

Seeds of *Striga hermonthica* were collected from sorghum field in Gadarif, Sudan. Experiments using *S. hermonthica* seeds were performed under permission issued by the Japanese Ministry of Agriculture. Seeds of *Orobancha minor* were collected from Utsunomiya, Japan.

***Striga* seed conditioning**

Seed conditioning of *S. hermonthica* was as previously described (Toh et al. 2012). Briefly, seeds were surface-sterilized and sown on glass fiber filter paper (Whatman, GF/B 2.5 cm) in sterile 35 mm Petri dish, sealed with parafilm and incubated at 30 °C in dark until use. For conditioning with PAC, GA₃ or BX-112, seeds were incubated with the chemicals at indicated concentrations during the conditioning period. Before using for assays, PAC, GA₃ or BX-112 were removed by washing thoroughly with water.

***Striga* germination assay**

7 to 10 d conditioned seeds were used for germination assays which showed similar results and representative data of 7 d conditioned seeds were presented. All germination assays were performed in 96-well plates at 100 µL final volume in water and about 30 seeds per well. Racemic mixture of GR24 was used to induce *Striga* germination at indicated concentrations. Plates were incubated at 30 °C in dark for 2 days and germination was scored as radicle emergence. Germination rate was calculated from three replicates for each treatment. All chemicals were dissolved in DMSO except BX-112 was dissolved directly in water. DMSO was used as the control at a final concentration of < 1 %.

***Striga* root elongation**

After counting germination rate on day 2, images of each well were taken with stereo microscope equipped with camera (Zeiss Stemi 508). Root length of germinated *Striga* seedlings was calculated in Fiji software.

***Orobanche minor* seed conditioning and germination assay**

Seeds of *O. minor* were first washed with 70 % EtOH for 1 min, surface sterilized with 2 % bleach solution for 1.5 min and washed thoroughly with sterilized water. Seeds were resuspended in PAC or DMSO control solution and sowed on glass fiber filter paper in sterile 35 mm Petri dish, sealed with parafilm and conditioned at 22 °C in dark for 7 d. PAC was washed away before inducing germination with GR24 and germination assays were performed as described above for *Striga* except the plates were incubated at 22 °C in dark and germination rate was calculated after 7 d.

RT-qPCR analysis

Total RNA was extracted from 30 mg of *Striga* seeds using illustra RNAspin Mini (GE Healthcare). 500 ng of total RNA was used for reverse transcription using ReverTra Ace (Toyobo) according to the instructions provided by manufacturer. qPCR was performed using THUNDERBIRD SYBR qPCR Mix (Toyobo) and CFX Connect Real-Time PCR System (Bio-Rad). Primer sequences were listed in Supplementary Table 1. Expression levels of *ShGA20ox1*, *ShGA3ox1* and *ShGA2ox1* were normalized against *ShUBQ1* while *ShHTLs* against *Sh18SrRNA* internal control, and calculated with $2^{-\Delta\Delta Ct}$ method. Data were presented as relative expression to unconditioned seeds (Fig. 2B) or DMSO control (Fig. 4).

BLAST search analysis and construction of phylogenetic tree

Genome sequence of *Striga hermonthica* was downloaded from database (https://www.ncbi.nlm.nih.gov/assembly/GCA_902706635.1/) and local BLAST was performed using amino acid sequences of *Arabidopsis* homologs (AtGA20ox1, AtGA3ox1, AtGA2ox1, AtGID1, AtSLY1 and AtRGL2 respectively) as queries. Amino acid sequences from *S. hermonthica* was aligned with homologs in *Arabidopsis* (sequence obtained from <https://www.arabidopsis.org>) and rice (sequence obtained from <http://rice.uga.edu>) by ClustalW and phylogenetic trees were constructed by Maximum Likelihood method and a bootstrap analysis of 1000 replicates using default parameters in MEGA X software ver. 10.2.6.

YLGW time-lapse movies

Striga seed coats were removed with autoclaved toothpick under microscope. Dissected *Striga* embryos were placed on 200 μ L volume of 1% agarose gel with approximately 30 embryos per

sample per gel. The gel was placed upside-down on 35 mm glass bottom dish (Matsunami, glass 14mm ϕ , uncoated) and wet tissue was placed around the gel to keep it moist. 20 μ L of 10 μ M YLGW solution was added to the gel right before the movie started. Time-lapse images were taken in dark at 20 min interval for 48 h with Leica DMI8 inverted microscope.

Kymograph analysis

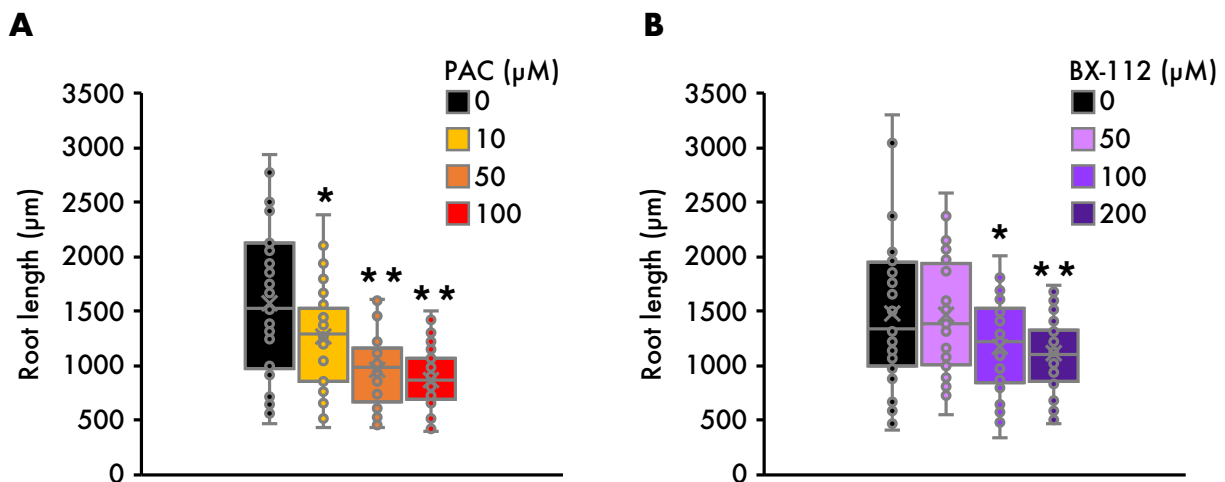
Time-lapse images were background subtracted and kymographs of each embryo were generated from time-lapse movie of YLGW fluorescence in Fiji software. Details of kymograph analysis were as previously described (Tsuchiya et al. 2015).

1.5 Supplementary Materials

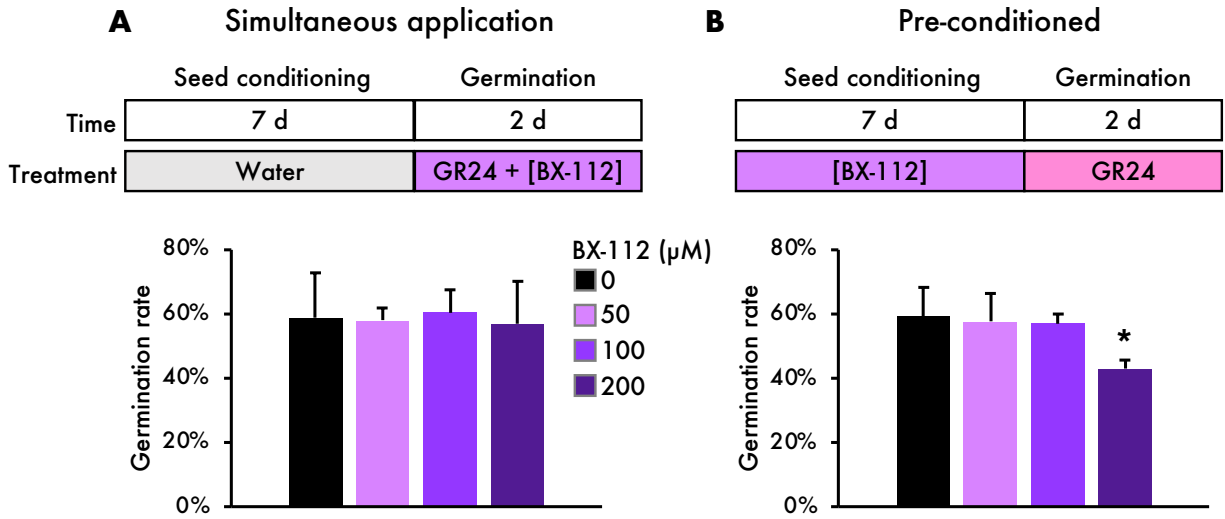
Supplementary Table 1: List of primers used for RT-qPCR.

Annotation	Name of primer	Sequence (5' to 3')	Reference
Internal control	Sh18SrRNA-qPCR-F	ACGCATGCATGTAAGTATGA	
	Sh18SrRNA-qPCR-R	CAAGGTTCAACTACGAGCTT	
SL signaling	ShHTL4-qPCR-F	AGATCAACCAAATGAACACT	Bunsick et al., 2020
	ShHTL4-qPCR-R	TGGAGATACTCAGCTACAG	
	ShHTL5-qPCR-F	AGCACAGTCGGGTCAGCA	
	ShHTL5-qPCR-R	CTCTCCATGGCACCGTA	
	ShHTL6-qPCR-F	ATGGGCACAGTCGGAGC	
	ShHTL6-qPCR-R	TTCCTCCATGGCGGCTTG	
	ShHTL7-qPCR-F	GCTCAATTGGATTAGCCCAT	
	ShHTL7-qPCR-R	TCCAAGGACCTCAGCGT	
	ShHTL8-qPCR-F	GATCTGCGCCGCTTTTAT	
	ShHTL8-qPCR-R	CTTGCTGAGGTACTION	
	ShHTL9-qPCR-F	ATGAGCACAGTTGGAGCA	This study.
	ShHTL9-qPCR-R	AGTAGTCTTTCGTGTTTCGAC	
	ShHTL1-qPCR-F	GTCCACAGACCGTAGTCCTG	
	ShHTL1-qPCR-R	CCCACATAAACGCACGAGCTT	
	ShHTL2-qPCR-F	TGGTGGACGACTATCGGGTC	
	ShHTL2-qPCR-R	GAGGATGAGGAGGAGGTCGCT	
	ShHTL3-qPCR-F	ATGAATAGAGTGGAGGCAGC	
	ShHTL3-qPCR-R	GGATGTAAACTCGTGGAG	
	ShHTL10-qPCR-F	CATGGTGTTCGACGCGAC	
	ShHTL10-qPCR-R	GGGTAGCGGAAATCATGATC	
GA biosynthetic	ShGA20ox1-qPCR-F	ACGACCACTCGTCCAGAAAC	
	ShGA20ox1-qPCR-R	CGTTGCGAGAGTAACCGTCT	

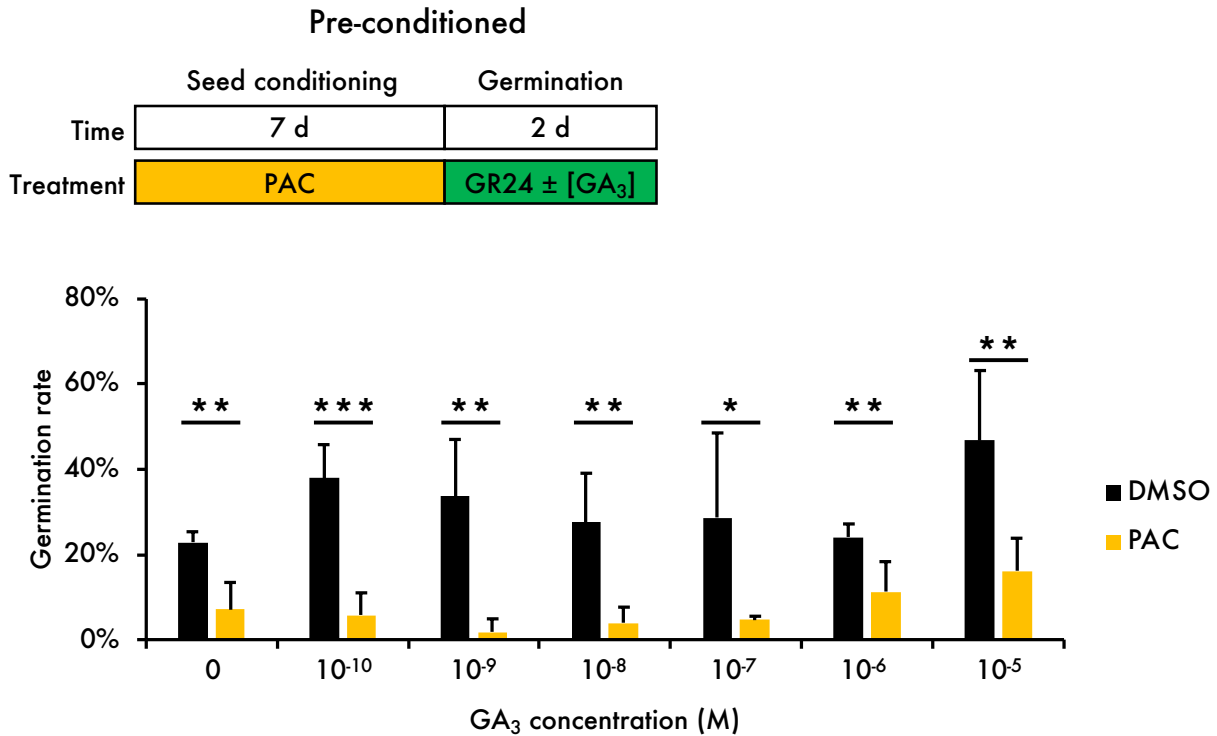
	ShGA3ox1-qPCR-F	GAACTACCCGACTCCCATGC	
	ShGA3ox1-qPCR-R	CATGACCGACTAGCCCGATT	
GA catabolic	ShGA2ox1-qPCR-F	GCCGCCAGAGAGTGAAAAGA	
	ShGA2ox1-qPCR-R	CCTATTGTCCCCAAGCCTCG	
Internal control	ShUBQ1-qPCR-F	CATCCAGAAAGAGTCGACTTTG	Fernández- Aparicio et al., 2013
	ShUBQ1-qPCR-R	CATAACATTTGCGGCAAATCA	



Supplementary Figure 1 Effect of GA biosynthetic inhibitors on the root elongation of germinating *Striga* seedlings. Root length was calculated from germinated *Striga* seedlings at day 2 after simultaneously treated with 0.1 μM GR24 and indicated concentrations of (A) PAC or (B) BX-112. 0.1 % DMSO or water was used as control for PAC or BX- 112 respectively. Asterisks indicate significant differences compared to control (Student's *t*-test, * $p < 0.05$, ** $p < 0.01$).

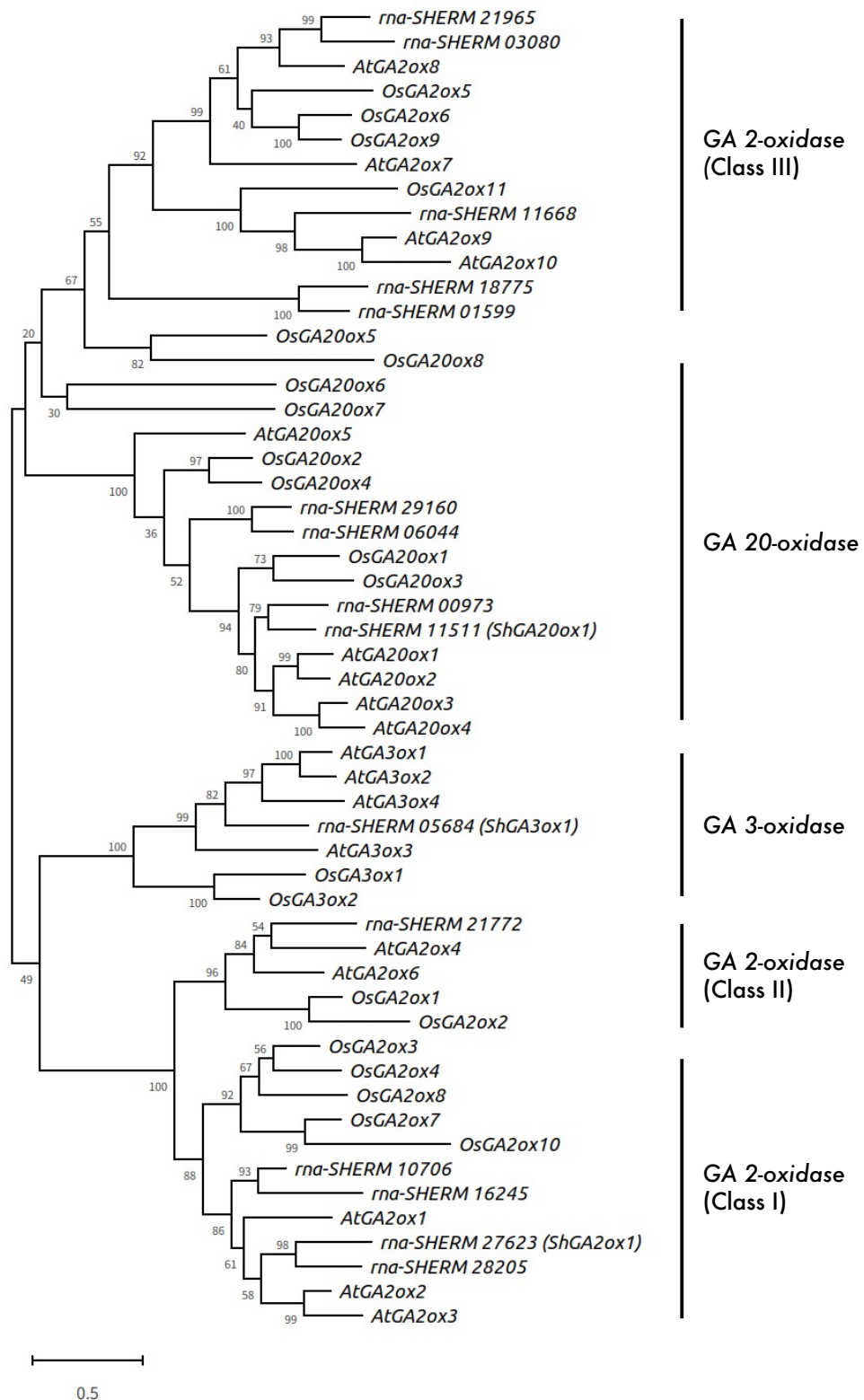


Supplementary Figure 2 Timeline and effect of BX-112 treatment during *Striga* seed germination or conditioning. (A) *Striga* seeds were conditioned in water for 7 d and induced germination with 0.1 μM GR24 and increasing concentration of 50 μM , 100 μM or 200 μM BX-112. (B) After 7 d of conditioning in BX-112, *Striga* seeds were washed with water and induced germination with GR24. Germination was counted after 2 d and scored as radicle emergence. BX-112 was directly dissolved in water and water was used as control. Error bars represent SD ($n = 3$). Asterisks indicate significant differences compared to water control (Student's t -test, $*p < 0.05$). Brackets highlighted changing in BX-112 concentrations.

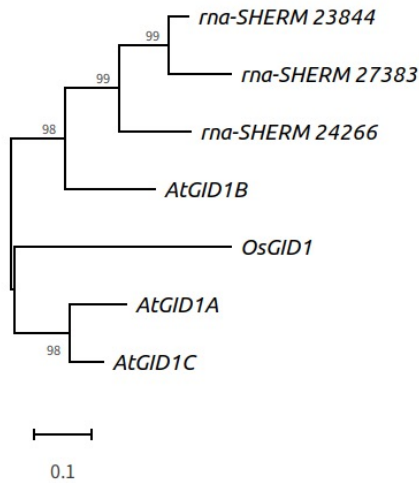


Supplementary Figure 3 Exogenous GA added simultaneously with GR24 was less effective in alleviating PAC inhibition on *Striga* seed conditioning. After 7 d conditioning in 0.1 % DMSO or 10 μ M PAC, PAC was removed by washing with water. Germination was then stimulated with 0.1 μ M of GR24 and increasing concentration of GA₃ ranging from 100 pM to 10 μ M. Germination rate was calculated after 2 d. Error bars represent SD (n = 3). Asterisks indicate significant differences compared to DMSO control (Student's *t*-test, **p*= 0.1, ***p*< 0.05, ****p*< 0.01). Brackets highlighted changing in GA₃ concentrations.

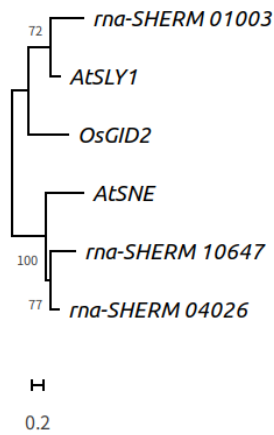
A. GA 20-, 3-, 2-oxidases



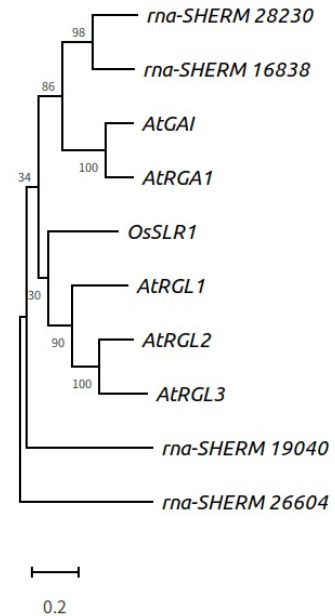
B. GA receptors



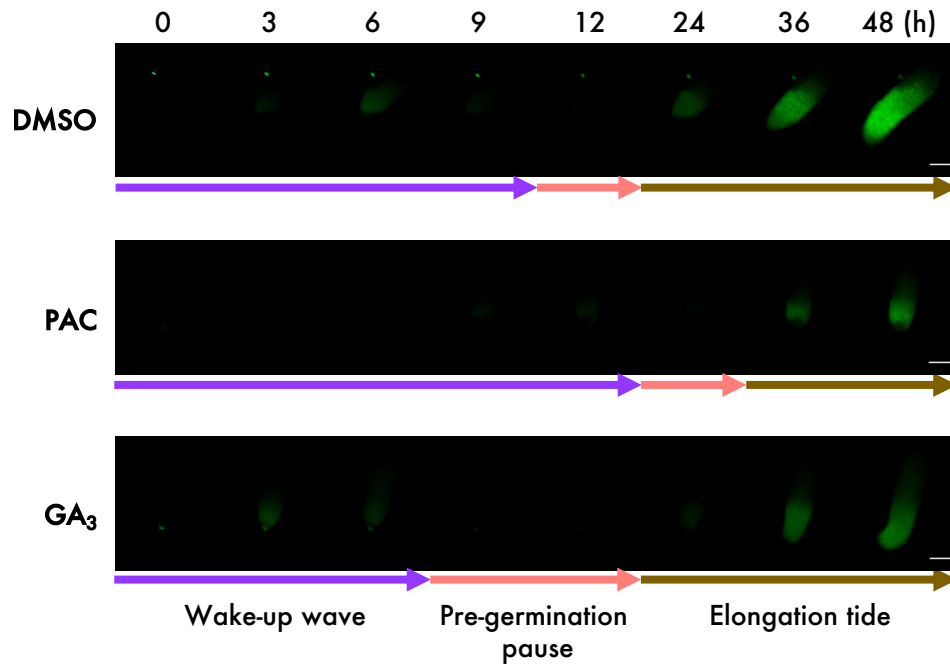
C. F-box protein



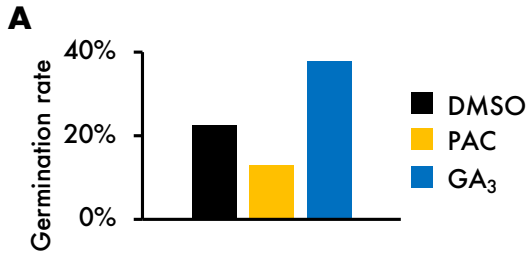
D. DELLA repressors



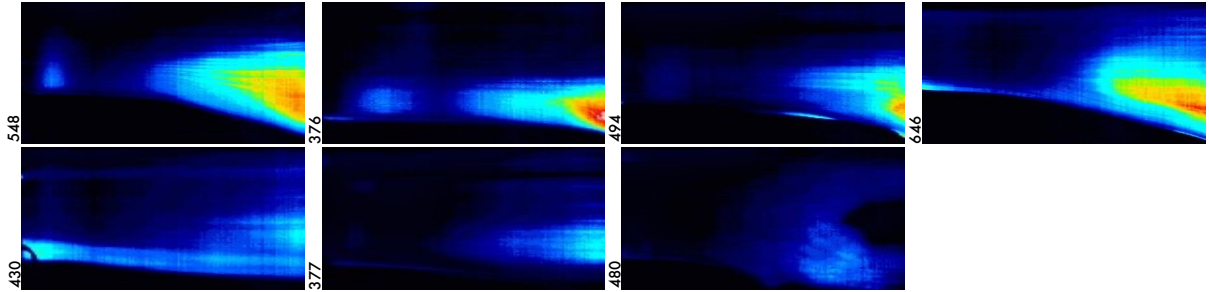
Supplementary Figure 4 Phylogenetic analysis of GA biosynthesis, catabolic and signaling genes in *S. hermonthica*. Phylogenetic trees of (A) GA 20-oxidases, GA 3-oxidases and GA 2-oxidases that regulate GA biosynthesis and catabolism. Two *GA 20-oxidases* (*ShGA20ox1* and *rna-SHERM 00973*), one *GA 3-oxidase* (*ShGA3ox1*) and two *GA 2-oxidases* (*ShGA2ox1* and *rna-SHERM 28205*) were closely related to *AtGA20ox3*, *AtGA3ox1* and *AtGA2ox2* respectively, but attempt to design primer pairs for gene expression analysis by RT-qPCR was only successful for *ShGA20ox1*, *ShGA3ox1* and *ShGA2ox1*, while another two genes showed multiple bands amplification in five primer sets targeting to different regions of the genes. (B) GA receptors, (C) F-box protein and (D) DELLA repressors that regulate GA signaling pathway were also conserved in *S. hermonthica*. Phylogenetic trees were built with amino acid sequences from *S. hermonthica*, *Arabidopsis* and rice.



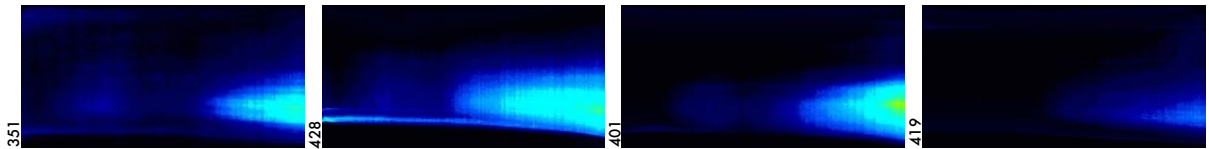
Supplementary Figure 5 Time-lapse movie images of green fluorescence produced from YLGW hydrolysis by ShHTL receptors in representative germinating *Striga* embryos in Fig. 5 that were conditioned for 10 d in 0.1 % DMSO control, 10 μ M PAC, or 100 nM GA₃. Arrows represent duration of three-step process during *Striga* germination: wake-up wave (purple), pre-germination pause (pink) and elongation tide (brown). Scale bar represents 100 μ m.



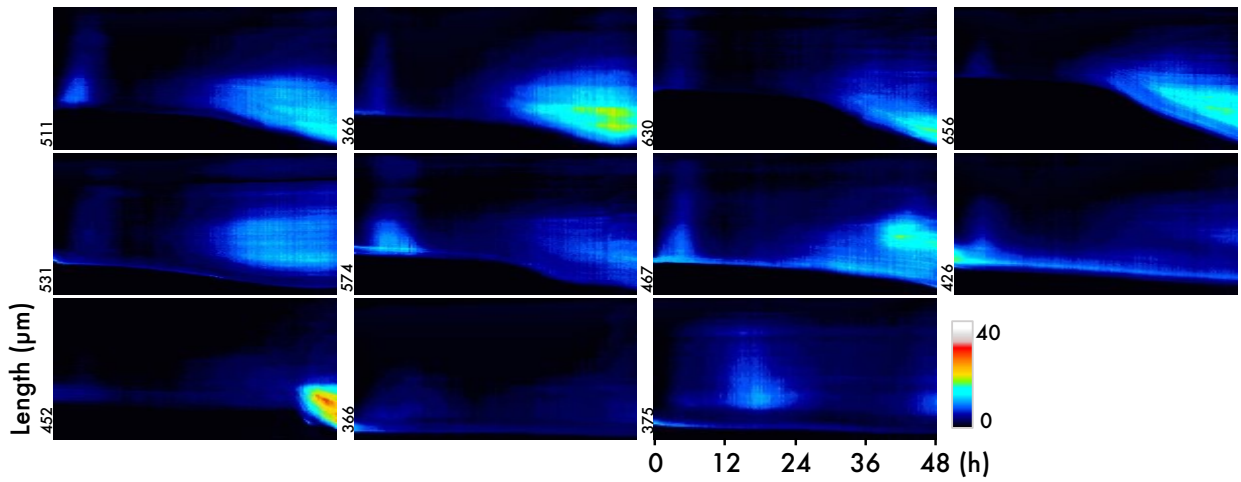
B Germinated seeds conditioned with DMSO



C Germinated seeds conditioned with PAC

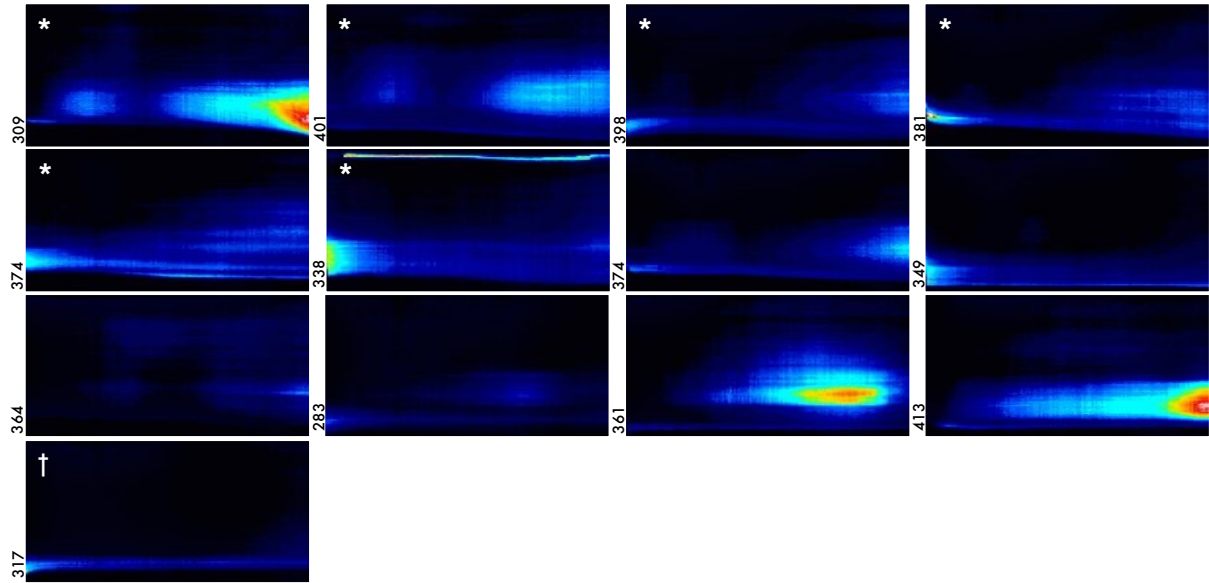


D Germinated seeds conditioned with GA₃

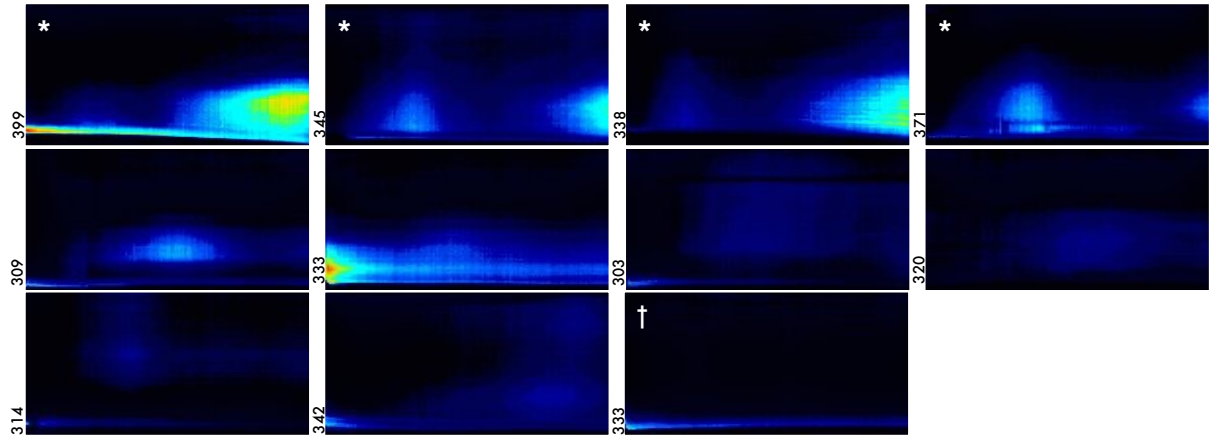


Supplementary Figure 6 (A) Germination rate of *Striga* embryos in YLGW time-lapse movies after conditioning with DMSO, 10 μ M PAC or 100 nM GA₃. Germination was scored as more than 10 % elongation at 48 h after 10 μ M YLGW application compared to 0h. Note that even with seed coats removed, PAC conditioned seeds still showed reduced germination whereas GA₃ treated seeds showed better germination than DMSO control. Kymographs of germinating embryos of seeds conditioned with (B) DMSO, (C) PAC and (D) GA₃. X-axis represents time after YLGW addition and y-axis represents root elongation. Look-up table indicating grey value was shown on right.

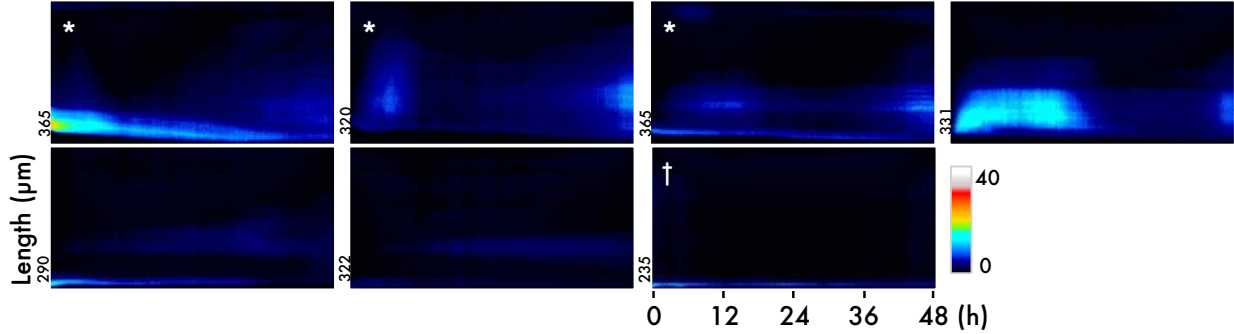
A Non-germinated seeds conditioned with DMSO



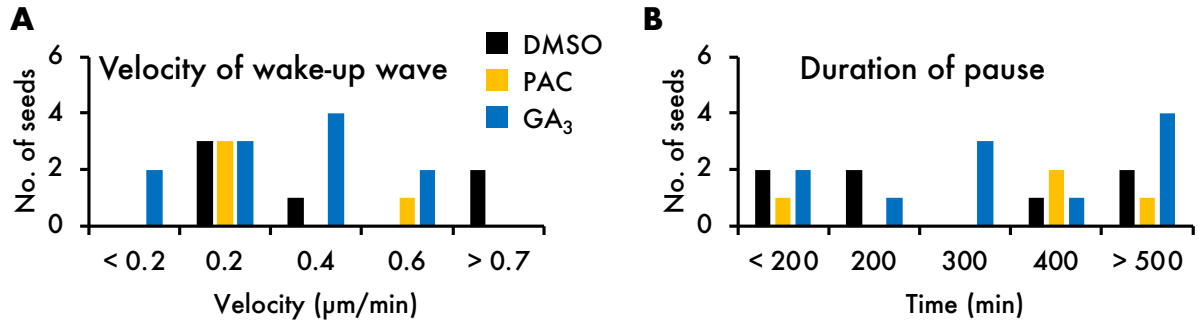
B Non-germinated seeds conditioned with PAC



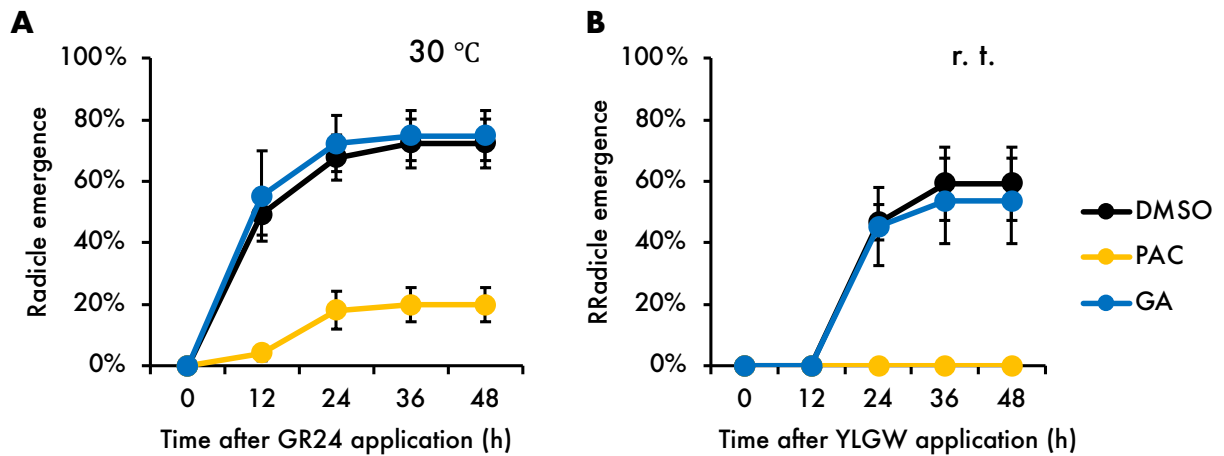
C Non-germinated seeds conditioned with GA₃



Supplementary Figure 7 Kymographs of non-germinating embryos conditioned with (A) DMSO, (B) 10 μ M PAC or (C) 100 nM GA₃. Embryos that elongated slightly but not more than 10 % compared to 0 h were highlighted in asterisks. Notably, these embryos still showed the typical three-step germination waves whereas other embryos either showed non-specific fluorescence propagation patterns or no fluorescence as previously reported (Tsuchiya *et al.*, 2015). † Kymographs represented other embryos (11 for DMSO, 16 for PAC and 11 for GA₃) with similar pattern in which no fluorescence or only weak fluorescence was detected towards the end of 48 h. Look-up table indicating grey value was shown on right.



Supplementary Figure 8 Kymograph analysis of germinating seeds. (A) Velocity of the wake-up wave was displacement traveled by the fluorescence over total duration. (B) Pre-germination pause represented the duration of time between wake-up wave and elongation tide where fluorescence disappeared.



Supplementary Figure 9 Radicle emergence of *Striga* seeds conditioned for 7 d in DMSO, 10 μ M PAC or 100 nM GA₃. Seed germination was induced with (A) 0.1 μ M GR24 at 30 °C or (B) 10 μ M YLGW at room temperature in dark. Radicle emergence was scored every 12 h. Error bar represents SD (n = 3).

Chapter 2

Functional analysis of parasitic plant *Striga hermonthica* germination inhibitor RTC2

Abstract

Parasitic plant *Striga hermonthica* (hereinafter referred to as *Striga* in this chapter) germinates in response to plant hormone strigolactones (SLs) exuded from host roots. This process is evoked by SL receptors encoded by *HYPOSENSITIVE TO LIGHT (HTL)* genes. SLs alter conformation of ShHTLs and induce protein-protein interaction with downstream F-box protein MORE AXILLARY GROWTH 2 (MAX2) and negative regulator SUPPRESSOR OF MAX2 1 (SMAX1) which trigger ubiquitination and proteasomal degradation of SMAX1 that activates SL signaling for germination. However, molecular mechanisms underlying *Striga* germination pathway are still largely unknown. In this chapter, I performed chemical suppressor screening to study *Striga* germination pathway elicited by a selective SL mimic called Splynolactone-7 (SPL7) that binds preferentially to ShHTL7, the most sensitive SL receptor in *Striga*. From *Striga* germination-based screening, I identified 41 small-molecule inhibitors that suppressed SPL7-mediated germination. 9 of these inhibitors, later named as Receptor-Targeting Compounds (RTCs), were able to bind ShHTL7 and/or other ShHTLs *in vitro*. I further clarified the role of RTC2 and propose an allosteric inhibitory mode of this inhibitor based on my current findings from structure-activity relationship studies, effect on protein-protein interaction of ShHTLs with MAX2 and SMAX1 as well as receptor stability.

2.1 Introduction

Obligate parasitic weed *Striga hermonthica* (*Striga*) senses plant hormone strigolactones (SLs) exuded from roots of its host plants as seed germination cues. SLs are perceived by SL receptors encoded by at least eleven *HYPOSENSITIVE TO LIGHT* (*HTL*) genes in *Striga*. ShHTLs are α/β hydrolase receptors that retain enzymatic activity to bind and hydrolyze SLs. Among them, ShHTL4-ShHTL9 are evidently the important receptors that elicit SL-dependent germination signals through binding to F-box protein MORE AXILLARY GROWTH 2 (MAX2) to direct negative regulator SUPPRESSOR OF MAX2 1 (SMAX1) for proteasomal degradation.

Despite the recent advances in parasitic plant research, many unknowns, such as the downstream targets in ShHTL signaling pathway, remain to be elucidated. This is mainly due to the lack of mutant availability as there is still no efficient transformation method. Hence, it remains difficult to perform conventional mutagenesis screen to study germination pathway in *Striga* itself. However, this limitation was circumvented by extensive chemical biology approaches to develop small-molecule tools for parasitic plant research.

One excellent example is the development of a fluorogenic SL mimic called Yoshimulactone Green (YLG) and its derivative YLGW that enabled the properties of ShHTLs to be probed *in vitro* and *in vivo* (Tsuchiya et al., 2015). For instance, YLG was applied to set up an *in vitro* competitive binding assay with SL receptors like ShHTLs to perform high-throughput screening for small-molecule modulators (Yoshimura et al., 2018). Using this system, our group previously identified a SL agonist called Sphynolactone-7 (SPL7) that targets preferentially to the most reactive receptor ShHTL7 and stimulates *Striga* germination at femtomolar level, which is equivalent to the most potent natural SLs 5-deoxystrigol (5DS) (Uraguchi et al., 2018).

In effort to elicit the detailed mechanism in SL-ShHTLs dependent *Striga* germination process, utilizing selective agonist like SPL7 will be ideal to dissect the ShHTL7-dependent pathway comparing to those that involve multiple receptors. Therefore, in this chapter, I performed a chemical suppressor screening to study the *Striga* germination pathway elicited by SPL7 through ShHTL7.

2.2 Results

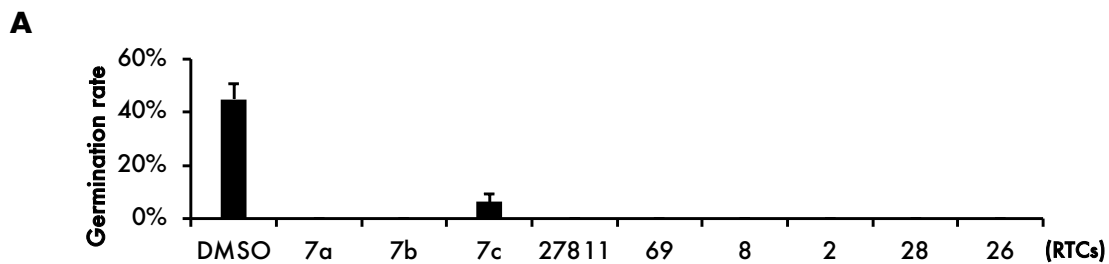
Identification of RTC2 as inhibitor of SPL7-induced *Striga* germination

Chemical suppressor screening of SPL7-induced germination was performed in a two-step procedure. Firstly, conditioned *Striga* seeds were incubated with 100 μ M chemical library compounds for 2 d and germination inducers were recorded. Next, SPL7 was applied to stimulate germination and inhibitors that fully suppressed germination were selected. Subsequently, hit compounds were subjected to germination assay two more times. This chemical screening performed with 10,400 random compounds in ITbM Chemical Library resulted in identification of 3 germination inducers along with 41 germination inhibitors that consistently suppressed SPL7-stimulated germination (Fig. S1).

Since I am mainly interested in studying SPL7-mediated germination pathway, I focused my studies on the germination inhibitors. I considered two main possibilities of how these molecules could inhibit *Striga* germination, either by targeting to the receptor and perturb SPL7 from eliciting signal, or by inhibiting components that act downstream of the receptor in the signaling pathway. To clarify these two possibilities, 41 germination inhibitors were tested for binding to the receptors using *in vitro* YLG competitive binding assay (Tsuchiya et al., 2015). Instead of evaluating with only ShHTL7, which is the main target of SPL7, all other ShHTLs were also investigated to confirm the selectivity of these inhibitors. Initial screen at 10 μ M concentration identified 12 hits that caused more than 50 % reduction of YLG fluorescence derived from receptor hydrolysis (Fig. S2). These 12 hits were further examined at a range of concentrations from 0.01 μ M to 10 μ M to calculate for their half maximal inhibitory concentrations (IC_{50}) of YLG hydrolysis by the target receptors. Using this approach, 9 out of 12 inhibitors were confirmed binding to ShHTLs at IC_{50} values below 10 μ M (Fig. 1A, B). On the other hand, the other 32 inhibitors likely bind to the downstream unknown components, or they could possibly also target to the receptors at higher concentration.

The 9 receptor-targeting inhibitors were named as Receptor-Targeting Compounds (RTCs). Among them, RTC7a, RTC7b and RTC7c were selective binders of ShHTL7 (Fig. 1B). RTC27811 preferentially binds to ShHTL7, but also binds to other three receptors with IC_{50} values below 3

μM . Interestingly, other RTCs preferentially bind to other receptors than ShHTL7, and the IC_{50} values to ShHTL7 were above $10 \mu\text{M}$. I was particularly intrigued by RTC2, RTC26 and RTC28 because they share similar core structure of *N*-phenylbenzenesulfonamide, which suggested that their common target should be important for SPL7-mediated germination pathway (Fig. 1C). As they all bind to ShHTL2, I wondered if that would imply on possible interaction between ShHTL2 and ShHTL7 pathways during germination process. Therefore, I decided to focus on the investigation of RTC2, as it has the highest affinity and selectivity to ShHTL2, as shown by the lowest IC_{50} value in YLG competitive binding assay.



B

IC₅₀ of YIG binding assay (μM)

	SPL7	7a	7b	7c	27811	69	8	2	28	26 (RTCs)
ShHTL2	> 10	> 10	> 10	> 10	2.88 ± 1.10	> 10	> 10	0.95 ± 0.86	2.43 ± 1.50	4.56 ± 1.79
ShHTL3	> 10	> 10	> 10	> 10	> 10	> 10	> 10	> 10	> 10	> 10
ShHTL4	> 10	> 10	> 10	> 10	> 10	> 10	> 10	> 10	> 10	> 10
ShHTL5	> 10	> 10	> 10	> 10	> 10	> 10	> 10	> 10	> 10	> 10
ShHTL6	> 10	> 10	> 10	> 10	> 10	1.24 ± 0.07	> 10	> 10	> 10	2.03 ± 0.30
ShHTL7	0.31 ± 0.06	1.67 ± 0.91	3.27 ± 0.43	7.48 ± 3.22	0.75 ± 0.15	> 10	> 10	> 10	> 10	> 10
ShHTL8	1.2 ± 0.1	> 10	> 10	> 10	1.24 ± 0.62	> 10	4.58 ± 0.62	> 10	3.11 ± 0.28	> 10
ShHTL9	> 10	> 10	> 10	> 10	> 10	5.33 ± 1.18	> 10	> 10	> 10	> 10
ShHTL10	> 10	> 10	> 10	> 10	> 10	> 10	> 10	> 10	> 10	> 10
ShHTL11	7.8 ± 0.29	> 10	> 10	> 10	1.35 ± 0.28	> 10	> 10	> 10	> 10	> 10

0 >10 μM

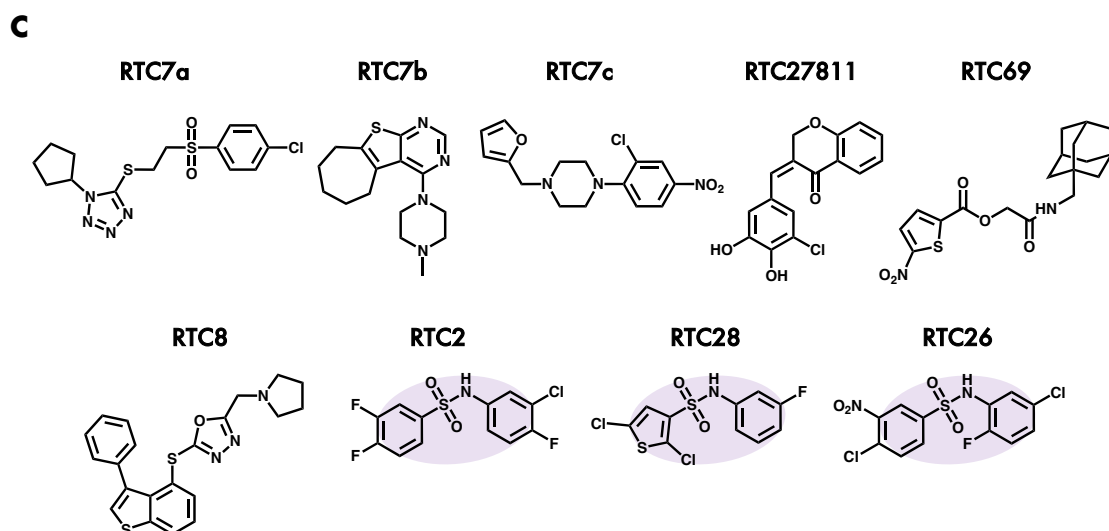


Figure 1 9 RTCs suppressed *Striga* germination induced by SPL7 and bind to ShHTLs. (A) Germination of conditioned *Striga* seeds was stimulated with 10 nM SPL7 in the presence of 100 μ M RTCs. Germination rate was counted after 2 d. 1 % DMSO was used as control. Error bars represent SD (n = 3). (B) Binding affinity of RTCs to ShHTL2-ShHTL11 in *in vitro* YLG competitive binding assay. IC₅₀ values for each RTC were represented as heat map with SD (n = 3). Previously reported IC₅₀ values of SPL7 were listed for comparison (Uraguchi et al., 2018). (C) Chemical structures of RTCs. *N*-phenylbenzenesulfonamide core structure of RTC2, RTC26 and RTC28 was highlighted in purple.

Structure-activity relationship (SAR) studies of RTC2

I reasoned that if RTC2 targets ShHTL2 to inhibit SPL7-mediated germination, RTC2 derivatives with higher ShhTL2 binding affinity supposedly impose stronger inhibition on *Striga* germination. Hence, I evaluated this hypothesis through structure-activity relationship (SAR) studies using RTC2 derivatives. Synthesis of RTC2 was first performed to establish a general chemical synthetic route. Activity of the synthesized molecule was confirmed to also inhibit *Striga* germination and binds strongly to ShHTL2 like RTC2 from the chemical library (Fig. 2A, S3). However, when tested at higher concentration of up to 100 μ M in YLG binding assay, binding of RTC2 to most of the ShHTLs was also observed.

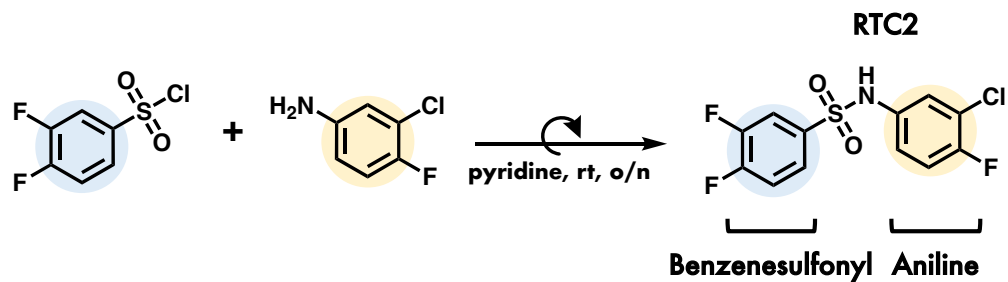
Despite the high structure similarities of RTC2, RTC26 and RTC28, they displayed different binding affinities to ShHTL2, which is potentially accounted by different substituents on the benzene rings. Therefore, the structure of RTC2 was modified by substituting the halogens on the benzene rings with hydrogens. Firstly, aniline moiety of RTC2 was retained whereas two fluorine atoms on the benzenesulfonyl moiety were modified either by removing both fluorine (J1) or leaving only one fluorine at *meta* (J2) or *para* position (J3) (Fig. 2A). Alternately, benzenesulfonyl moiety was remained whereas chlorine and fluorine atoms on the aniline moiety were both removed (J4) or keeping only *meta*-chlorine (J5) or *para*-fluorine (J6). Next, J1-J6 derivatives were compared for their binding affinity to ShHTL2 in YLG binding assay. Interestingly, modifications of J1, J2 and J5 showed enhanced affinity to ShHTL2 with a five-fold reduction in IC_{50} values (Fig. 2B). Taking the results into account, I speculated that binding affinity of RTC2 could be further improved by combining benzenesulfonyl modification of J1 or J2 with aniline modification of J5. Indeed, J7 and J8 that carries such modifications could bind at 10-fold greater affinity compared to RTC2. In addition to that, the selectivity of RTC2 derivatives was also investigated, where J4 and J6 were more selective to ShHTL2 despite they had weaker binding.

To gain insights on the relationship between binding affinity to ShHTL2 and inhibitory effect for *Striga* germination, sensitivity of SPL7-induced germination to inhibition by RTC2 derivatives were compared by concentration required to reduce the germination rate of SPL7 by half (IC_{50} of *Striga* germination). Surprisingly, the strong binders of ShHTL2 such as J8 showed weaker germination inhibitors compared to RTC2 (Fig. 2C). Instead, RTC2 showed the strongest

inhibitory activity as portrayed by its lowest IC₅₀ value of *Striga* germination. Additionally, J4 and J6 that lost binding to most ShHTLs were greatly defective of *Striga* germination inhibition. Thus, results from SAR studies collectively inferred that binding to ShHTL2 is insufficient to account for RTC2 inhibition, but rather its action more likely requires binding to other ShHTLs.

If RTC2 targets the receptors to inhibit *Striga* germination, then its suppression should be alleviated by exogenous application of plant hormone ethylene, since SL signaling was previously shown to upregulate ethylene biosynthesis genes (Sugimoto et al., 2003). Consistent with this idea, 1-aminocyclopropane-1-carboxylic acid (ACC), the direct precursor of ethylene, partially alleviated the inhibitory effect of RTC2 (Fig. S4). Therefore, the target site of RTC2 should be upstream of ethylene biosynthesis where SL signaling occurs.

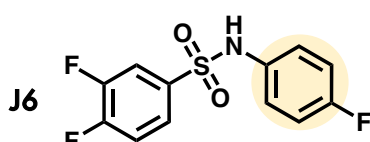
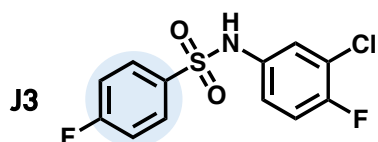
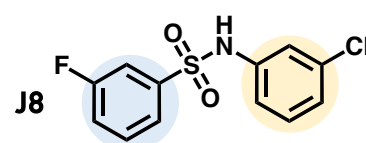
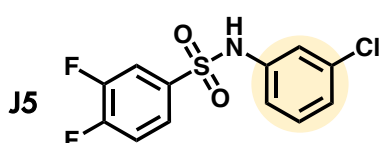
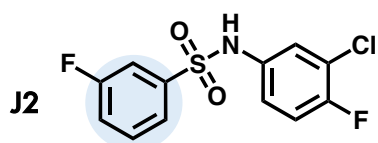
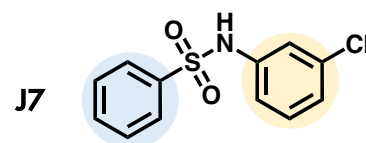
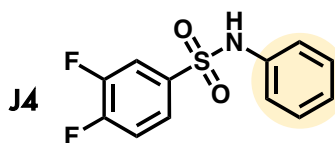
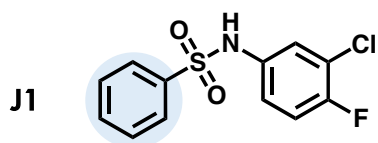
A



● **Modification of benzenesulfonyl**

● **Modification of aniline**

Modification of both rings



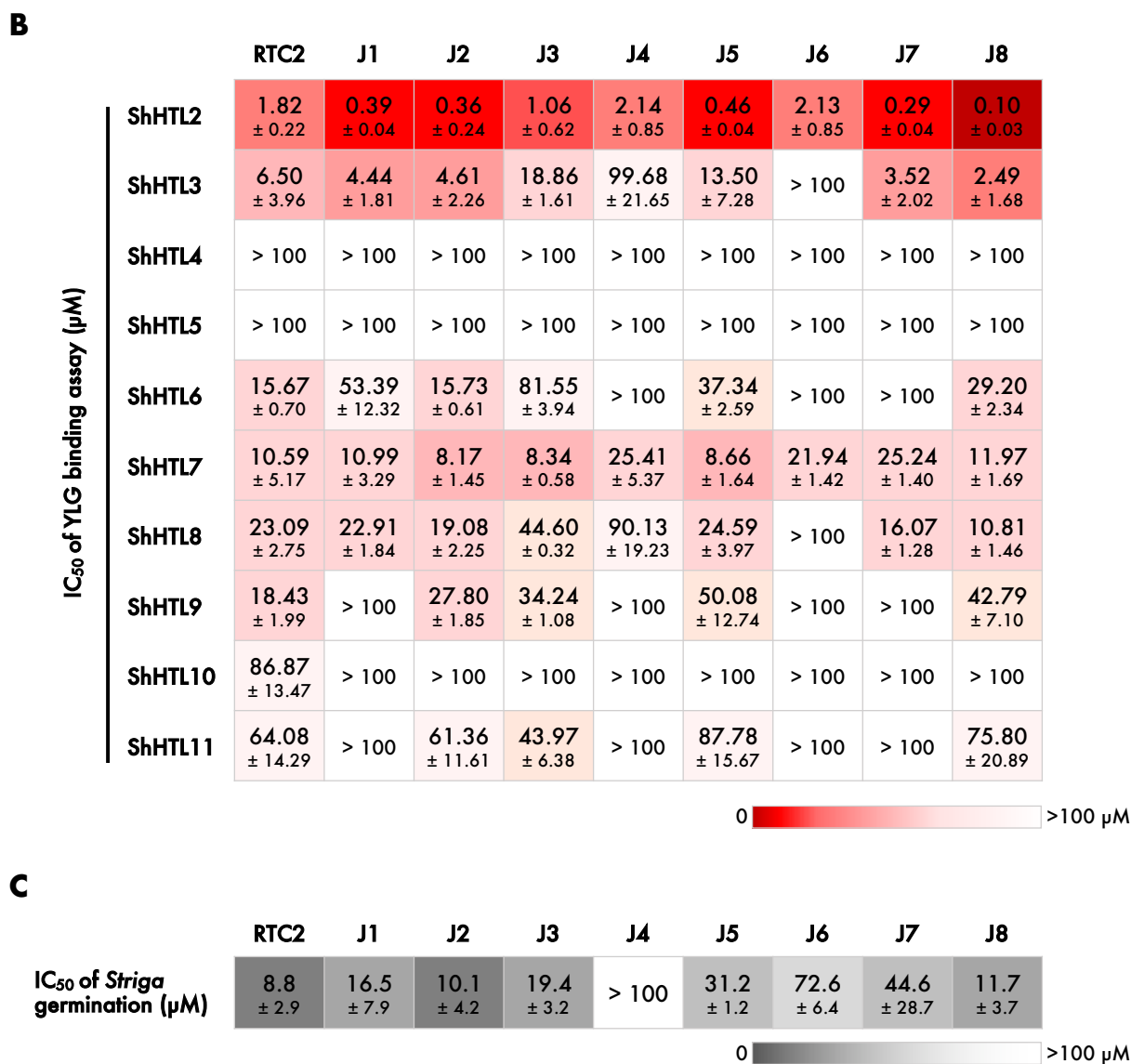


Figure 2 Chemical synthesis and structure-activity relationship studies of RTC2 derivatives. (A) RTC2 and derivatives were synthesized through a general procedure by reacting appropriate benzenesulfonyl chloride and aniline. The derivatives were either substituted on benzenesulfonyl ring (J1-J3) or aniline ring (J4-J6) or both (J7 and J8). (B) Binding affinity of RTC2 derivatives to ShHTL2-ShHTL11 in *in vitro* YLG competitive binding assay. IC₅₀ values were represented as heat map with SD (n = 3). (C) Inhibitory strength of RTC2 derivatives on *Striga* germination. Germination was stimulated with 10 nM SPL7 in the presence of 0.1-100 μM of RTC derivatives. Germination rate was counted after 2 d. 1 % DMSO was used as control. IC₅₀ values for *Striga* germination were represented as heat map with SD (n = 3).

RTC2 decoupled binding of ShHTLs with downstream MAX2 and SMAX1

Next, I investigated if binding of RTC2 to ShHTLs would impact on SLs-dependent interaction with downstream proteins, MAX2 and SMAX1 through yeast two-hybrid or three-hybrid (Y2H or Y3H) assays. First, I established Y2H assay for HTL-MAX2 and HTL-SMAX1 interaction, as well as Y3H assay for HTL-MAX2-SMAX1 interactions by validating with SPL7 dose-dependent binding (Fig. S5A). *AtSMAX1* from *Arabidopsis* was used in the assay because the homologous genes in *Striga* have not been identified yet. Also, ShHTL1, ShHTL4 and ShHTL6 that constitutively interacted with ShMAX2 or AtSMAX1 in this system were excluded from analysis. Firstly, SPL7 encouraged protein-protein interaction between ShHTL7 and ShMAX2 at concentration as low as 100 pM, which agrees with its high selectivity toward ShHTL7. Nevertheless, high concentration of SPL7 (100 nM or higher) also induced other ShHTLs (ShHTL5, 8 and 9) to interact with ShMAX2. In contrast, for AtSMAX1, only ShHTL7-AtSMAX1 interaction was elicited even at high concentration of 10 μ M SPL7 in Y2H assays. With the presence of ShMAX2 effector in Y3H assays, however, other ShHTLs (ShHTL8 and 9) interacted with AtSMAX1 at 100 nM or higher concentrations of SPL7. Moreover, the stronger ShHTL7-AtSMAX1 interaction was also observed in the Y3H assay, which is consistent with the enhancement observed with GR24 reported previously (Wang et al., 2021). Collectively, SPL7 activates not only ShHTL7, but also other ShHTLs at high concentration, and these dose-dependent protein-protein interactions between ShHTLs and their downstream partners can be monitored by the Y2H and Y3H assays.

Using this system, I next tested if RTC2 encourages these interactions. However, even high concentration of 50 μ M RTC2 did not show observable differences from DMSO, suggesting that RTC2 alone could not induce protein-protein interaction (Fig. S5B). On the contrary, when applied with SPL7, RTC2 weakened the binding of most ShHTLs with ShMAX2 and AtSMAX1 (Fig. 3). This indicated that RTC2 most likely inhibits SPL7-mediated germination pathway by decoupling the binding of receptor to downstream components, thereby preventing the activation signal to be elicited.

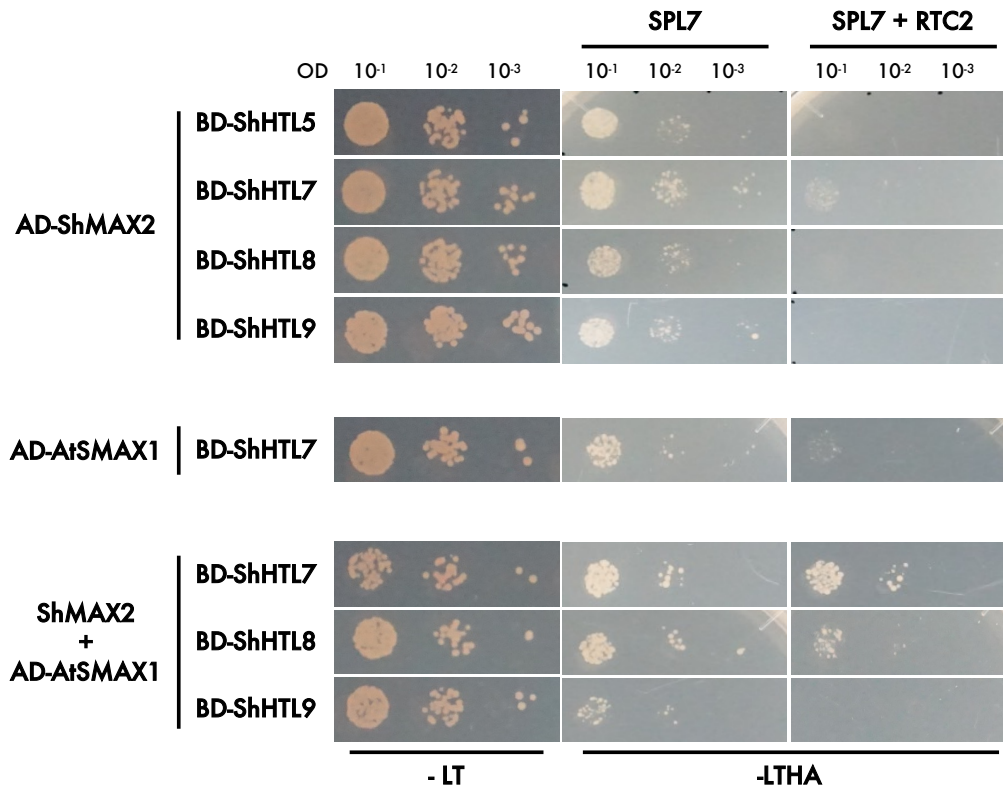


Figure 3 RTC2 weakened SPL7-dependent protein-protein interactions of ShHTLs with downstream ShMAX2 and AtSMAX1 in Y2H and Y3H assays. In Y2H assays, ShHTLs were fused with GAL4 DNA binding domain (BD) whereas ShMAX2 or AtSMAX1 was fused with GAL4 activation domain (AD). In Y3H assays, ShHTLs and AtSMAX1 were fused with BD and AD respectively whereas ShMAX2 was expressed as a free effector. Serial 10-fold dilution of yeast was loaded onto -LT control or -LTHA selection media plate supplemented with SPL7 ± RTC2. Minimum SPL7 concentration (either 1 nM, 10 nM, 100 nM or 1 μM) required to encourage protein-protein interaction for each ShHTLs and 50 μM RTC2 was used in the assays. 0.2 % DMSO was used as control. The plates were incubated at 30 °C for 3 d. -L, -Leu; -T, -Trp; -H, -His; -A, -Ade; OD, Optical density.

RTC2 further destabilized SPL7-bound ShHTL7

Despite signal activation mechanism remains debatable, SL-induced destabilization and degradation of receptor is well-recorded in the studies of SL receptor in non-parasitic plants that is encoded by *DWARF14 (D14)*. Consistently, SL agonists also caused receptor destabilization whereas SL antagonists caused an opposite effect to stabilize the receptor and prevent it from degradation (Nakamura et al., 2019). The findings thus far suggested that RTC2 shares similar properties with novel antagonists that also decouple the receptor from binding to downstream components. Thus, I tested the effect of RTC2 on the stability of ShHTL7 in the next step.

I set up an *in vitro* protein thermal shift assay called differential scanning fluorimetry (DSF) assay to test the stability of recombinant ShHTL7 subjected to different ligands by monitoring the change in melting temperature. Firstly, I validated the assay by treating ShHTL7 with increasing concentrations of SPL7 and observed a dose-dependent shift of lower melting temperature, which is consistent with the destabilizing effect of SLs or SL agonists (Fig. 4A). Next, I tested the effect of RTC2 but it did not induce any changes up to highest concentration of 100 μ M tested (Fig. 4B). However, interestingly, when RTC2 was co-applied with SPL7, it caused a further destabilization of the receptor, which is a direct opposite effect with reported antagonists (Fig. 4C).

The further destabilizing effect of RTC2 was unexpected and could not be explained by simple antagonist model. However, this further destabilizing effect could lead dysfunctionalization of ShHTL7 *in vivo*, by which RTC2 could suppress SPL7-dependent seed germination. To test the idea, I confirmed the effect of RTC2 on ShHTL7 stability *in planta* by checking the protein level of ShHTL7 in 7 d old seedlings of *Arabidopsis* transgenic line constitutively expressing *ShHTL7-FLAG* in *htl-3* mutant background. Since the SL receptor undergoes degradation after perceiving SLs (Zhao et al., 2015). I first examined the time dependent degradation and observed gradual decrease of ShHTL7 and were mostly degraded 4 h after SPL7 treatment (Fig. S6). I then selected 1 h treatment where ShHTL7 was slightly degraded as a suitable timing to observe the destabilizing effect of RTC2. Consistent with the results of *in vitro* DSF assay, RTC2 alone did not affect ShHTL7 level but with SPL7, a lower protein level in relative to SPL7 alone was detected (Fig. 4D, E). Collectively, the current findings suggested RTC2 is unlikely an antagonist, but reduces the protein level of ShHTL7 in SPL7-dependent manner.

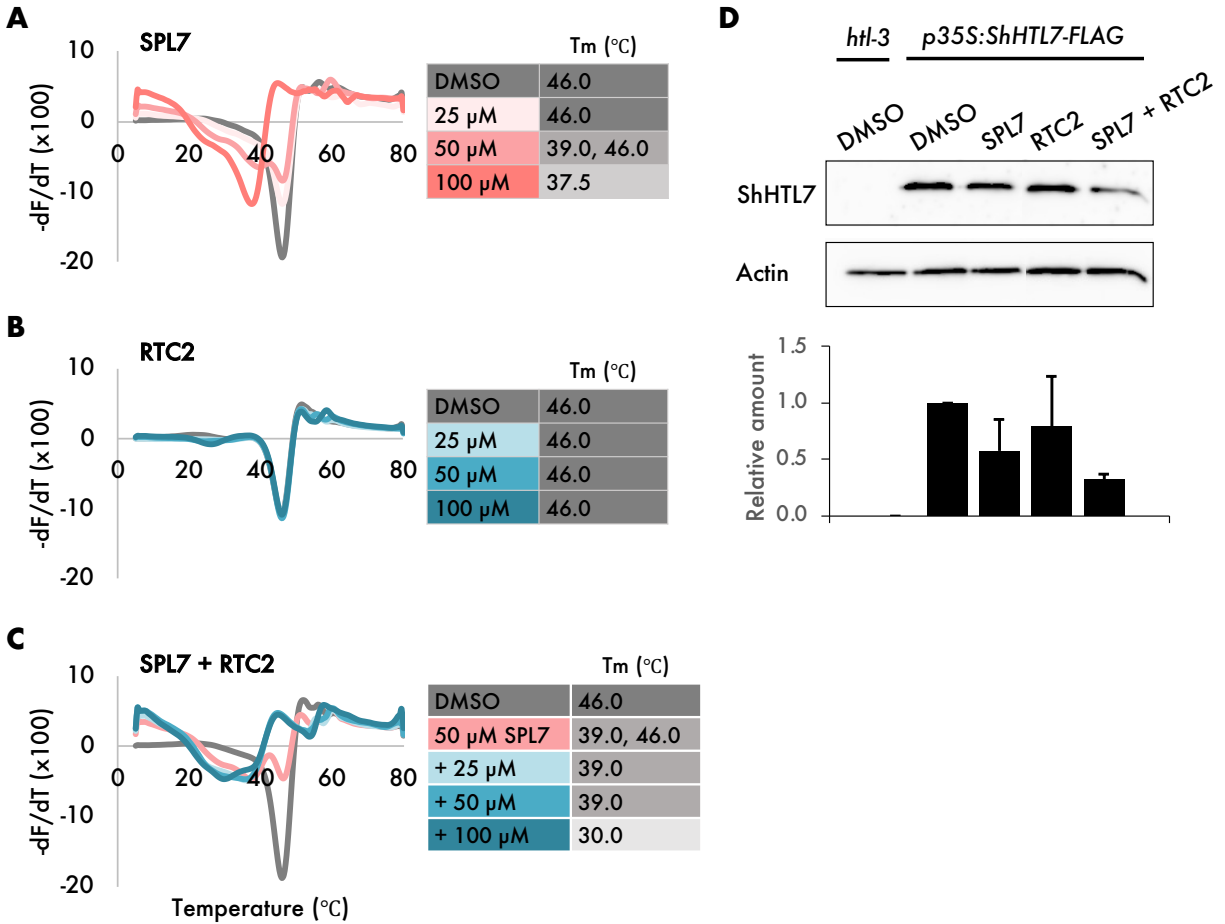


Figure 4 RTC2 destabilized SPL7-bound ShHTL7 *in vitro* and *in planta*. DSF assays of ShHTL7 incubated with (A) SPL7, (B) RTC2, (C) SPL7 and RTC2 at indicated concentrations. 1 % DMSO was used as control. Apparent melting temperature (T_m) presented as inverted peak was shown on right (n = 3). (D) Representative western blot and relative ShHTL7-FLAG protein level in 7-day-old *Arabidopsis* seedlings expressing *ShHTL7-FLAG* in *htl-3* background after 1 h treatment with 1 μ M SPL7 or 5 μ M RTC2 or both. 0.1 % DMSO was used as the control. Protein level of ShHTL7-FLAG was normalized against actin and presented in relative to DMSO control. Data was calculated from three biological samples from two different *ShHTL7* expressing lines.

2.3 Discussion

In this study, *Striga*-germination based screening together with biochemical analysis successfully uncovered inhibitors that targets to different sites of the SPL7-ShHTL7 mediated germination pathway. Discovery of RTC2 as a receptor-targeting inhibitor that was initially thought to act through another receptor ShHTL2 leads to its unexpected mode-of-action suggested in later experiments that it is more likely to act through further destabilization of SPL7-bound ShHTL7. These results raised a new inhibitory mode that could not be explained by the findings from currently reported antagonist. Importantly, SPL7 must be present for RTC2 to impact on ShHTL7 stability. Based on this observation, an allosteric inhibition mode is proposed for RTC2 (Fig. 5). Firstly, ShHTL7 must perceive SPL7. Then, either binding or hydrolysis of SPL7 leads to conformational change of the protein and creates a new target site for binding of RTC2 that further destabilized the protein.

In future work, I aim to elucidate the target site of RTC2 from several methods. Firstly, I considered protein crystallography likely challenging, as RTC2 would highly destabilize the receptor together with SPL7, not mentioning many attempts to crystalize SL receptor bound to intact SL by other groups were unsuccessful. However, some useful information was provided by a recent study that reported a crystal structure of intact GR24 binding to ShHTL5 with mutated catalytic serine residue that impaired its hydrolytic activity (Arellano-Saab et al., 2023). The ligand-bound crystal structure showed conformational shifts of the receptor but is insufficient to promote interaction with downstream MAX2 and SMAX1. Instead, it forms an internal tunnel that explains how ABC-ring of SLs exits the receptor after hydrolysis. Based on this finding, a few hypotheses of RTC2 inhibition can be postulated: it possibly targets to the exist of the tunnel to prevent the release of SPL7 after hydrolysis by ShHTL7 and further destabilize the protein; alternately, RTC2 with a chemical structure that resembles piperazine fragment of SPL7 might hijack into the tunnel after the fragment exists. In either way, I will test these hypotheses through molecular dynamic simulations. Meanwhile, I have synthesized RTC2 derivative attached with a photoaffinity group to identify the target site on SPL7-bound ShHTL7 by photoaffinity crosslinking. Alternatively, I am also performing random mutation screening of ShHTL7 in Y2H assay to look for mutations that could rescue the inhibition of RTC2 on SPL7-induced protein-

protein interaction with ShMAX2. In anyways, I expected the results from this finding would provide useful insights on clarifying the SL signal perception and activation mechanism of HTL receptors in parasitic plants that perceive different ligand from HTLs in non-parasitic plants, which action mechanism remains debatable even for SL receptor encoded by *D14*.

Besides identifying the target site, I would also investigate in detail on the effect of RTC2 during seed conditioning as previous report of a ShHTL7 antagonist showed greater inhibition when applied during conditioning which suggested a possible role of ShHTLs in regulating seed conditioning of *Striga* in conjunction with the role of GA that I elucidated in Chapter 1. Altogether, the inhibitors identified from this study have huge potential to uncover the unknowns in *Striga* germination process, especially the non-RTCs could contribute to identification of unknown components downstream of the pathway.

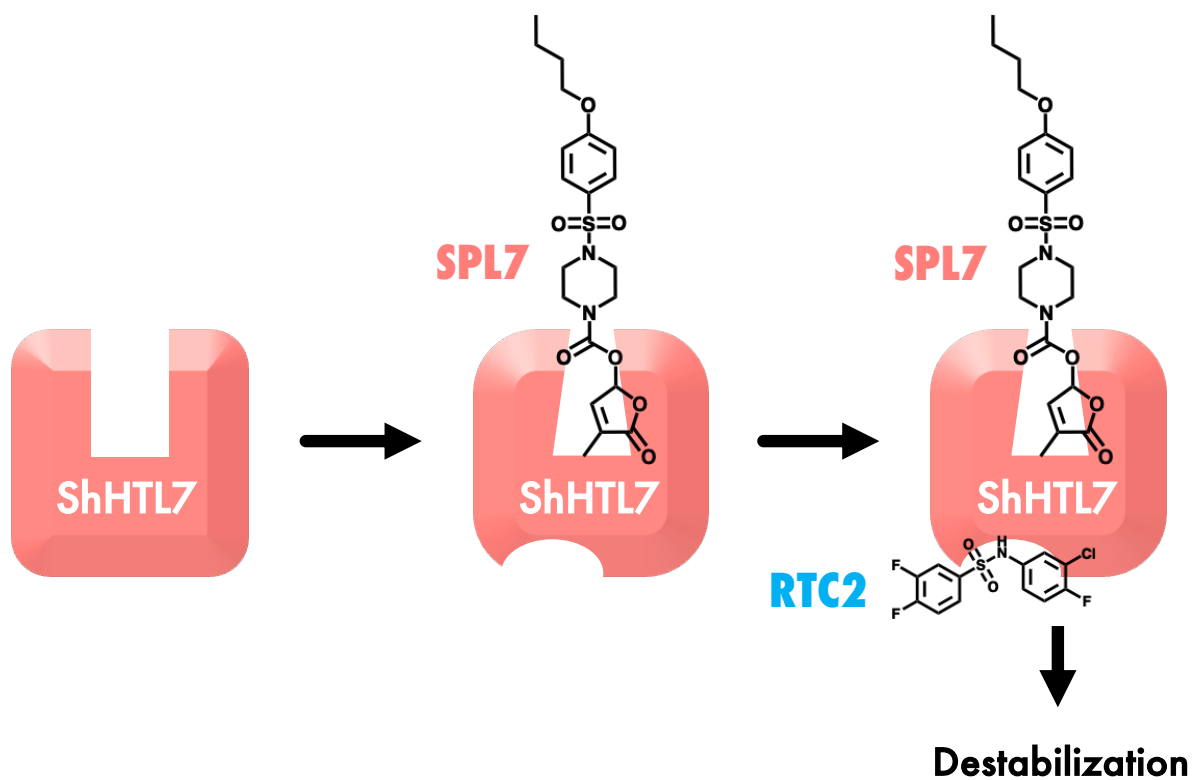


Figure 5 A proposed model for allosteric inhibition of RTC2. SPL7 first binds to the receptor. Binding or hydrolysis of SPL7 alters the conformation of ShHTL7 and destabilizes the protein. Meanwhile, this conformational change creates an allosteric site targeted by RTC2. Binding of RTC2 to the allosteric site further destabilizes ShHTL7.

2.4 Materials and Methods

Plant materials

Seeds of *Striga hermonthica* were collected from sorghum field in Gadarif, Sudan. Experiments using *S. hermonthica* seeds were performed under permission issued by the Japanese Ministry of Agriculture. *Arabidopsis thaliana* used in this study was Columbia-0 (Col-0) accession. Seeds of *ShHTL7* transgenic lines were in *htl-3* background (Toh et al., 2015).

Striga seed conditioning and germination assay

Seeds of *S. hermonthica* were conditioned with water and germination assays were performed in the same way as previously described in Chapter 1. 7 d to 14 d conditioned seeds were used for chemical screening and 7 d conditioned seeds were used for comparing the inhibitory effect of RTC2 derivatives. All compounds were dissolved in DMSO except ACC was dissolved in water. DMSO was used as the control at a final concentration of ≤ 1 %. IC_{50} values of *Striga* germination were calculated with curve fitting function (Rodbard) in Fiji software.

Chemical screening of *Striga* germination inhibitor

7 d to 14 d conditioned *Striga* seeds were treated with chemical library compounds at 100 μ M final concentration and 100 μ L final volume in 96-well plates. After 2 d incubation at 30 °C in dark, the plates were observed under microscope and the wells that germinated were recorded as germination inducers. Then, 10 μ L of SPL7 or its D-ring derivative was added to plates to stimulate germination at 10 nM final concentration. After another 2 d of incubation, the plates were observed under microscope again and the wells that did not germinate were recorded as germination inhibitors. Corresponding chemical library compounds selected from first screening were repeated for germination assay in second screening, and those that completely suppressed germination in second screening were repeated for third screening. Finally, 41 chemical library compounds that consistently suppressed SPL7-induced germination in three rounds of screening were selected as the most potent germination inhibitors. Due to low solubility of SPL7, first and second screening were performed with SPL7 D-ring analog, allyl-SPL7 in duplicate and triplicate respectively, and third screening was performed with another D-ring analog, H-SPL7 with higher selectivity towards ShHTL7 in triplicate. Both analogs used in screening still confer high selectivity towards ShHTL7

(Uraguchi et al., 2018). In subsequent germination assays, the original SPL7 was used and was simultaneously applied with germination inhibitors unless otherwise specified. DMSO control was loaded to all screening plates at ≤ 1 % final concentration.

Protein expression and purification

Purification of 6XHis-ShHTLs was as previously described (Tsuchiya et al., 2015). Purified recombinant proteins were suspended in assay buffer (100 mM HEPES, 150 mM NaCl, pH 7.0) and used for subsequent biochemical analysis.

***In vitro* YLG competitive binding assays**

In primary screening, 10 μ M final concentration of 41 germination inhibitors were co-incubated with 1 μ g of recombinant ShHTL and 1 μ M of YLG in assay buffer (100 mM HEPES, 150 mM NaCl, pH 7.0) on 96-well black plates (Greiner) at final volume of 100 μ L. Plates were reacted for 1 h at room temperature in dark. Fluorescence intensity was measured by SpectraMax i3 at 480 nm excitation wavelength and 520 nm detection wavelength. Relative fluorescence compared to DMSO control was calculated with Microsoft Excel. 12 hits that reduced YLG fluorescence level to below 50 % were repeated for binding assay to target ShHTL(s) with concentrations ranging from 0.01-10 μ M and IC_{50} values were calculated with curve fitting function (Rodbard) in Fiji software.

Relative YLG fluorescence of RTC2 derivatives to DMSO were compared at 10 μ M and 100 μ M final concentration. Derivatives that reduced YLG fluorescence level to below 50 % were repeated for binding assay to target ShHTLs with concentrations ranging from 0.01-10 μ M or 0.1-100 μ M and IC_{50} values were calculated.

Y2H and Y3H Assays

pGBE9 vector was constructed from pGBT9 vector (Takara) backbone by inserting a second multiple cloning site (MCS) fused to nuclear localizing signal and a FLAG tag at the N-terminus and expressed under constitutive *PGK* promoter. The insertion was validated with YFP expression in the nucleus (Tsuchiya, unpublished). Overall cloning of *ShHTLs* was performed by introducing common 15-basepair linker with the sequence 5'-TTGTATTTCCAGGGC-3' (forward) or 5'-

CAAGCTTCGTCATCA-3' to gene-specific primers by PCR reaction and inserted into MCS1 of pGBE9 carrying the same linker sequence by NEBuilder HiFi DNA Assembly (NEB; E2621). To stabilize ShMAX2, *ARABIDOPSIS SKP1-LIKE1* (*AtASK1*) was attached to N-terminus of *ShMAX2* with two GGSG repeats. All primer sequences used for cloning *ASK1-ShMAX2* or *AtSMAX1* into respective vector were listed in Supplementary Table 1.

For Y2H assays, pGBE9 vector carrying *ShHTL1-ShHTL11* in MCS1 with empty MCS2, and pGADT7 vector (Takara) carrying *ShMAX2* fused with *ARABIDOPSIS SKP1-LIKE1* (*AtASK1*) through two GGSG repeats at N-terminus, or full-length *AtSMAX1*, were transformed into Y2H Gold yeast strain (Takara) by lithium acetate method. For Y3H assays, pGBE9 vector carrying *ShHTL1-ShHTL11* in MCS1 and *ASK1-ShMAX2* in MCS2, and pGADT7 vector carrying *AtSMAX1*, were transformed into Y2H Gold. Transformed yeast was incubated on SD (-LT) plate for plasmid selection. Protein-protein interactions were detected on SD (-LTHA) plates containing indicated concentration of ligands after 3 d incubation at 30 °C.

DSF assay

10 µg of recombinant ShHTL7 was added to indicated ligand concentration and final 5X SYPRO Tangerine (Lonza) dye in 20 µL total volume of assay buffer (100 mM HEPES, 150 mM NaCl, pH 7.0) in a 96-well plate. The mixture was allowed to react for 10 min at room temperature in dark and the plate was loaded to Bio-Rad CFX connect real-time PCR machine for initial incubation at 5 °C for 5 min and gradual heat denaturation from 5 °C to 80 °C at 0.5 °C per 20 s interval with lid temperature set at 80 °C. The fluorescence change was detected with FRET channel and the melting temperature was calculated with CFX Maestro software and presented as inverted melting peak.

***Arabidopsis* protein degradation assay**

Arabidopsis seeds expressing *35S:ShHTL7-FLAG* in *htl-3* background were germinated on half strength Murashige and Skoog (MS) plate under constant light at 22 °C. Approximately twenty 7 d old seedlings per well were incubated with indicated ligand concentration in 1 mL half strength MS liquid by gentle shaking under constant light at 22 °C for 1 h, 2 h or 4 h. The samples were flash frozen with liquid nitrogen and lysed with TissueLyser II (Qiagen). Total proteins were

extracted with chilled lysis buffer (50 mM Tris-HCl, pH 7.5, 15 mM MgCl₂, 15 mM EGTA, pH 8.0, 1 mM DTT, 10 μL/mL protease inhibitor, 50 μM MG-132, 0.5 % NP-40) by 5 min incubation on ice followed by centrifugation at 14,000 rpm for 10 min at 4 °C. The supernatant was transferred to a new tube and protein concentration was measured by Bradford assay. Protein was denatured by heating at 95 °C for 5 min in SDS-PAGE sample buffer. *Arabidopsis htl-3* mutant was used as the background control.

Immunoblotting

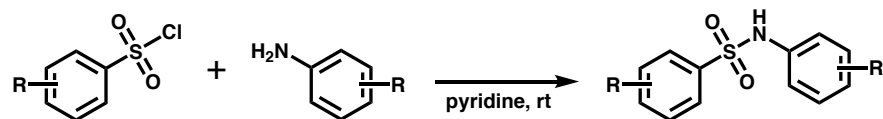
10 μg of total protein per sample was separated with 15 % SDS-PAGE mini gel and transferred to nitrocellulose membrane by Trans-Blot Turbo Transfer System (Bio-Rad). The membrane was washed for 30 min at room temperature with blocking buffer (5 % non-fat dry milk, 20 mM Tris-HCl, pH 7.4, 140 mM NaCl, 0.05% Tween-20). For ShHTL7-FLAG detection, the membrane was incubated overnight at 4 °C with mouse anti-FLAG primary antibody (Sigma; F1804; 1:3000 dilution), rinse for 5 min with TBS-T buffer (20 mM Tris-HCl, pH 7.4, 140 mM NaCl, 0.05% Tween-20) for three times, and incubated with goat anti-mouse IgG-HRP conjugate secondary antibody (Bio-Rad; 1706516; 1:3000 dilution) for 2 h at room temperature. After signal detection, antibodies were removed by 5 min rinse with Milli Q water, 10 min incubation with stripping buffer (7 M guanidinium chloride, 50 mM glycine, 0.05 mM EDTA-2Na, 0.1 M KCl, 20 mM 2-mercaptoethanol) and 10 min rinse with TBS-T buffer for two times. The membrane was then washed for 30 min at room temperature with blocking buffer and detected for actin with the same procedure as ShHTL7-FLAG using mouse anti-actin (plant) primary antibody (Sigma; A0480; 1:20000 dilution) and goat anti-mouse IgG-HRP conjugate secondary antibody (Bio-Rad; 1706516; 1:20000 dilution). All antibodies were diluted in blocking buffer and signal detection was performed using SuperSignal West Pico Chemiluminescence (Thermo Scientific; 34580) as the substrate and detected by Amersham Imager (GE Healthcare).

Chemical Synthesis

General information: ¹H NMR spectra were recorded on a JEOL JNM-ECS500 (500 MHz) spectrometer. Chemical shifts are reported in ppm from tetramethylsilane (0.0 ppm) resonance as the internal standard (CD₃OD and CDCl₃). The high resolution mass spectra were conducted on Thermo Fischer Scientific Exactive (ESI and APCI). Analytical thin layer chromatography (TLC)

was performed on Merck precoated TLC plates (silica gel 60 GF₂₅₄, 0.25 mm). Flash column chromatography was conducted on silica gel 60 (spherical, 40-50 μm; Kanto Chemical Co., Inc.), silica gel 60 N (spherical, 40-50 μm; Kanto Chemical Co., Inc.) and silica gel 60 (Merck 1.09385.9929, 230-400 mesh). Recycling preparative high-performance liquid chromatography (HPLC) was performed using YMC HPLC LC-forte/R equipped with a silica gel column [φ 20 mm × 250 mm, YMC-Pack SIL SL12S05-2520WT].

General Procedure for the Preparation of RTC2 and derivatives:



To a solution of the appropriate benzenesulfonyl chloride (0.5 mmol, 1 equiv) in pyridine (5 mL, 0.1 M) was added the appropriate aniline (0.5 mmol, 1 equiv) at 0 °C. The reaction mixture was stirred at room temperature for overnight and quenched with 1 N HCl. The product was extracted with CH₂Cl₂ (three times) and concentrated to afford the crude residue. Purification of the residue was performed by silica gel column chromatography (EtOAc : *n*-Hexane = 1:2) and HPLC to give the final product.

RTC2: Using 3,4-difluorobenzenesulfonyl chloride and 3-chloro-4-fluoroaniline to afford a white solid (62 % yield). HRMS (ESI) Calculated for C₁₂H₆ClF₃NO₂S⁻ ([M+H]⁻) 319.9765. Found 319.9754.

J1: Using benzenesulfonyl chloride and 3-chloro-4-fluoroaniline to afford a white solid (12 % yield). HRMS (ESI) Calculated for C₁₂H₈ClFNO₂S⁻ ([M+H]⁻) 283.9954. Found 283.9944.

J2: Using 3-fluorobenzenesulfonyl chloride and 3-chloro-4-fluoroaniline to afford a light pink solid (31 % yield). HRMS (ESI) Calculated for C₁₂H₇ClF₂NO₂S⁻ ([M+H]⁻) 301.9860. Found 301.9850.

J3: Using 4-fluorobenzenesulfonyl chloride and 3-chloro-4-fluoroaniline to afford a pink solid (49 % yield). HRMS (ESI) Calculated for C₁₂H₇ClF₂NO₂S⁻ ([M+H]⁻) 301.9860. Found 301.9852.

J4: Using 3,4-difluorobenzenesulfonyl chloride and aniline to afford a light purple solid (64 % yield). HRMS (ESI) Calculated for $C_{12}H_8F_2NO_2S^-$ ($[M+H]^-$) 268.0249. Found 268.0241.

J5: Using 3,4-difluorobenzenesulfonyl chloride and 3-chloroaniline to afford a white solid (30 % yield). HRMS (ESI) Calculated for $C_{12}H_7ClF_2NO_2S^-$ ($[M+H]^-$) 301.9860. Found 301.9852.

J6: Using 3,4-difluorobenzenesulfonyl chloride and 4-fluoroaniline to afford a white solid (36 % yield). HRMS (ESI) Calculated for $C_{12}H_7F_3NO_2S^-$ ($[M+H]^-$) 286.0155. Found 268.0147.

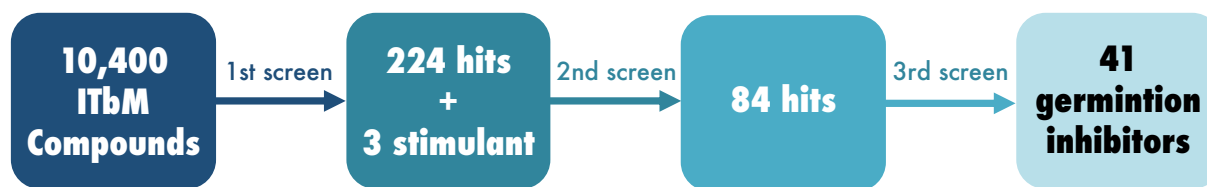
J7: Using benzenesulfonyl chloride and 3-chloroaniline to afford a light yellow solid (48 % yield). HRMS (ESI) Calculated for $C_{12}H_9ClNO_2S^-$ ($[M+H]^-$) 268.0048. Found 266.0043.

J8: Using 3-fluorobenzenesulfonyl chloride and 3-chloroaniline to afford a white solid (34 % yield). HRMS (ESI) Calculated for $C_{12}H_8ClFNO_2S^-$ ($[M+H]^-$) 283.9954. Found 283.9947.

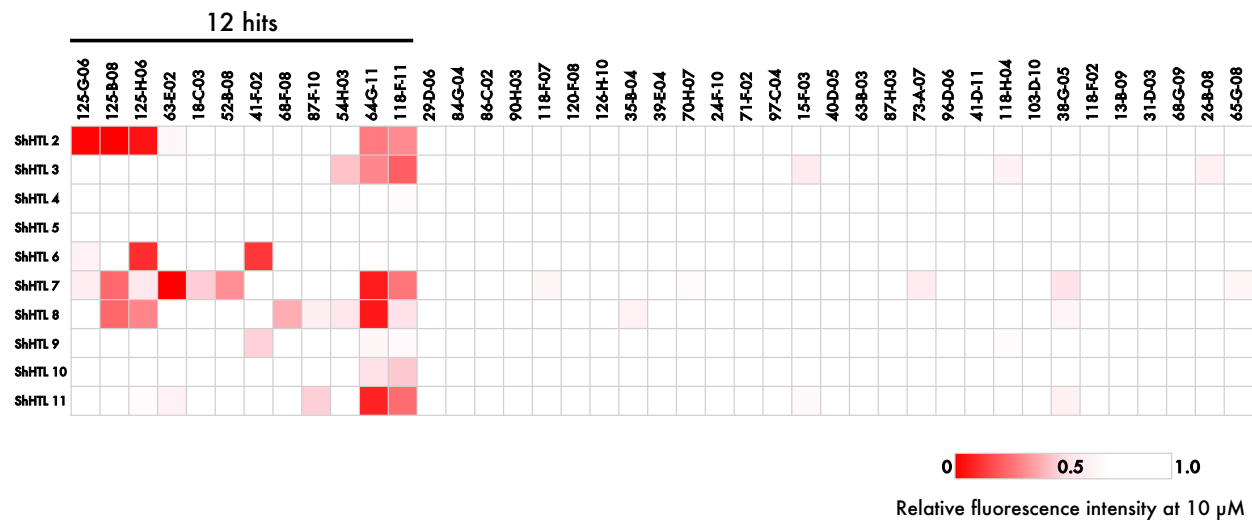
2.5 Supplementary Materials

Supplementary Table 1: List of primers used for Y2H and Y3H assays.

Annotation	Name of primer	Sequence (5' to 3')
For cloning AtASK1-ShMAX2 into pGADT7	pGADT7-F	<u>TGATGACGAAGCTTG</u> ATACTGAAAAACCCCGCAAGTTC
	pGADT7-R	<u>GCCCTGGAAATACAA</u> AGCGTAATCTGGTACGTCGTA
	AtASK1-F	<u>TTGTATTTCCAGGGC</u> ATGTCTGCGAAGAAGATTGTG
	ShMAX2-R	<u>CAAGCTTCGTCATCA</u> ATCAGAGATCTGGCGCCTGTT
For cloning AtASK1-ShMAX2 into MCS2 of pGBE9	pGBE9-MCS2-F	<u>TAGCTGGCGGCCGCGATCAATT</u>
	pGBE9-MCS2-R	<u>AACACCTTTCTCTTCTTCTTAGG</u>
	AtASK1-MCS2-F	<u>AAGAGAAAGGTGTTTCTCCAGGGC</u> ATGTCTGCGAAGAAGATTGTG
	ShMAX2-MCS2-R	<u>CGCGGCCGCCAGCTACGTCATCA</u> ATCAGAGATCTGGCGCCTGTT
For cloning AtSMAX1 into pGADT7	pGADT7-F	Same sequence as above.
	pGADT7-R2	<u>GAATTC</u> ACTGGCCTCCATGG
	AtASMAX1-F	<u>GAGGCCAGTGAATTC</u> ATGAGAGCTGGTTTAAGTACGATT
	AtSMAX1-R	<u>CAAGCTTCGTCATCA</u> TACTGCCAAAGTAATAGTTGTC




Supplementary Figure 1 The flow of chemical suppressor screening. *Striga* seeds were incubated with chemical library compounds for 2 days and germination inducers were noted. SPL7 was then to stimulate germination and inhibitors that completely suppressed germination were selected. From 10,400 compounds, 224 hits were tested for second screening and 84 hits for third screening, and 41 inhibitors that completely suppressed germination in all three screening were selected. Further details of screening were described in Materials and Methods.

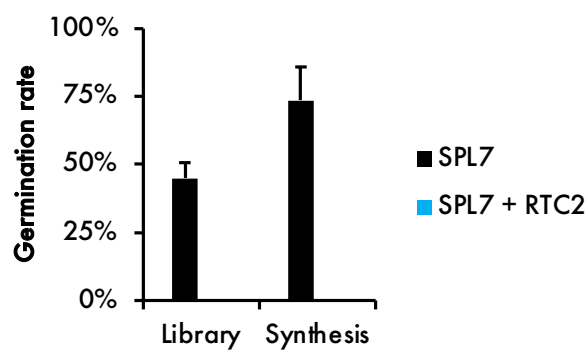


Supplementary Figure 2 YLG binding assay of 41 germination inhibitors at 10 μ M final concentration. Relative fluorescence to DMSO control is presented as a heatmap (n = 2).

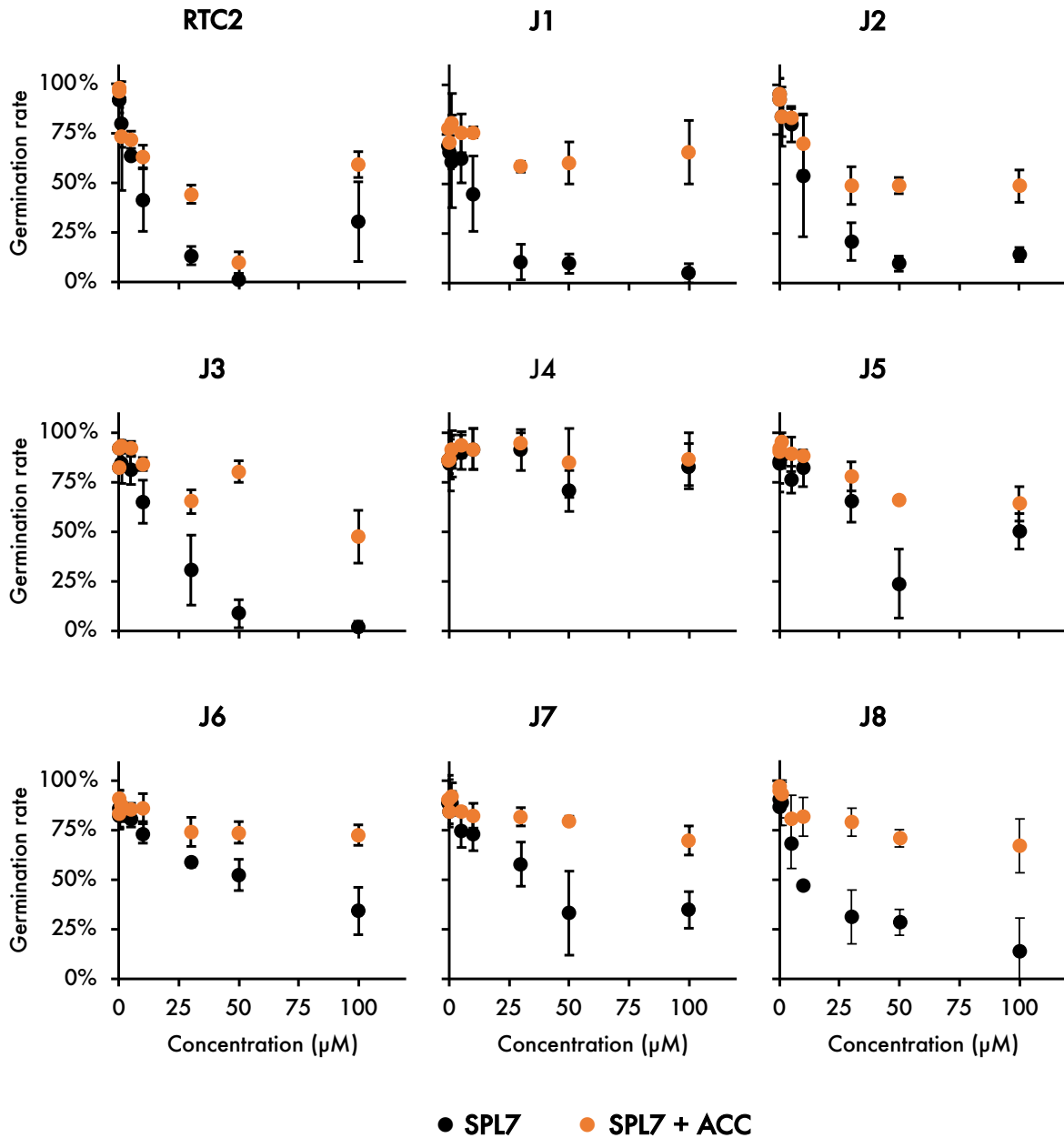
A

	Library Synthesis	
	Library	Synthesis
ShHTL2	0.95 ± 0.86	1.82 ± 0.22
ShHTL3	> 10	6.50 ± 3.96
ShHTL4	>10	> 100
ShHTL5	> 10	> 100
ShHTL6	> 10	15.67 ± 0.70
ShHTL7	> 10	10.59 ± 5.17
ShHTL8	> 10	23.09 ± 2.75
ShHTL9	> 10	18.43 ± 1.99
ShHTL10	> 10	86.87 ± 13.47
ShHTL11	> 10	64.08 ± 14.29

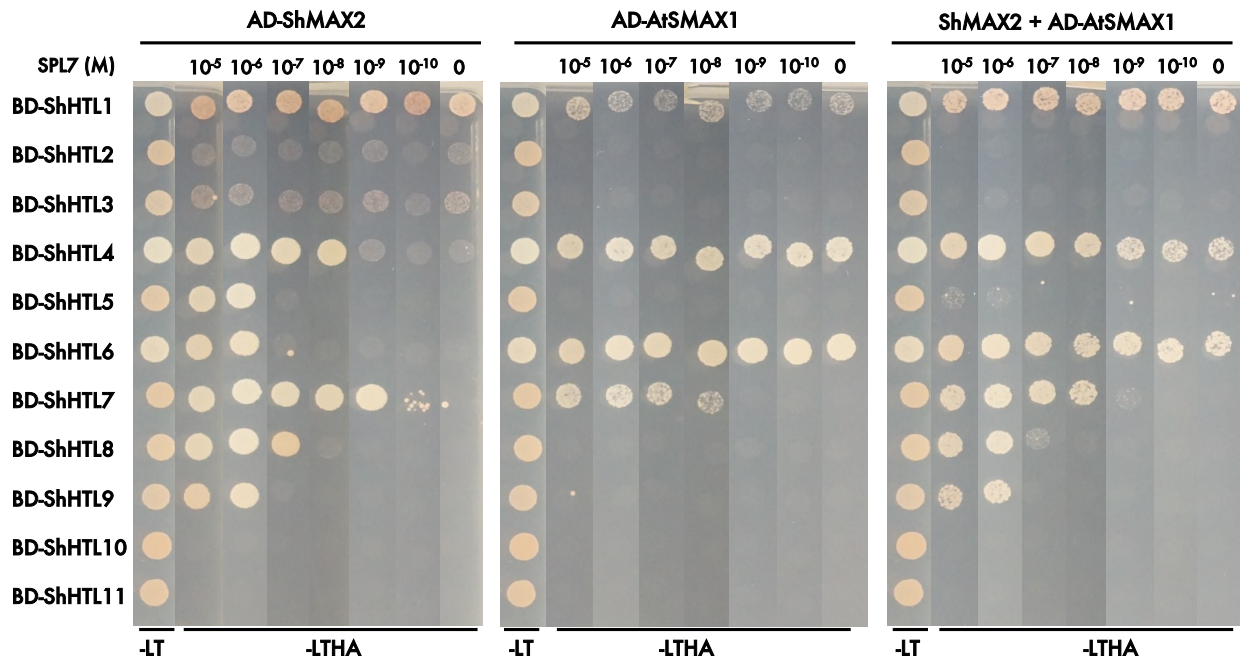
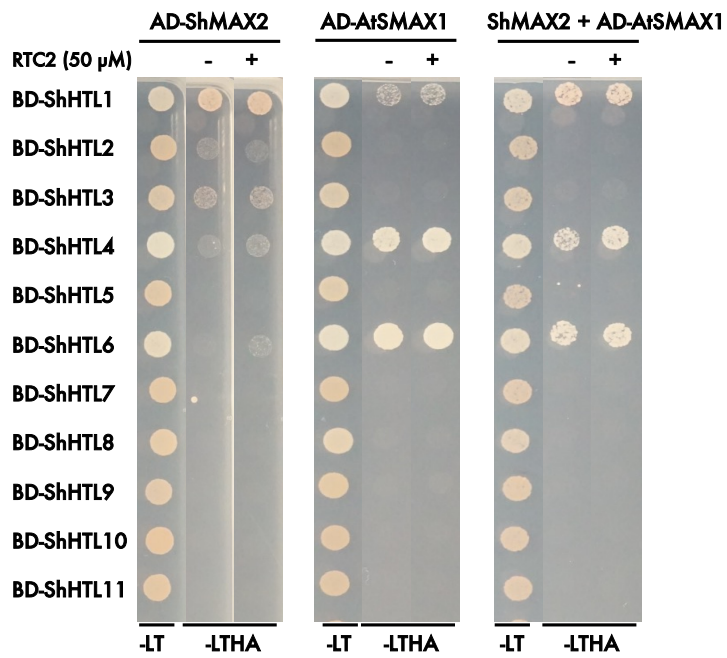
0  >100 μM

B

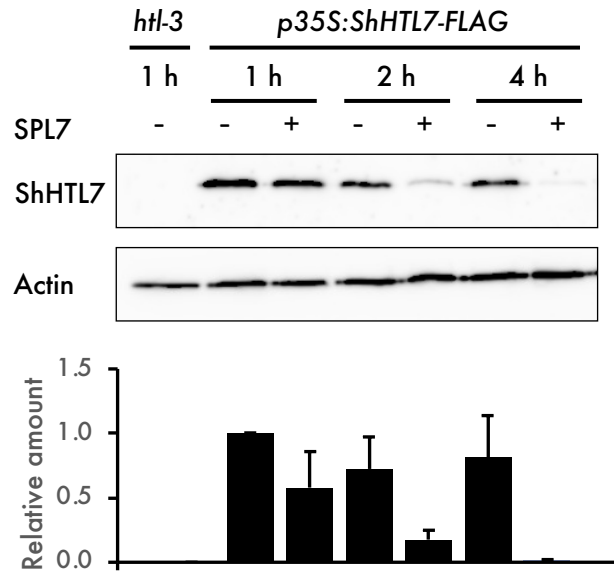
Supplementary Figure 3 Comparison of RTC2 from chemical library and synthesized compound. Both inhibited *Striga* germination induced by SPL7 and bound strongly to ShHTL2 in YLG binding assay at similar IC_{50} values. When tested at higher concentration, RTC2 also targeted to other ShHTLs. 100 μ M RTC2 and 10 nM SPL7 were used for germination assay and error bars represent SD ($n = 3$). 1 % DMSO was used as control.



Supplementary Figure 4 ACC treatment partially rescued RTC2 inhibition. *Striga* germination assay of 10 nM SPL7 co-incubated with RTC2 and derivatives at increasing concentration of 0.1, 1, 5, 10, 30, 50, 100 µM. After calculating germination rate on day 2, 100 µM ACC was added and further incubated 2 d before calculating germination. 0.2% DMSO was used as control. Error bars represent SD (n = 3 replicates).

A**B**

Supplementary Figure 5 Protein-protein interactions of ShHTLs, ShMAX2 and AtSMAX1 in Y2H and Y3H assays. In Y2H assays, ShHTLs were fused with GAL4 DNA binding domain (BD) whereas ShMAX2 or AtSMAX1 was fused with GAL4 activation domain (AD). In Y3H assays, ShHTLs and AtSMAX1 were fused with BD and AD respectively whereas ShMAX2 was expressed as a free effector. Yeast was loaded onto -LT control or -LTHA selection media plate supplemented with (A) SPL7 or (B) RTC2. Serial 10-fold increasing SPL7 concentration from 100 pM to 10 μ M and 50 μ M RTC2 was used in the assays. 0.2 % DMSO was used as control. The plates were incubated at 30 °C for 3 d. -L, -Leu; -T, -Trp; -H, -His; -A, -Ade.



Supplementary Figure 6 Time course degradation of ShHTL7 induced by SPL7. Representative western blot and relative ShHTL7-FLAG protein level in 7 d old *Arabidopsis* seedlings expressing *ShHTL7-FLAG* in *htl-3* background after 1 h, 2 h or 4 h treatment with 1 μ M SPL7. 0.1 % DMSO was used as the control. Protein level of ShHTL7-FLAG was normalized against actin and presented in relative to DMSO control at 1 h treatment. Data was calculated from three biological samples from two different *ShHTL7* expressing lines.

Concluding Remarks

In this research, I applied chemical genetic approaches to successfully provide new insights on seed germination of *Striga hermonthica*. In Chapter 1, I uncovered a role for plant hormone gibberellins in promoting seed conditioning of *S. hermonthica* that indirectly contributes to the seed germination pathway by up-regulating the expression level of receptors required to perceive germination stimulants released from the host plants. In Chapter 2, I performed a chemical suppressor screening of strigolactone-dependent germination pathway and identified a series of small-molecule inhibitors that could potentially clarify molecular mechanism of the pathway such as receptor perception activation mechanism as well as the downstream unknown components. In conclusion, I envisaged that this work would contribute to development of better solutions for parasitic plant control.

Acknowledgement

Research is never a solo work, and I will never accomplish this far without the continuous support from the following people whom I would like to sincerely highlight here.

I would like to thank my supervisor, Dr. Yuichiro Tsuchiya, for his tremendous support throughout the years that we have been working together. Without his guidance and encouragements, I would not persist so far in doing research, happily and freely expressing my thoughts.

I would also like to thank our lab members, both Tsuchiya Group and Kinoshita Group, for always willing to support whenever I ask for help and for all the constructive advice given to strengthen my work.

I would like to also express my gratitude to ITbM members, Dr. Ayato Sato and his group for kindly providing and preparing the chemical libraries and provide useful suggestions on the chemical aspects, as well as Dr. Daisuke Uraguchi who was previously in Ooi Group and the students for their assistance during the chemical synthesis of RTC2 derivatives.

I would like to acknowledge Dr. A. Babikier for kindly providing us *S. hermonthica* seeds, Dr. Masanori Okamoto for providing us *O. minor* seeds, Dr. Shigeo Toh for providing us *Arabidopsis ShHTL7* lines and Dr. Masahiko Yoshimura for providing us YLGW.

And I would like to also thank Sato Yo International Scholarship Foundation for their financial support during my PhD study and for attending conferences.

Many more people contributed to the work, whom I am not able to list out everyone here, but I truly appreciate anyone of you who had provided useful comments for my work, or your kind words to help me to overcome the hurdles in research.

Lastly, not forgetting also my beloved family and friends. I would not be who I am today without their endless love and support.

Reference

- Aflakpui, G.K.S., Gregory, P.J. and Froud-Williams, R.J. (1998) Effect of temperature on seed germination rate of *Striga hermonthica* (Del.) Benth., *Crop Production*, 17(2), 129-133.
- Akiyama, K., Matsuzaki, K. I., & Hayashi, H. (2005) Plant sesquiterpenes induce hyphal branching in arbuscular mycorrhizal fungi. *Nature*, 435(7043), 824–827.
- Arellano-Saab, A., McErlean, C. S. P., Lumba, S., Savchenko, A., Stogios, P. J. and McCourt, P. (2022) A novel strigolactone receptor antagonist provides insights into the structural inhibition, conditioning, and germination of the crop parasite *Striga*, *Journal of Biological Chemistry*, 298(4).
- Arellano-Saab, A., Skarina, T., Xu, Z., McErlean, C. S. P., Savchenko, A., Lumba, S., Stogios, P. J., & McCourt, P. (2023) Structural analysis of a hormone-bound *Striga* strigolactone receptor. *Nature Plants*, 9(6), 883–888.
- Arite, T., Umehara, M., Ishikawa, S., Hanada, A., Maekawa, M., Yamaguchi, S. et al.. (2009) d14, a Strigolactone-Insensitive Mutant of Rice, Shows an Accelerated Outgrowth of Tillers, *Plant and Cell Physiology*, 50(8), 1416-1424.
- Ariizumi, T., Lawrence, P. K., & Steber, C. M. (2011) The Role of Two F-Box Proteins, SLEEPY1 and SNEEZY, in Arabidopsis Gibberellin Signaling. *Plant Physiology*, 155(2), 765–775.
- Besserer, A., Puech-Pagès, V., Kiefer, P., Gomez-Roldan, V., Jauneau, A., Roy, S., Portais, J. C., Roux, C., Bécard, G., & Séjalon-Delmas, N. (2006) Strigolactones Stimulate Arbuscular Mycorrhizal Fungi by Activating Mitochondria. *PLOS Biology*, 4(7), e226.
- Bewley, J. D. (1997) *Seed Germination and Dormancy: American Society of Plant Physiologists*. Available at: <https://academic.oup.com/plcell/article/9/7/1055/5986415>.
- Brown, R. and Edwards, M. (1946) The germination of the seed of *Striga lutea*: II. The effect of time of treatment and of concentration of then host stimulant, *Annals of Botany*, 10(2).
- Bunsick, M., Toh, S., Wong, C., Xu, Z., Ly, G., McErlean, C. S. P. et al. (2020) SMAX1-dependent seed germination bypasses GA signalling in Arabidopsis and *Striga*, *Nature Plants*, 6(6), 646-652.

Bythell-Douglas, R., Rothfels, C. J., Stevenson, D. W. D., Graham, S. W., Wong, G. K. S., Nelson, D. C., & Bennett, T. (2017) Evolution of strigolactone receptors by gradual neo-functionalization of KAI2 paralogues. *BMC Biology*, 15(1), 1–21.

Cardoso, C., Zhang, Y., Jamil, M., Hepworth, J., Charnikhova, T., Dimkpa, S. O. N., Meharg, C., Wright, M. H., Liu, J., Meng, X., Wang, Y., Li, J., McCouch, S. R., Leyser, O., Price, A. H., Bouwmeester, H. J., & Ruyter-Spira, C. (2014) Natural variation of rice strigolactone biosynthesis is associated with the deletion of two MAX1 orthologs. *Proceedings of the National Academy of Sciences of the United States of America*, 111(6), 2379–2384.

Cheng, H., Qin, L., Lee, S., Fu, X., Richards, D. E., Cao, D., Luo, D., Harberd, N. P., & Peng, J. (2004). Gibberellin regulates Arabidopsis floral development via suppression of DELLA protein function. *Development*, 131(5), 1055–1064.

Chevalier, F., Nieminen, K., Sánchez-Ferrero, J. C., Rodríguez, M. L., Chagoyen, M., Hardtke, C. S., & Cubas, P. (2014) Strigolactone Promotes Degradation of DWARF14, an α/β Hydrolase Essential for Strigolactone Signaling in Arabidopsis. *The Plant Cell*, 26(3), 1134–1150.

Conn, C. E., Bythell-Douglas, R., Neumann, D., Yoshida, S., Whittington, B., Westwood, J. H. et al. (2015) Convergent evolution of strigolactone perception enabled host detection in parasitic plants, *Science*, 349(6247), 540-543.

Cook, C. E., Whichard, L. P., Turner, B., Wall, M. E., & Egle, G. H. (1966) Germination of Witchweed (*Striga lutea* Lour.): Isolation and Properties of a Potent Stimulant, *Science*, 154(3753), 1189–1190.

de Saint Germain, A., Clavé, G., Badet-Denisot, M.-A. A., Pillot, J.-P. P., Cornu, D., Le Caer, J.-P. P. et al. (2016) An histidine covalent receptor and butenolide complex mediates strigolactone perception, *Nature Chemical Biology*, 12(10), 787-794.

Delaux, P. M., Xie, X., Timme, R. E., Puech-Pages, V., Dunand, C., Lecompte, E., Delwiche, C. F., Yoneyama, K., Bécard, G., & Séjalon-Delmas, N. (2012) Origin of strigolactones in the green lineage. *New Phytologist*, 195(4), 857–871.

Desta, B., & Amare, G. (2021) Paclobutrazol as a plant growth regulator, *Chemical and Biological Technologies in Agriculture*, 8(1), 1–15.

Dill, A., Jung, H. S., & Sun, T. P. (2001) The DELLA motif is essential for gibberellin-induced degradation of RGA. *Proceedings of the National Academy of Sciences of the United States of America*, 98(24), 14162–14167.

Dohmann, E. M. N., Nill, C., & Schwechheimer, C. (2010) DELLA proteins restrain germination and elongation growth in *Arabidopsis thaliana* COP9 signalosome mutants. *European Journal of Cell Biology*, 89(2–3), 163–168.

Ejeta, G. (2007) The *Striga* scourge in Africa: A growing pandemic, *Integrating New Technologies for Striga Control: Towards Ending the Witch-hunt*, 3-15.

Fernández-Aparicio, M., Huang, K., Wafula, E. K., Honaas, L. A., Wickett, N. J., Timko, M. P., Depamphilis, C. W., Yoder, J. I., & Westwood, J. H. (2013) Application of qRT-PCR and RNA-Seq analysis for the identification of housekeeping genes useful for normalization of gene expression values during *Striga hermonthica* development, *Molecular Biology Reports*, 40(4), 3395–3407.

Fu, X., Richards, D. E., Fleck, B., Xie, D., Burton, N., & Harberd, N. P. (2004) The *Arabidopsis* Mutant *sleepy1gar2-1* Protein Promotes Plant Growth by Increasing the Affinity of the SCF^{SLY1} E3 Ubiquitin Ligase for DELLA Protein Substrates. *The Plant Cell*, 16(6), 1406–1418.

Fujioka, H., Samejima, H., Suzuki, H., Mizutani, M., Okamoto, M., & Sugimoto, Y. (2019) Aberrant protein phosphatase 2C leads to abscisic acid insensitivity and high transpiration in parasitic *Striga*. *Nature Plants*, 5(3), 258–262.

Gobena, D., Shimels, M., Rich, P. J., Ruyter-Spira, C., Bouwmeester, H., Kanuganti, S., Mengiste, T., & Ejeta, G. (2017) Mutation in sorghum LOW GERMINATION STIMULANT 1 alters strigolactones and causes *Striga* resistance. *Proceedings of the National Academy of Sciences of the United States of America*, 114(17), 4471–4476.

Gomez-Roldan, V., Fermas, S., Brewer, P. B., Puech-Pagès, V., Dun, E. A., Pillot, J.-P. P. et al. (2008) Strigolactone inhibition of shoot branching, *Nature*, 455(7210), 189-194.

Gomi, K., Sasaki, A., Itoh, H., Ueguchi-Tanaka, M., Ashikari, M., Kitano, H., & Matsuoka, M. (2004) GID2, an F-box subunit of the SCF E3 complex, specifically interacts with phosphorylated SLR1 protein and regulates the gibberellin-dependent degradation of SLR1 in rice. *The Plant Journal*, 37(4), 626–634.

Griffiths, J., Murase, K., Rieu, I., Zentella, R., Zhang, Z. L., Powers, S. J., Gong, F., Phillips, A. L., Hedden, P., Sun, T. P., & Thomas, S. G. (2006) Genetic Characterization and Functional Analysis of the GID1 Gibberellin Receptors in Arabidopsis. *The Plant Cell*, 18(12), 3399.

Ha, C. V., Leyva-Gonzalez, M. A., Osakabe, Y., Tran, U. T., Nishiyama, R., Watanabe, Y. et al. (2014) Positive regulatory role of strigolactone in plant responses to drought and salt stress, *Proceedings of the National Academy of Sciences of the United States of America*, 111(2), 851-856.

Hamiaux, C., Drummond, R. S. M., Janssen, B. J., Ledger, S. E., Cooney, J. M., Newcomb, R. D. et al. (2012) *DAD2* is an α/β hydrolase likely to be involved in the perception of the plant branching hormone, strigolactone, *Current Biology*, 22(21), 2032-2036.

Hu, Q., He, Y., Wang, L., Liu, S., Meng, X., Liu, G., Jing, Y., Chen, M., Song, X., Jiang, L., Yu, H., Wang, B., & Li, J. (2017) DWARF14, a receptor covalently linked with the active form of strigolactones, undergoes strigolactone-dependent degradation in rice. *Frontiers in Plant Science*, 8, 301560.

Ikeda, A., Ueguchi-Tanaka, M., Sonoda, Y., Kitano, H., Koshioka, M., Futsuhara, Y., Matsuoka, M., & Yamaguchi, J. (2001) slender Rice, a Constitutive Gibberellin Response Mutant, Is Caused by a Null Mutation of the SLR1 Gene, an Ortholog of the Height-Regulating Gene GAI/RGA/RHT/D8. *The Plant Cell*, 13(5), 999–1010.

Ito, T., Okada, K., Fukazawa, J., & Takahashi, Y. (2018) DELLA-dependent and -independent gibberellin signaling. *Plant Signaling & Behavior*, 13(3), 1445933.

Jacobsen, S. E. and Olszewski, N. E. (1993) Mutations at the *SPINDLY* Locus of Arabidopsis Alter Gibberellin Signal Transduction: American Society of Plant Physiologists.

Jiang, L., Liu, X., Xiong, G., Liu, H., Chen, F., Wang, L. et al. (2013) *DWARF53* acts as a repressor of strigolactone signalling in rice, *Nature*, 504(7480), 401-405.

Kagiyama, M., Hirano, Y., Mori, T., Kim, S. Y., Kyojuka, J., Seto, Y., Yamaguchi, S., & Hakoshima, T. (2013) Structures of D14 and D14L in the strigolactone and karrikin signaling pathways. *Genes to Cells*, 18(2), 147–160.

Kapulnik, Y., Delaux, P. M., Resnick, N., Mayzlish-Gati, E., Wininger, S., Bhattacharya, C. et al. (2011) Strigolactones affect lateral root formation and root-hair elongation in *Arabidopsis*, *Planta*, 233(1), 209-216.

Khosla, A., Morffy, N., Li, Q., Faure, L., Chang, S. H., Yao, J. et al. (2020) Structure-Function Analysis of *SMAX1* Reveals Domains That Mediate Its Karrikin-Induced Proteolysis and Interaction with the Receptor *KAI2*, *The Plant cell*, 32(8), 2639-2659.

Koornneef, M., & van der Veen, J. H. (1980) Induction and analysis of gibberellin sensitive mutants in *Arabidopsis thaliana* (L.) heynh. *Theoretical and Applied Genetics*, 58(6), 257–263.

Lee, S., Cheng, H., King, K. E., Wang, W., He, Y., Hussain, A., Lo, J., Harberd, N. P., & Peng, J. (2002) Gibberellin regulates *Arabidopsis* seed germination via *RGL2*, a *GAI/RGA*-like gene whose expression is up-regulated following imbibition. *Genes & Development*, 16(5), 646.

Lechat, M.M., Burn, G., Montiel, G., Véronési, C. Simier, P., Thoiron, S. et al (2015) Seed response to strigolactone is controlled by abscisic acid-independent DNA methylation in the obligate root parasitic plant, *Phelipanche ramosa* L. Pomel, *Journal of Experimental Botany*, 66(11), 3129-3140.

Li, W., Nguyen, K. H., Chu, H. D., Ha, C. Van, Watanabe, Y., Osakabe, Y., Leyva-González, M. A., Sato, M., Toyooka, K., Voges, L., Tanaka, M., Mostofa, M. G., Seki, M., Seo, M., Yamaguchi, S., Nelson, D. C., Tian, C., Herrera-Estrella, L., & Tran, L. S. P. (2017) The karrikin receptor *KAI2* promotes drought resistance in *Arabidopsis thaliana*. *PLOS Genetics*, 13(11), e1007076.

Liu, Q., Zhang, Y., Matusova, R., Charnikhova, T., Amini, M., Jamil, M., Fernandez-Aparicio, M., Huang, K., Timko, M. P., Westwood, J. H., Ruyter-Spira, C., van der Krol, S., & Bouwmeester,

- H. J. (2014) *Striga hermonthica* MAX2 restores branching but not the Very Low Fluence Response in the *Arabidopsis thaliana* max2 mutant. *New Phytologist*, 202(2), 531–541.
- Mallu, T. S., Irafasha, G., Mutinda, S., Owuor, E., Githiri, S. M., Odeny, D. A. et al. (2022) Mechanisms of pre-attachment *Striga* resistance in sorghum through genome-wide association studies, *Molecular Genetics and Genomics*, 297(3), 751-762.
- McGinnis, K. M., Thomas, S. G., Soule, J. D., Strader, L. C., Zale, J. M., Sun, T. P., & Steber, C. M. (2003) The *Arabidopsis* SLEEPY1 gene encodes a putative F-box subunit of an SCF E3 ubiquitin ligase. *The Plant Cell*, 15(5), 1120–1130.
- Mohammed, R., Are, A. K., Munghate, R. S., Bhavanasi, R., Polavarapu, K. K. B., & Sharma, H. C. (2016) Inheritance of resistance to sorghum shoot fly, *Atherigona soccata* in Sorghum, *Sorghum bicolor* (L.) Moench. *Frontiers in Plant Science*, 7(APR2016), 175264
- Nakamura, H., Hirabayashi, K., Miyakawa, T., Kikuzato, K., Hu, W., Xu, Y., Jiang, K., Takahashi, I., Niiyama, R., Dohmae, N., Tanokura, M., & Asami, T. (2019) Triazole Ureas Covalently Bind to Strigolactone Receptor and Antagonize Strigolactone Responses. *Molecular Plant*, 12(1), 44–58.
- Nakamura, H., Xue, Y. L., Miyakawa, T., Hou, F., Qin, H. M., Fukui, K., Shi, X., Ito, E., Ito, S., Park, S. H., Miyauchi, Y., Asano, A., Totsuka, N., Ueda, T., Tanokura, M., & Asami, T. (2013) Molecular mechanism of strigolactone perception by DWARF14. *Nature Communications*, 4(1), 1–10.
- Nakayama, I., Miyazawa, T., Kobayashi, M., Kamiya, Y., Abe, H., & Sakurai, A. (1990) Effects of a New Plant Growth Regulator Prohexadione Calcium (BX-112) on Shoot Elongation Caused by Exogenously Applied Gibberellins in Rice (*Oryza sativa* L.) Seedlings, *Plant and Cell Physiology*, 31(2), 195–200.
- Nelson, D. C., Scaffidi, A., Dun, E. A., Waters, M. T., Flematti, G. R., Dixon, K. W., Beveridge, C. A., Ghisalberti, E. L., & Smith, S. M. (2011) F-box protein MAX2 has dual roles in karrikin and strigolactone signaling in *Arabidopsis thaliana*. *Proceedings of the National Academy of Sciences of the United States of America*, 108(21), 8897–8902.

Nomura, S., Nakashima, H., Mizutani, M., Takikawa, H., & Sugimoto, Y. (2013) Structural requirements of strigolactones for germination induction and inhibition of *Striga gesnerioides* seeds. *Plant Cell Reports*, 32(6), 829–838.

Peng, J., Carol, P., Richards, D. E., King, K. E., Cowling, R. J., Murphy, G. P., & Harberd, N. P. (1997) The Arabidopsis GAI gene defines a signaling pathway that negatively regulates gibberellin responses. *Genes & Development*, 11(23), 3194–3205.

Ogawa, M., Hanada, A., Yamauchi, Y., Kuwahara, A., Kamiya, Y., & Yamaguchi, S. (2003) Gibberellin Biosynthesis and Response during Arabidopsis Seed Germination. *The Plant Cell*, 15(7).

Qiu, S., Bradley, J.M., Zhang, P., Chaudhuri, R., Blaxter, M., Butlin, R.K. et al. (2022) Genome-enabled discovery of candidate virulence loci in *Striga hermonthica*, a devastating parasite of African cereal crops, *New Phytologist*, 236, 622-638.

Ruyter-Spira, C., Kohlen, W., Charnikhova, T., Van Zeijl, A., Van Bezouwen, L., De Ruijter, N., Cardoso, C., Antonio Lopez-Raez, J., Matusova, R., Bours, R., Verstappen, F., & Bouwmeester, H. (2011) Physiological Effects of the Synthetic Strigolactone Analog GR24 on Root System Architecture in Arabidopsis: Another Belowground Role for Strigolactones? *Plant Physiology*, 155, 721–734.

Sasaki, A., Itoh, H., Gomi, K., Ueguchi-Tanaka, M., Ishiyama, K., Kobayashi, M., Jeong, D. H., An, G., Kitano, H., Ashikari, M., & Matsuoka, M. (2003) Accumulation of phosphorylated repressor for Gibberellin signaling in an F-box mutant. *Science*, 299(5614), 1896–1898.

Scaffidi, A., Waters, M. T., Sun, Y. K., Skelton, B. W., Dixon, K. W., Ghisalberti, E. L., Flematti, G. R., & Smith, S. M. (2014) Strigolactone Hormones and Their Stereoisomers Signal through Two Related Receptor Proteins to Induce Different Physiological Responses in Arabidopsis. *Plant Physiology*, 165(3), 1221–1232.

Seto, Y., Yasui, R., Kameoka, H., Tamiru, M., Cao, M., Terauchi, R., Sakurada, A., Hirano, R., Kisugi, T., Hanada, A., Umehara, M., Seo, E., Akiyama, K., Burke, J., Takeda-Kamiya, N., Li, W.,

Hirano, Y., Hakoshima, T., Mashiguchi, K., ... Yamaguchi, S. (2019) Strigolactone perception and deactivation by a hydrolase receptor DWARF14. *Nature Communications*, 10(1), 1–10.

Shabek, N., Ticchiarelli, F., Mao, H., Hinds, T. R., Leyser, O., & Zheng, N. (2018) Structural plasticity of D3–D14 ubiquitin ligase in strigolactone signalling. *Nature*, 563(7733), 652–656.

Silverstone, A. L., Mak, P. Y. A., Martínez, E. C., & Sun, T. P. (1997) The New RGA Locus Encodes a Negative Regulator of Gibberellin Response in *Arabidopsis thaliana*. *Genetics*, 146(3), 1087–1099.

Song, W. J., Zhou, W. J., Jin, Z. L., Cao, D. D., Joel, D. M., Takeuchi, Y., & Yoneyama, K. (2005) Germination response of Orobanche seeds subjected to conditioning temperature, water potential and growth regulator treatments, *Weed Research*, 45(6), 467–476.

Stanga, J. P., Smith, S. M., Briggs, W. R. and Nelson, D. C. (2013) *SUPPRESSOR OF MORE AXILLARY GROWTH2 1* controls seed germination and seedling development in *Arabidopsis*, *Plant Physiology*, 163(1), 318-330.

Sugimoto, Y., Mukhtar, A., Abdelbagi, Yabuta, S., Kinoshita, H., Inanaga, S. et al. (2003) Germination strategy of *Striga hermonthica* involves regulation of ethylene biosynthesis, *PHYSIOLOGIA PLANTARUM*, 119, 137-145.

Sun, X. D., & Ni, M. (2011) HYPOSENSITIVE TO LIGHT, an Alpha/Beta Fold Protein, Acts Downstream of ELONGATED HYPOCOTYL 5 to Regulate Seedling De-Etiolation. *Molecular Plant*, 4(1), 116–126.

Sun, Y. K., Flematti, G. R., Smith, S. M., & Waters, M. T. (2016) Reporter gene-facilitated detection of compounds in *Arabidopsis* leaf extracts that activate the karrikin signaling pathway. *Frontiers in Plant Science*, 7(DECEMBER2016), 238405.

Swarbreck, S. M., Guerringue, Y., Matthus, E., Jamieson, F. J. C., & Davies, J. M. (2019) Impairment in karrikin but not strigolactone sensing enhances root skewing in *Arabidopsis thaliana*. *The Plant Journal*, 98(4), 607–621.

Takahashi, I., & Asami, T. (2018) Target-based selectivity of strigolactone agonists and antagonists in plants and their potential use in agriculture. *Journal of Experimental Botany*, 69(9), 2241–2254.

Takeuchi, Y., Omigawa, Y., Ogasawara, M., Yoneyama, K., Konnai, M., & Worsham, A. D. (1995) Effects of brassinosteroids on conditioning and germination of clover broomrape (*Orobanche minor*) seeds, *Plant Growth Regulation*, 16(2), 153–160.

Tal, L., Palayam, M., Ron, M., Young, A., Britt, A., & Shabek, N. (2022) A conformational switch in the SCF-D3/MAX2 ubiquitin ligase facilitates strigolactone signalling. *Nature Plants*, 8(5), 561–573.

Toh, S., Holbrook-Smith, D., Stogios, P. J., Onopriyenko, O., Lumba, S., Tsuchiya, Y. et al. (2015) Structure-function analysis identifies highly sensitive strigolactone receptors in *Striga*, *Science*, 350(6257), 203-208.

Toh, S., Holbrook-Smith, D., Stokes, M. E., Tsuchiya, Y., & McCourt, P. (2014) Detection of Parasitic Plant Suicide Germination Compounds Using a High-Throughput Arabidopsis HTL/KAI2 Strigolactone Perception System. *Chemistry & Biology*, 21(8), 988–998.

Toh, S., Kamiya, Y., Kawakami, N., Nambara, E., McCourt, P. and Tsuchiya, Y. (2012) Thermoinhibition uncovers a role for strigolactones in Arabidopsis seed germination, *Plant and Cell Physiology*, 53(1), 107-117.

Tsuchiya, Y., Yoshimura, M., & Hagihara, S. (2018) The dynamics of strigolactone perception in *Striga hermonthica*: a working hypothesis. *Journal of Experimental Botany*, 69(9), 2281–2290.

Tsuchiya, Y., Yoshimura, M., Sato, Y., Kuwata, K., Toh, S., Holbrook-Smith, D. et al. (2015) Probing strigolactone receptors in *Striga hermonthica* with fluorescence, *Science*, 349(6250), 864-868.

Ueda, H., & Kusaba, M. (2015) Strigolactone Regulates Leaf Senescence in Concert with Ethylene in Arabidopsis. *Plant Physiology*, 169(1), 138–147.

Ueguchi-Tanaka, M., Ashikari, M., Nakajima, M., Itoh, H., Katoh, E., Kobayashi, M., Chow, T. Y., Hsing, Y. I. C., Kitano, H., Yamaguchi, I., & Matsuoka, M. (2005) GIBBERELLIN INSENSITIVE DWARF1 encodes a soluble receptor for gibberellin. *Nature*, 437(7059), 693–698.

Umehara, M., Hanada, A., Yoshida, S., Akiyama, K., Arite, T., Takeda-Kamiya, N. et al. (2008) Inhibition of shoot branching by new terpenoid plant hormones, *Nature*, 455(7210), 195-200.

Uraguchi, D., Kuwata, K., Hijikata, Y., Yamaguchi, R., Imaizumi, H., Sathiyarayanan, A.M. et al. (2018) A femtomolar-range suicide germination stimulant for the parasitic plant *Striga hermonthica*, *Science*, 362(6420), 1301-1305.

Villaécija-Aguilar, J. A., Hamon-Josse, M., Carbonnel, S., Kretschmar, A., Schmidt, C., Dawid, C., Bennett, T., & Gutjahr, C. (2019) SMAX1/SMXL2 regulate root and root hair development downstream of KAI2-mediated signalling in Arabidopsis. *PLOS Genetics*, 15(8), e1008327.

Wang, L., Wang, B., Jiang, L., Liu, X., Li, X., Lu, Z., Meng, X., Wang, Y., Smith, S. M., & Lia, J. (2015) Strigolactone Signaling in Arabidopsis Regulates Shoot Development by Targeting D53-Like SMXL Repressor Proteins for Ubiquitination and Degradation. *The Plant Cell*, 27(11), 3128–3142.

Wang, L., Waters, M. T., & Smith, S. M. (2018). Karrikin-KAI2 signalling provides Arabidopsis seeds with tolerance to abiotic stress and inhibits germination under conditions unfavourable to seedling establishment. *New Phytologist*, 219(2), 605–618.

Wang, Y., Yao, R., Du, X., Guo, L., Chen, L., Xie, D. et al. (2021) Molecular basis for high ligand sensitivity and selectivity of strigolactone receptors in *Striga*, *Plant Physiology*, 185(4), 1411-1428.

Waters, M. T., Nelson, D. C., Scaffidi, A., Flematti, G. R., Sun, Y. K., Dixon, K. W., & Smith, S. M. (2012) Specialisation within the DWARF14 protein family confers distinct responses to karrikins and strigolactones in Arabidopsis. *Development*, 139(7), 1285–1295.

Waters, M. T., Scaffidi, A., Flematti, G., & Smith, S. M. (2015a) Substrate-induced degradation of the α/β -fold hydrolase KARRIKIN INSENSITIVE2 requires a functional catalytic triad but is independent of MAX2. *Molecular Plant*, 8(5), 814–817.

Waters, M. T., Scaffidi, A., Moulin, S. L. Y., Sun, Y. K., Flematti, G. R., & Smith, S. M. (2015b) A *Selaginella moellendorffii* Ortholog of KARRIKIN INSENSITIVE2 Functions in Arabidopsis Development but Cannot Mediate Responses to Karrikins or Strigolactones. *The Plant Cell*, 27(7), 1925.

Xu, Y., Miyakawa, T., Nosaki, S., Nakamura, A., Lyu, Y., Nakamura, H. et al. (2018) Structural analysis of HTL and D14 proteins reveals the basis for ligand selectivity in *Striga*, *Nature Communications*, 9(1).

Yao, R., Ming, Z., Yan, L., Li, S., Wang, F., Ma, S. et al. (2016) DWARF14 is a non-canonical hormone receptor for strigolactone, *Nature*, 536(7617), 469-473.

Yao, R., Wang, F., Ming, Z., Du, X., Chen, L., Wang, Y., Zhang, W., Deng, H., & Xie, D. (2017) ShHTL7 is a non-canonical receptor for strigolactones in root parasitic weeds. *Cell Research* 2017 27:6, 27(6), 838–841.

Yamaguchi, S. (2008) Gibberellin Metabolism and its Regulation, *Annual Review of Plant Biology*, 59, 225–251.

Yokota, T., Sakai, H., Okuno, K., Yoneyama, K., & Takeuchi, Y. (1998) Alectrol and orobanchol, germination stimulants for *Orobanche minor*, from its host red clover, *Phytochemistry*, 49(7), 1967–1973.

Yoshimura, M., Sato, A., Kuwata, K., Inukai, Y., Kinoshita, T., Itami, K., Tsuchiya, Y., & Hagihara, S. (2018). Discovery of Shoot Branching Regulator Targeting Strigolactone Receptor DWARF14. *ACS Central Science*, 4(2), 230–234.

Zehhar, N., Ingouff, M., Bouya, D., & Fer, A. (2002) Possible involvement of gibberellins and ethylene in *Orobanche ramosa* germination, *Weed Research*, 42(6), 464–469.

Zhao, L. H., Zhou, X. E., Yi, W., Wu, Z., Liu, Y., Kang, Y., Hou, L., De Waal, P. W., Li, S., Jiang, Y., Scaffidi, A., Flematti, G. R., Smith, S. M., Lam, V. Q., Griffin, P. R., Wang, Y., Li, J., Melcher, K., & Xu, H. E. (2015) Destabilization of strigolactone receptor DWARF14 by binding of ligand and E3-ligase signaling effector DWARF3. *Cell Research* 2015 25:11, 25(11), 1219–1236.

Zhou, F., Lin, Q., Zhu, L., Ren, Y., Zhou, K., Shabek, N. et al. (2013) D14-SCF D3 -dependent degradation of D53 regulates strigolactone signalling, *Nature*, 504(7480), 406-410.